SPRINGER BRIEFS IN
PETROLEUM GEOSCIENCE & ENGINEERING

Jebraeel Gholinezhad
John Senam Fianu
Mohamed Galal Hassan

Challenges in Modelling and Simulation of Shale Gas Reservoirs

Springer

SpringerBriefs in Petroleum Geoscience & Engineering

The SpringerBriefs series in Petroleum Geoscience & Engineering promotes and expedites the dissemination of substantive new research results, state-of-the-art subject reviews and tutorial overviews in the field of petroleum exploration, petroleum engineering and production technology. The subject focus is on upstream exploration and production, subsurface geoscience and engineering. These concise summaries (50–125 pages) will include cutting-edge research, analytical methods, advanced modelling techniques and practical applications. Coverage will extend to all theoretical and applied aspects of the field, including traditional drilling, shale-gas fracking, deepwater sedimentology, seismic exploration, pore-flow modelling and petroleum economics. Topics include but are not limited to:

- Petroleum Geology & Geophysics
- Exploration: Conventional and Unconventional
- Seismic Interpretation
- Formation Evaluation (well logging)
- Drilling and Completion
- Hydraulic Fracturing
- Geomechanics
- Reservoir Simulation and Modelling
- Flow in Porous Media: from nano- to field-scale
- Reservoir Engineering
- Production Engineering
- Well Engineering; Design, Decommissioning and Abandonment
- Petroleum Systems; Instrumentation and Control
- Flow Assurance, Mineral Scale & Hydrates
- Reservoir and Well Intervention
- Reservoir Stimulation
- Oilfield Chemistry
- Risk and Uncertainty
- Petroleum Economics and Energy Policy

Contributions to the series can be made by submitting a proposal to the responsible Springer contact, Charlotte Cross at charlotte.cross@springer.com or the Academic Series Editor, Prof Dorrik Stow at dorrik.stow@pet.hw.ac.uk.

More information about this series at http://www.springer.com/series/15391

Jebraeel Gholinezhad · John Senam Fianu
Mohamed Galal Hassan

Challenges in Modelling and Simulation of Shale Gas Reservoirs

Springer

Jebraeel Gholinezhad
School of Engineering
University of Portsmouth
Portsmouth, Hampshire
UK

Mohamed Galal Hassan
School of Engineering
University of Portsmouth
Portsmouth, Hampshire
UK

John Senam Fianu
School of Engineering
University of Portsmouth
Portsmouth, Hampshire
UK

ISSN 2509-3126 ISSN 2509-3134 (electronic)
SpringerBriefs in Petroleum Geoscience & Engineering
ISBN 978-3-319-70768-6 ISBN 978-3-319-70769-3 (eBook)
https://doi.org/10.1007/978-3-319-70769-3

Library of Congress Control Number: 2017960202

Printed on acid-free paper

This Springer imprint is published by Springer Nature
The registered company is Springer International Publishing AG
The registered company address is: Gewerbestrasse 11, 6330 Cham, Switzerland

Preface

The depletion of conventional oil and gas reservoirs as well as the rise in the energy demand has compelled the upstream oil industry to search for alternative energy sources such as unconventional hydrocarbon reservoirs to meet the demand. Shale gas reservoirs as an unconventional energy source are organic-rich formations considered as both the source rock and the reservoir. Gas is stored in the limited pore space of the rock while substantial fraction of gas is adsorbed on the organic material. These reservoirs exhibit extremely low permeability and thus require effective stimulation strategies in place to produce economically.

The "shale gas boom" occurred in the last decade in the USA has stimulated huge production of oil and natural gas from shale gas reservoirs. The advances in production technology and application of combined horizontal drilling and hydraulic fracturing have facilitated such production. However, long-term exploitation of shale gas reservoirs poses some inherent challenges to upstream oil industry. These challenges emanate from the characteristics of shale gas reservoirs which differ from those of conventional gas reservoirs. They contain natural gas both in the pore spaces of reservoir rock and as adsorbed gas on the surface of rock grain. Very low permeability in shale formations means that the fluid flow mechanisms are different and in general more complicated than permeable reservoirs. In addition, a major factor determining the productivity of this type of reservoirs is the existence of a natural fracture network. Drilling long horizontal wells with multiple hydraulic fracturing has been established as the method of depleting shale gas reservoirs. The combination of an ultra-tight shale matrix with hydraulic fractures, natural fractures and a horizontal well results in a complicated flow system that cannot be modelled accurately using the existing conventional models. Exploring these challenges and the relevant advancements in modelling and simulation of shale gas reservoirs has been the main drive for writing this book.

Although there has been a tremendous research to understand the underlying differences between these formations and conventional reservoirs and major steps have been taken towards modelling of shale reservoirs with natural fracture network coupled with hydraulic fracturing, due to the numerous challenges in characterisation of shale formations, the fundamental differences in modelling and simulation

of such formations compared with conventional reservoirs are poorly understood. On the other hand, the results of the investigations on the area are very much scattered and fragmented while the various studies are yet to be integrated and assimilated. The aim of the present book is to try to bring much of the relevant fundamental understandings together into one place and to present a unified approach to the ideas produced for modelling of shale gas reservoirs.

"Challenges in Modelling and Simulation of Shale Gas Reservoirs", therefore, tends to be an insightful book about modelling aspects of shale gas reservoirs considering their ingrained dissimilarities with conventional gas reservoirs. The book starts with an introduction to the shale gas reservoirs and the inherent challenges encountered in simulation of them in Chap. 1. Then, different modelling and simulation challenges such as complexity of fracture network, adsorption phenomena, non-Darcy flow, natural fracture network, etc. are discussed in detail and the latest findings in those areas are presented. These are covered in Chaps. 2 and 3. Chapter 4 addresses the available techniques for evaluation of production performance and the ways they can be adapted to shale gas reservoirs.

We, the authors, believe that the book would be of interest to the scientific community of petroleum industry in both industry and academia and hope that the readers can learn and understand the complications present in developing shale gas models and compare analytical modelling as well as numerical simulation of shale gas with those of conventional reservoirs. They can also benefit from a comprehensive review of the state of the art in developing shale gas models and simulators in the upstream oil industry, which can eventually lead to a better understanding of these reservoirs and facilitate the systematic research on efficient development of shale gas plays.

In this book, we aim to cover the cutting-edge information about analytical and numerical modelling of shale gas reservoirs and elaborate on the various challenges about simulation of these reservoirs which may, if not considered, lead to erroneous results when doing the calculations related to exploration and production of these resources. While we have endeavoured to gather as many research works and publications as possible from the subject experts, it is not unlikely to have missed a particular paper with noticeable outcomes. Furthermore, it is possible to misinterpret some statements from the work of others. In other words, the book we have produced will not be flawless. Therefore, any feedback or comments with regards to the contents of this book will be most welcome and will help us to improve the future editions.

We take this opportunity to thank many people who have helped, in different ways, in the preparation of this book. In particular, we thank Mr. Michael Kenomore for his inputs on the status of shale gas in the UK. We would also like to express our appreciation to the editorial staff of Springer International Publishing Company for their patience and understanding.

Portsmouth, UK
November 2017

Jebraeel Gholinezhad
John Senam Fianu
Mohamed Galal Hassan

Contents

Nomenclature

Chapter 2

K_n	Knudsen number
λ	Diameter of the pores
d_p	Gas mean free path
$k(p_{avg})$	Gas permeability at mean pressure
k_D	Darcy or liquid permeability
b	Klinkenberg permeability
k_{app}	Apparent permeability
T	Temperature
M	Molar mass
α	Tangential momentum accommodation coefficient
r	Pore radius
μ	Viscosity
$A\&B$	Empirical fitting constants (Eg. 2.8)
D_k	Knudsen diffusion coefficient
$\delta^{'}$	Ratio of normalised molecular size (d_m) to local average pore diameter (d_p)
R_{avg}	Average pore diameter
x_f	Fracture half length
w_o	Maximum fracture opening
p_w	Wellbore pressure
G	Shear modulus
Q	Fluid injection rate
t	Time
v	Poison's ratio
h	Height
V	Volume of adsorbed gas
P	Pressure
V_L	Langmuir volume or maximum gas adsorption at infinite pressure
P_L	Langmuir pressure corresponding to one half of Langmuir volume

P_o Saturation pressure
n Maximum number of adsorption layers (Eg. 2.16)
C Constant related to the net heat of adsorption
V_m Maximum volume of gas adsorption
k_o Permeability at atmospheric condition
P_e Effective pressure
α Slope of the curve of permeability vs effective pressure (Eg. 2.19)
E Young's modulus
φ Porosity

Chapter 3

β Non-Darcy flow coefficient (Eg. 3.1)
ρ Density
v Superficial velocity
c Constant related to pore size distribution
τ Tortuosity
K Permeability
a, b Constants determined by experiments based on proppant type
S_{wr} Residual water saturation
K_{rel} Relative gas permeability
k_d Constant Darcy permeability
k_{mr} Minimum permeability relative to Darcy permeability

Chapter 4

D_i Initial decline rate
q_i Initial rate
D Arps "loss ratio"
D_∞ Decline constant at "infinite time"
D_1 Decline constant "intercept" at 1 time unit
n Time exponent (Eg. 4.4)
q_o Flow rate at time $t = 0$
Q Cumulative production
τ Characteristics time parameter for SEPD model (Eg. 4.6)
m Slope
a Intercept constant (Eg. 4.8)
s Fracture surface skin
s_p Pseudo-skin factor
B Formation volume factor
r_w Well radius
c_t Total compressibility
h Formation thickness
x_s Fracture spacing
x_f Fracture half length

Δp_{wf}	Drawdown pressure drop
n	Fracture number, dimensionless
t_e	End of early time linear flow
V_p	SRV pore volume
V_r	Reservoir pore volume
r_e	External boundary radius
t_d	Dimensionless time
q_{Dd}	Decline curve dimensionless rate
q_d	Dimensionless rate
z	Gas compressibility factor
c_g	Gas compressibility
p_i	Initial pressure
m	Real gas potential (Eq. 4.25)
G	Original gas in place (Eg. 4.26)
μ_g	Gas viscosity
J_g	Gas productivity index
t_n	Normalised time, days
T_{sc}	Temperature at standard conditions
p_{sc}	Pressure at standard conditions
C_A	Dietz shape factor
$\bar{\mu}, \bar{c_g}$	Evaluated at averaged reservoir pressure
q_g	Gas flow rate
p_{wf}	Wellbore flowing pressure
γ	Euler's constant = 0.577216
pss	Pseudo-steady state
t_a	Pseudo-time
A	Area
t_{DA}	Dimensionless time based on area
t_{aD}	Dimensionless time based on r_{wa}^2
Q_{AD}	Dimensionless cumulative production based on area
r_{wa}	Apparent wellbore radius
p_{wd}	Dimensionless wellbore pressure

Chapter 1
Shale Gas Reservoirs—A Comparative Approach

Abstract Until recently, shales were regarded by the oil industry as a setback hindering the operations while drilling to target sandstone and limestone reservoirs. Also, it was considered as the source rock for hydrocarbons migrating into conventional reservoirs and as the seal for trapping oil and gas in underlying sediments. Thanks to the "shale gas revolution" in the USA, however, it is known today that shales, as the most abundant form of sedimentary rock on Earth, can form low-permeable reservoirs containing huge quantities of hydrocarbons. Unlike the conventional reservoirs, production from shale gas resources would not be economically feasible due to the very low rates of flow of natural gas from the formation of ultra-low permeability. Yet, this is only one of the characteristics of shale gas reservoir which makes them different from conventional resources. Outlining the fundamental differences between shale gas plays and conventional gas reservoirs along with a brief description of status of shale gas development is the subject of this chapter. Furthermore, the potential of shale gas in the UK and the problems associated with its development compared to the US shale gas are presented.

1.1 Introduction

It has now become evident that there is a considerable volume of hydrocarbons remaining within shale source rocks due to its inherently ultra-low permeability preventing it from migration to permeable formations. For many years, the trapped hydrocarbons within this source rock were thought to be uneconomic to produce. The advanced techniques of hydraulic fracturing and horizontal drilling, however, led to bringing these source rocks into markets in the USA. These shale reservoirs are often described as unconventional reservoirs because commercial rates of hydrocarbons cannot be achieved without hydraulic stimulation. Production from shale gas and associated gas from tight oil plays is the largest contributor to natural gas production growth in the USA and will account for nearly two-thirds of total USA production by 2040. Tight gas production, however, is the second largest

J. Gholinezhad et al., *Challenges in Modelling and Simulation of Shale Gas Reservoirs*, SpringerBriefs in Petroleum Geoscience & Engineering,
https://doi.org/10.1007/978-3-319-70769-3_1

source of the US domestic natural gas supply but its share falls through the late 2020s as the result of growing development of shale gas and tight oil plays.

The Marcellus and Utica plays in the East are the main driver for growth in total US shale gas production and the main source of total US dry natural gas production. Furthermore, production from the Eagle Ford and Haynesville plays along the Gulf Coast is a secondary contributor to domestic dry natural gas production, with production stabilising in the 2030s. Improvement in industry best practices and continuous technological advancement can be expected to lower costs and increase the expected ultimate recovery per well especially in plays having large undeveloped resources such as Marcellus, Utica and Haynesville plays. Nations around the world, including the UK, are now attempting to replicate the success of shale gas in America.

The UK is no stranger to shale gas. In 1875, the first well to encounter shale gas within the UK was drilled—at that time, the importance of it went unknown and unnoticed because of the abundant supply of conventional reservoirs making shale gas extraction uneconomic (The Royal Society 2012). The possibility of exploring for shale gas was later proposed in 1980s in the UK (Selley 1987). Presently, the decline in the domestic generation of conventional gas has led to a notable increase in gas imports from other countries like Qatar (Stevens 2013) and the decrease in the oil and gas production in the North Sea has resulted in a rapid expansion in attempting to develop shale in the UK. According to EIA (2013), the UK has large prospective shale gas volumes within carboniferous shale formations that are mainly situated in the north and central areas of the country.

1.2 Shale Gas Versus Conventional Reservoirs

Shale gas refers to natural gas that is confined or trapped in shale formation. Shale formations are formed by the weathering of rocks which are then transported and eventually deposited as fine grains into lakes, lagoons, river deltas and the sea floor along with large quantities of dead plankton or marine plants (Energy Institute 2015). In terms of geology, shale gas-bearing formations are rich in organic matter, fine-grained and porous with low permeability (Javadpour et al. 2007). This very low permeability feature is one of the properties that distinguish the shale source rock from conventional gas reservoirs. Unconventional shale reservoirs formed from sediments are characterised by low or ultra-low permeability of less than 0.1 mD (milli-Darcy). This means that the flow of gas is restricted and always needs artificial pathways to the well, through stimulation by creating fractures which can enhance flow and production (Green 2011). The gas is generated and stored within the rock (shale) which acts as both source rock and reservoir at the same time.

There are two fundamental characteristics of shale that control its ability to produce gas; this includes chemical and physical characteristics. The chemical characteristics involve the quality and quantity (maturity and composition) of the organic matter while porosity and permeability refer to the physical features of the

shale rock (Selley 2012). Moreover, hydraulic fracturing relies on two geo-meical characteristics of the formation; these are the mineral composition of the shale rock and the ductility/brittleness of the formation. Brittleness is a combination of both Poisson's ratio and Young's modulus. Poisson's ratio exhibits the ability of the rock to fail when put under stress, and Young's modulus reflects the ability of the rock to maintain fracture. Fracture pressure is higher in ductile shale formations as the shale formation initially deforms before finally fracturing—this tends to result in an inefficient fracture network (Arogundade and Sohrabi 2012). However in brittle shale formations, high fracturing pressures are not needed to create an efficient fracture network hence these formations are desired (Arogundade and Sohrabi 2012). The reason for this contrast is the magnitude of Poisson's ratio which gives an indication of quartz/clay content. Accordingly, a high Poisson's ratio (low quartz–clay ratio) indicates a ductile formation and vice versa. A high quartz–clay ratio means the shale formation has a higher porosity and thus lower fracture pressures (Arogundade and Sohrabi 2012).

Other important geological factors that play a significant role in the reservoir stimulation process are bedding plane arrangement, stratigraphy, clay content and shale water absorption. These parameters can change the direction of fracture propagation, the rate of gas recovery and wellbore stability (Mallick and Achalpurkar 2014).

Figure 1.1 illustrates the key elements necessary to have a commercial and productive play (Kundert and Mullen 2009).

These elements exist in various percentages in a shale reservoir but the essential features on Fig. 1.1 are maturity, free gas and total gas in place, thickness, natural fractures and reservoir pressure. Desirable properties are organic richness, brittleness and mineralogy (which affects brittleness). If the rock is ductile, the fracking technique can be improved to achieve good results provided that there is sufficient free gas in the shale (Kundert and Mullen 2009).

Chopra et al. (2012) suggested that the depth of the shale gas reservoir needs to be a factor because it will have an effect on the economics of the gas recovery. Locations of desirable shale properties that enable high shale gas production are commonly described as shale sweet spots. The sweets spots in shale gas reservoirs generally exhibit low clay volumes, mid to high organic content, high effective porosity, low water saturation, high Young's modulus and low Poisson's ratio (Holden et al. 2015).

Initial gas production from shale is mainly from the depletion of gas in the fracture network but production from these finite fractures declines rapidly due to limited storage capacity (Speight 2013). As pressure diffuses slowly through the shale rock compared to conventional reservoirs due to the extremely low permeability, tight well spacing is required to lower the reservoir pressure significantly to allow large amount of gas to desorb (Speight 2013). Recovery factor from shale gas reservoirs was suggested by Speight (2013), to be approximately between 28 and 40%. However, most shale gas reservoirs commonly achieve a recovery factor of around 20% (Chopra et al. 2012) compared to conventional reservoirs with recovery factors as high as 90%. In a conventional reservoir, each well is capable of

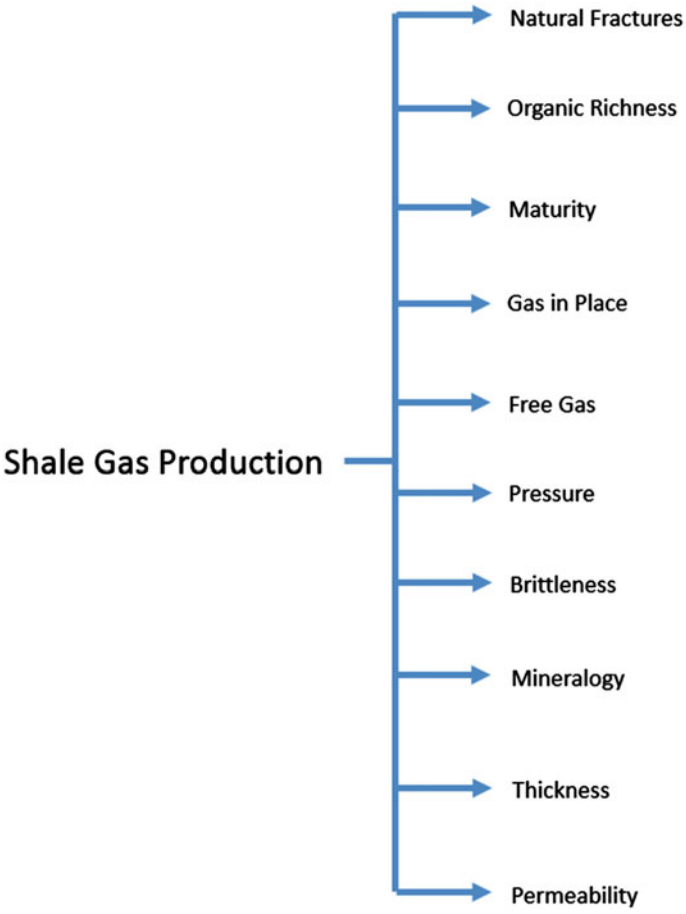

Fig. 1.1 Key elements needed for a successful shale gas play (Kundert and Mullen 2009)

draining a large area of oil or gas therefore only a few vertical wells might be needed to produce at commercial rates from the field (Speight 2013).

Most shale reservoirs typically have a net shale thickness of 50–600 ft, a porosity of 2–8%, total organic carbon content ranging between 1 and 14% and are found at depths ranging from 1000 to 13,000 ft (Cipolla et al. 2010). The economic development of these unconventional resources is based on successful stimulation of these extremely low permeability rocks, typically 10–100 nano-Darcies (10^{-5}–10^{-4} mD) (Cipolla et al. 2010). Physically, conventional reservoirs have enough porosity, so they have enough gas storage capacity, and sufficient permeability to allow gas flow. Therefore, without extensive stimulation procedures or long lateral wells, economic volumes of gas or oil can be produced at high commercial flow rates (Naik 2003).

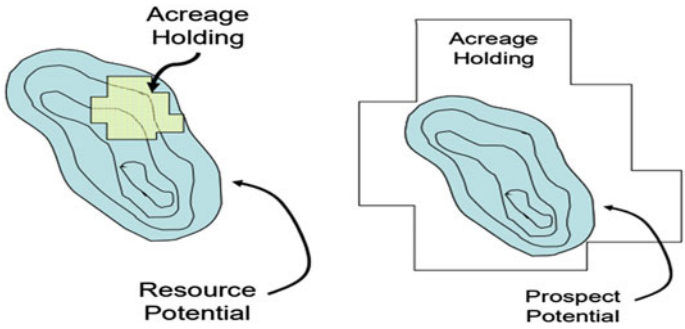

Fig. 1.2 Extension of conventional (left) and unconventional (right) resources in relation to area under evaluation (Haskett and Brown 2005)

Chan et al. (2010) also described conventional resources as those that exist in discrete petroleum accumulations localised to a structural or stratigraphic trap. These accumulations are typically bounded by an aquifer and are significantly affected by hydrodynamics based on the buoyancy of petroleum in water. Conventional resources require minimal processing before sale.

Some of the differences between shale gas formations and conventional reservoirs are summarised below:

- Conventional prospect assessment has clear boundaries to the potential reservoir or is usually enclosed within a specific geographical area, whereas unconventional resource potential extends far beyond the area being assessed and there are no definite boundaries (Fig. 1.2). In other words, analysis and assessment of unconventional resources are not feasible using traditional volumetric determinations (Haskett and Brown 2005).
- The shale rock acts as the source reservoir and seal compared to conventional rock types. Andrews (2013) further illustrated that owing to this characteristic, exploration of shale gas reservoirs occurs in the extensive basin centres rather than in traps or in structural highs for conventional reservoirs.
- The presence of natural fractures which are native to the formation and secondary fractures induced due to the creation of hydraulic fractures is common feature of shale gas reservoirs. These complex fracture networks serve as an added challenge when modelling shale gas reservoirs compared to conventional gas reservoirs. Also, porosity can be represented as primary and secondary porosity systems in shale gas reservoirs.
- Shale gas reservoirs generally have significantly lower permeability and porosity compared to conventional gas reservoirs (Williams-Kovacs 2012). Permeability of shale gas is in the nano- to micro-Darcy range compared to the milli-Darcy to micro-Darcy range in conventional reservoirs (Williams-Kovacs

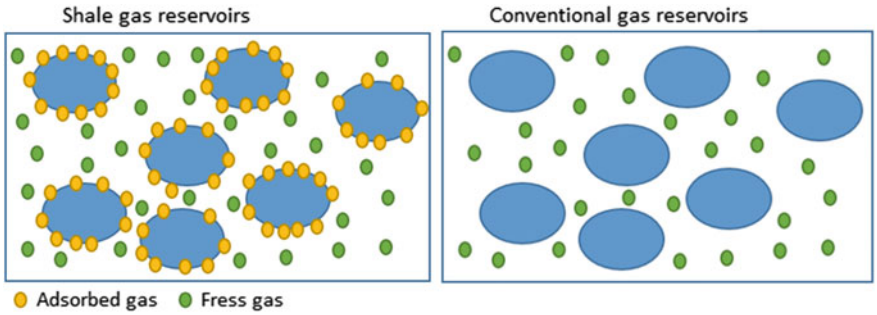

Fig. 1.3 Gas storage system in shale gas reservoirs and conventional gas reservoirs

2012). Hence, the flow of gas is minimal in shale formations and hydraulic fracturing is needed to flow economic quantities of gas (Mallick and Achalpurkar 2014). Low permeability of shale also implies flow is represented by non-Darcy flow compared to Darcy flow that occurs in most conventional gas reservoirs.

- Gas adsorption is a key component of the overall gas storage in shale gas reservoirs. Majority of the gas stored in shale gas reservoirs are through gas adsorption, whereas for conventional gas reservoirs, gas is mostly stored as compressed gas within the pores of the matrix (see Fig. 1.3).
- The low permeability characteristic in shale prevents the migration of gas to more permeable reservoirs (Sun et al. 2014), whereas gas present in conventional reservoirs has migrated from a source rock, through carrier beds over geological time into the discrete traps of the conventional reservoir located in structural highs on the margin of the basin centre (Andrews 2013).
- According to Sun et al. (2014), Swami et al. (2012), prevalent pore diameters in shale are at most 2 nm compared to an approximate range of 1–100 mm in conventional sandstone and carbonate reservoirs.
- Hydraulic fracturing is a necessity for economic production from shale gas reservoirs which is not the case for conventional reservoirs (Williams-Kovacs 2012). High-volume unconventional fracking typically uses 3–7 million gallons of water to fracture a well (Wilkinson 2014). These large quantities of water are needed because unconventional wells are deeper and require higher pressure than offshore conventional wells (Wilkinson 2014). Conventional fracturing is referred to as low-volume fracking because less than 80,000 gallons of water are used to fracture a single well (Wilkinson 2014).
- Shale gas reservoirs contain gas-bearing strata that are not stratified based on density (i.e. gas is not necessarily above water) unlike conventional reservoirs with the gas lying near the top and the water at the bottom strata due to its higher density (Williams-Kovacs 2012).

1.3 Shale Gas Development in the World

Shale gas resources can be found extensively around the world. Advanced Resources International (ARI) conducted a world shale gas resource assessment in 2013 on behalf of the United States (U.S.) Energy Information Administration (EIA) and the U.S. Department of Energy (DOE)—the countries in the assessment within all the continents are shown on Table 1.1.

An overview of technically recoverable shale gas resources from the EIA/ARI assessment is shown on Table 1.2.

The study which was first released in 2011 by US EIA assessed 48 shale basins in 32 countries. However in 2013, 95 basins and 41 countries were assessed. In 2014, countries like Chad, Kazakhstan, Oman and United Arab were added (see Fig. 1.4).

The study estimated technically recoverable resources and did not consider whether these resources were commercially viable. Two groups of countries were noted where shale gas development might be attractive. The first group included countries like France, Poland, Turkey, Ukraine, South Africa, Morocco and Chile. This group depends on natural gas imports and has at least substantial shale gas resource relative to their current consumption (Sakmar 2014). Countries like USA, Canada, Mexico, China, Australia, Libya, Algeria, Argentina and Brazil belong to

Table 1.1 Countries with shale gas resources (EIA 2013)

Continent	Countries
Africa	South Africa, Algeria, Morocco, Tunisia, Libya, Egypt
Americas	Argentina, Canada, Mexico, USA[a], Brazil, Bolivia, Chile, Paraguay, Uruguay, Venezuela
Australia	Australia
Asia	China, Mongolia, Thailand, Jordan, Turkey, Saudi Arabia, India, Indonesia, Pakistan
Europe	Austria, Bulgaria, Spain, Denmark, France, Germany, Hungary, Ireland, Kaliningrad, Russia, Poland, Lithuania, Romania, Sweden, Ukraine and UK

[a]Assessment was not conducted for the USA but has been included here for completeness

Table 1.2 Technically recoverable shale gas resources (EIA 2013)

USA	1161
China	1115
Argentina	802
Algeria	707
Canada	573
Mexico	545
Australia	437
South Africa	390
Russia	285

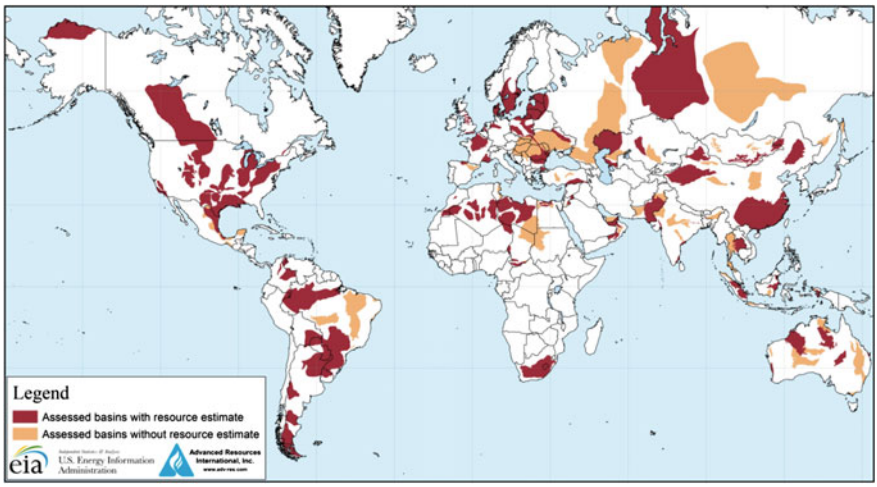

Fig. 1.4 Worldwide shale gas resources (EIA 2013)

the second group where their shale gas estimates are considered large and these countries have significant natural gas production infrastructure.

1.4 Potential of the UK Shale Gas

The BGS/DECC report in 2013 estimated shale gas in place values for the most prospective formation in the UK, i.e. the carboniferous Bowland Shale Gas Formation (Table 1.3 and Fig. 1.5). The formation is divided into upper and lower units—the upper unit of the Bowland Shale Formation is more prospective with more well control where prospective productive zones are up to 500 ft thick having a close resemblance to the Barnett shale in North America (Andrews 2013). The lower unit, however, is largely undrilled but has been penetrated and it has been estimated to contain up to 10,000 ft of organic shale intervals (Andrews 2013).

The UK-produced shale gas would offer better security of supply than relying on imports as it will help to insulate the UK from volatile changes of world demand, regional instability and politically motivated interruptions of gas supply (House of Lords 2014).

Table 1.3 Total gas in place for the Bowland Shale Formation (Andrews 2013)

	P90 (TCF)	P50 (TCF)	P10 (TCF)
Upper unit of Bowland Shale Formation	164	264	447
Lower unit of Bowland Shale Formation	658	1065	1834

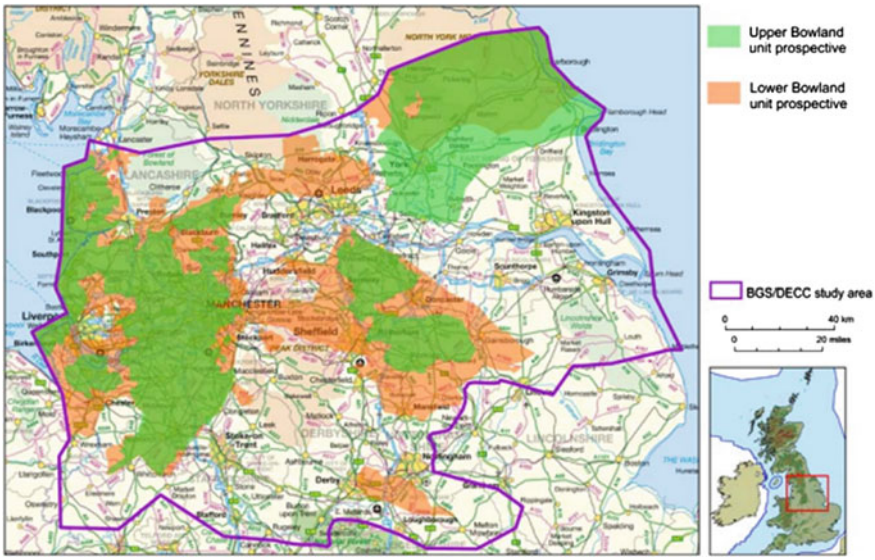

Fig. 1.5 Upper and lower Bowland units in the UK (Andrews 2013)

Nevertheless, the effect of shale gas production in the UK is less certain because the scale of economically recoverable gas reserves is not yet known. As a result, significant outputs of shale gas are not expected before the early 2020s (House of Lords 2014).

Uncertainty is large regarding shale gas resources in the UK/EU, and only around 50 exploration wells have been drilled in Europe (Spencer et al. 2014). Shale gas development in the UK is still at an early stage hence there is insufficient exploration and no production data. Therefore, resource estimates are mainly from geological data obtained from cores, seismic analysis and well log data from existing conventional onshore oil and gas fields (Spencer et al. 2014). Compared to the USA, onshore oil and gas production is less, hence geological data are scarcer. In the absence of sufficient data from shale gas plays in Europe, there is considerable uncertainty on the amount of shale that can be technically and economically recovered. There are several other subsurface and surface factors that can affect the prospect of shale gas production in the UK.

Subsurface geological factors can be assessed to get an initial evaluation of resource estimates—similar to the carboniferous Bowland–Hodder shale study carried out by (Andrews 2013). Some of the geological/geochemical factors include depth, formation extent, thickness, thermal maturity, organic content, mineralogy (shale's with high proportion of clays fracture inefficiently), pressure and porosity. These factors are hard to correlate in geological formations in Europe, but there are several generalizations; European shales are usually smaller, deeper, highly pressurised and higher in clay content suggesting that drilling techniques in the USA cannot be simply transposed to European shale gas development (Spencer et al. 2014).

Shale gas production requires intensive operation from the service industry with a large amount of drilling required to achieve and maintain significant production (Spencer et al. 2014). In the USA between 2005 and 2012, an average 1087 natural gas drilling rigs were in operation (Spencer et al. 2014). This is in contrast to Europe with a natural gas rig count of 32 as of December 2013, and only a small percentage of these rigs would have the capability to drill horizontal wells and frack (Spencer et al. 2014).

To produce around 30 bcm of shale gas per year, 700–1000 wells per year would be needed over several decades ~20–30 years (Gény 2010). Assuming 6 wells per year per rig, then approximately 110–170 active rigs with fracking and horizontal drilling capabilities would be needed (Gény 2010).

Forecasts of breakeven cost for European shale gas are much higher than those in the USA and Australia perhaps because European shale gas development is still at an appraisal/exploratory stage (Centrica Energy 2010).

Although shale gas development in the UK is still at an exploratory phase, the UK Government is keen on tapping this energy resource to improve energy security, create jobs (~77,000 jobs are estimated) and reduce dependency on coal. The Institute of Directors (IoD) estimates that 74,000 jobs could be supported through the development of shale in the UK (House of Lords 2014). This is to be carried out by encouraging safe and environmentally sound exploration to determine its potential (BEIS 2015). The need for energy affects every area of our lives. Over a third of the UK energy came from natural gas and another third from oil with coal (13%), nuclear (7%) and renewables (mostly biomass and wind at 10%) contributing to the rest (BEIS 2015). Only two-fifths of this natural gas came from the North Sea and the Irish Sea with the rest being imported from Belgium, Norway and the Netherlands via pipelines and also shipped from Qatar, Algeria and Trinidad and Tobago and Nigeria as Liquefied Natural Gas (BEIS 2015). Gas was also used to generate nearly a third of the UK electricity in 2014—the UK Government predicts by 2030 nearly three quarters of the UK gas will be imported (BEIS 2015).

References

Andrews IJ (2013) The carboniferous Bowland Shale gas study: geology and resource estimation. British Geological Survey for Department of Energy and Climate Change, London, UK

Arogundade O, Sohrabi M (2012) A review of recent developments and challenges in shale gas recovery. In: SPE Saudi Arabia Section Technical Symposium and Exhibition, pp 1–31. https://doi.org/10.2118/160869-MS

BEIS (2015) Developing shale oil and gas in the UK [WWW Document]. Department of Business, Energy & Industrial Strategy.GOV.UK. URL https://www.gov.uk/government/publications/about-shale-gas-and-hydraulic-fracturing-fracking/developing-shale-oil-and-gas-in-the-uk. Accessed 30 Oct 2017

Centrica Energy (2010) Unconventional gas in Europe response to DECC consultation. Report number: DECC_Gas_195, Available at: https://ukccsrc.ac.uk/system/files/publications/ccs-reports/DECC_Gas_195.pdf

Chan PB, Etherington JR, Aguilera R (2010) A process to evaluate unconventional resources. In: SPE Annual Technical Conference and Exhibition. Society of Petroleum Engineers. pp 19–22. https://doi.org/10.2118/134602-MS

Chopra S, Sharma RK, Keay J, Marfurt KJ (2012) Shale gas reservoir characterization workflows. In: SEG Technical Program Expanded Abstracts 2012. Society of Exploration. 99:1–5. https://doi.org/10.1190/segam2012-1344.1

Cipolla C, Lolon E, Erdle J, Rubin B (2010) Reservoir modeling in shale-gas reservoirs. SPE Reserv Eval Eng 13:23–25. https://doi.org/10.2118/125530-PA

EIA (2013) Technically recoverable shale oil and shale gas resources: an assessment of 137 shale formations in 41 countries outside the United States. U.S. Energy Information Administration, 76 pp. URL www.eia.gov/analysis/studies/worldshalegas/

Gény F (2010) Can unconventional gas be a game changer in European Gas Markets? The Oxford Institute For Energy Studies, UK

Green C (2011) Background Note on Shale gas. A factsheet prepared for DECC about the induced seismicity during hydraulic fracturing at the Preese Hall site. Lancashire, NW England

Haskett WJ, Brown PJ (2005) Evaluation of Unconventional Resource Plays. Society of Petroleum Engineers. doi:10.2118/96879-MS

Holden T, Pendrel J, Jenson F, Mesdag P (2015) GEO ExPro—a workflow for success in shales [WWW Document]. URL https://www.geoexpro.com/articles/2013/09/a-workflow-for-success-in-shales. Accessed 30 Oct 2017

House of Lords (2014) The economic impact on UK energy policy of shale gas and oil. 3rd Report of Session 2013–2014. London: Economics Affairs Committee. Available at: https://publications.parliament.uk/pa/ld201314/ldselect/ldeconaf/172/172.pdf

Javadpour F, Fisher D, Unsworth M (2007) Nanoscale gas flow in shale gas sediments. J Can Pet Technol 46:55–61. https://doi.org/10.2118/07-10-06

Kundert DP, Mullen MJ (2009) Proper evaluation of shale gas reservoirs leads to a more effective hydraulic-fracture stimulation. In: SPE Rocky Mountain Petroleum Technology Conference. https://doi.org/10.2118/123586-MS

Mallick M, Achalpurkar M (2014) Factors controlling shale gas production: geological perspective factors controlling shale-gas value. In: Abu Dhabi International Petroleum Exhibition and Conference, pp 10–13. https://doi.org/10.2118/171823-MS

Naik GC (2003) Tight gas reservoirs–an unconventional natural energy source for the future. Accessado em, 1(07):2008

Sakmar S (2014) The future of global shale gas development: will industry earn the social license to operate? In: 21st World Petroleum Congress. World Petroleum Congress.

Selley RC (1987) British shale gas potential scrutinized. Oil Gas J 85(24):62–64

Selley RC (2012) UK shale gas: the story so far. Mar Pet Geol 31:100–109. https://doi.org/10.1016/j.marpetgeo.2011.08.017

Energy Institute (2015) A guide to shale gas. London: Energy Inst. Available at: https://knowledge.energyinst.org/__data/assets/pdf_file/0020/124544/Energy-Essentials-Shale-Gas-Guide.pdf.

Speight JG (2013) Shale gas production processes. Gulf Professional Publishing, Houston

Spencer T, Sartor O, Iddri MM (2014) Unconventional wisdom: an economic analysis of US shale gas and implications for the EU. IDDRI Policy Br 5:1–4

Stevens P (2013) Shale gas in the United Kingdom. Chatham House: London, UK

Sun H, Chawathe A, Hoteit H, Shi X, Li L (2014) Understanding shale gas flow behavior using numerical simulation. SPE 20:1–13. https://doi.org/10.2118/167753-PA

Swami V, Clarkson CR, Settari A (2012) Non-darcy flow in shale nanopores: do we have a final answer? SPE Can Unconv Resour Conf 1–17. https://doi.org/10.2118/162665-MS

The Royal Society (2012) Shale gas extraction in the UK: a review of hydraulic fracturing. Royal Academy of Engineering. https://doi.org/10.1016/j.petrol.2013.04.023

Wilkinson G (2014) Hydraulic fracturing [WWW Document]. Intermountain Oil and Gas BMP Project. URL http://www.oilandgasbmps.org/resources/fracing.php

Williams-Kovacs J (2012) New methods for shale gas prospect analysis. ProQuest Dissertations & Theses 287

Chapter 2
Inherent Defying Features in Shale Gas Modelling

Abstract Accurate simulation and modelling of shale gas reservoirs are deemed crucial for efficient exploitation of these resources. Obtaining realistic results for resource estimation and performance predictions has a significant impact on the economics of the operating companies and all interested parties. Integrating all the unique characteristics of shale gas reservoirs within a single reservoir simulator for accurate predictions of future performance has become an increasingly intricate task. For many years now, various researchers have tried to tackle some of these challenges which include, but not limited to, how the natural fractures are simplified and represented in a simulator, the transport of gas within the matrix and fractures, adsorption and desorption phenomena within the shale gas system and also how the fractures are propagated within the shale formation upon hydraulic fracturing. This chapter provides an overview of the advances made in shale gas modelling and highlights the improved understanding conveyed by various researchers on the main defining characteristics of shale and the way these features of shale are modelled in numerical reservoir simulators.

2.1 Incorporation of Natural Fractures in Shale Gas Models

Natural fractures play an important role in the production of natural gas from shale gas reservoirs. Where these fractures are present, there must be an extensive network of the fractures intersecting to be able to contribute towards production of the natural gas. For instance, according to Walton and Mclennan (2013), the Devonian shale of the Appalachian basin is considered to be highly fractured with a fracture spacing of order 1–10 cm, whereas that of the Atrium shale of Michigan basin is more intensely fractured with fracture spacing of 1–2 ft.

Walton and Mclennan (2013) raised the question of whether these natural fractures, if present, is, in fact, open and if so, how they are maintained open against closure stress. According to the authors, if these natural fractures behave just like coal cleats, are they initially filled with water? And how much of this water

J. Gholinezhad et al., *Challenges in Modelling and Simulation of Shale Gas Reservoirs*, SpringerBriefs in Petroleum Geoscience & Engineering,
https://doi.org/10.1007/978-3-319-70769-3_2

production is actually observed? An assumption that they believed is commonly made is to assume that the fractures are open and gas filled.

The contribution of open natural fractures to economic gas production is perceived to be because of their large surface area. However, Walton and Mclennan (2013) argued in their paper that the contribution of this large surface area to gas production is possible only for the ultra-low-permeability shallow gas shales, whereas a much smaller surface area would be required for the deeper gas shales such as Barnett. The Barnett shale, in particular, is believed to have less natural fractures as it is often argued that the abundance of open natural fractures would have resulted in the expulsion and migration of the gas out of the shale into overlying rocks. Other arguments seek to suggest that the prolific abundance of natural gas within the Barnett shale could only be as a result of the presence of open natural fractures.

The storage capacity of the matrix is much higher than that of the fractures, and in many of the shale gas reservoirs, the fractures tend not to hold any gas at all. Bai et al. (1993) argued that the storage capacity of a fractured system should not always be considered negligible compared to the storage of the matrix. This is because, in most reservoirs that experience a high degree of production initially, most of the gas must have been stored in the fractures and hence there is always a drastic decline after a short period of time.

The open fractures may, however, be filled by fracturing fluid used in the hydraulic fracturing process. The permeability of the matrix is lower relative to that of the fractures.

There are basically two methods used in characterising fractured reservoirs. These are dual porosity/dual permeability models and discrete fracture network models.

2.1.1 Dual Porosity/Dual Permeability Model

Naturally fractured reservoirs are characterised by the presence of two distinct porous media, the matrix and fractures. Naturally fractured reservoirs have been referred to as dual porosity system as a result of the two porous media which are present (Barenblatt et al. 1960). The matrix feeds fluid locally to the fractures, and the fractures form a continuous system connected to the well.

Under the dual porosity model which was further modified by Warren and Root (1963), the matrix does not contribute directly to the wellbore. The system was seen as an orthogonal set of intersecting fractures and sugar cubic matrix block (Fig. 2.1), and by using differential equations, analytical solutions were obtained for well test analysis.

Warren and Root (1963) assumed flow from the matrix to the fracture occurs under a transfer function with Darcy characteristics and also flow occurs under pseudo-steady state conditions in the matrix blocks with a single value assigned to the pressure in the blocks. The pressure differential between the matrix and the

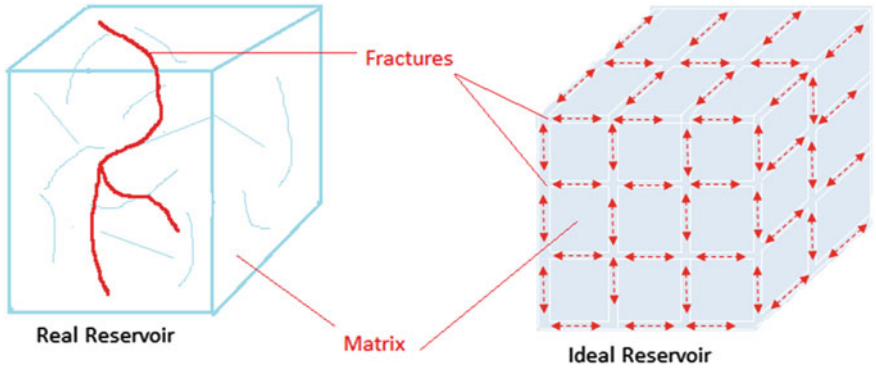

Fig. 2.1 Sugar cube model by Warren and Root

fractures, therefore, determines the mass transfer rate of the fluid. Thus, the inter-porosity flow has been described by two main mechanisms which are the pseudo-steady state and the transient flow. Warren and Root (1963) predicted that on a semi-log plot of the test data, two parallel straight lines will develop. The slope of the parallel lines represented the flow capacities of the formation, whereas the vertical separation of the lines represented the storage capacity of the fractures. This is shown in Fig. 2.2.

Odeh (1965) developed a simplified model with mathematical equations that described the unsteady state behaviour of fractured reservoirs. He concluded from his studies that there was no difference between fractured reservoir and

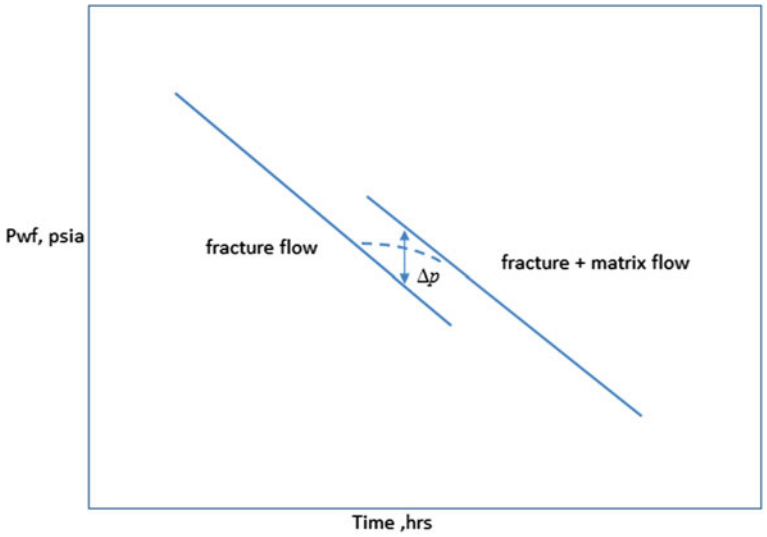

Fig. 2.2 Pseudo-steady state matrix flow pressure build-up curve (Warren and Root 1963)

homogeneous reservoir on the basis of drawdown and build-up curves using field measured data. This according to Kazemi (1969), contradicted the results of Warren and Root (1963) but with smaller block dimensions and a higher permeability, their results remain valid. Odeh (1965) used a similar model as Warren and Root (1963) although his results did not show the two parallel straight lines as depicted in Fig. 2.2.

The dual porosity model by Warren and Root (1963) was extended to include transient flow in the matrix block by Kazemi (1969). The main distinction for Kazemi (1969) was the use of transient flow within the matrix instead of assuming a pseudo-steady state as was done by Warren and Root (1963). Kazemi (1969) also used the slap model (sheets of parallel fracture sets) (Fig. 2.3) to describe the reservoir. By considering a direct flow to the well, he found that similar results to Warren and Root (1963) were obtainable without affecting the results in any sensible way, except for a smooth transitional zone which occurs due to the non-permanent flow regime of the fluid flow from the matrix to the fractures. Thus, deviations will occur in the transitional period when the rock matrix is described by a pseudo-steady state regime.

de Swaan (1976) expanded on the dual porosity model by using transient flow as the basis of flow from the matrix to the fractures. He defined his transient model by intrinsic properties of the matrix and the fractures as opposed to the bulk properties of the matrix and fractures used by both Warren and Root (1963) and Kazemi (1969). Both slab matrix shape model and a spherical matrix block solution were also presented in the same study.

Serra et al. (1983) also used the transient model to describe the fluid flow from the matrix to the fractures and based his model on intrinsic properties rather than bulk properties. Serra et al. (1983) model was very similar to de Swaan (1976) except for the use of different storativity ratio and inter-porosity coefficient.

Najurieta (1980) showed in a simplified description the pressure behaviour of naturally fractured reservoir based on appropriate solutions of the de Swaan

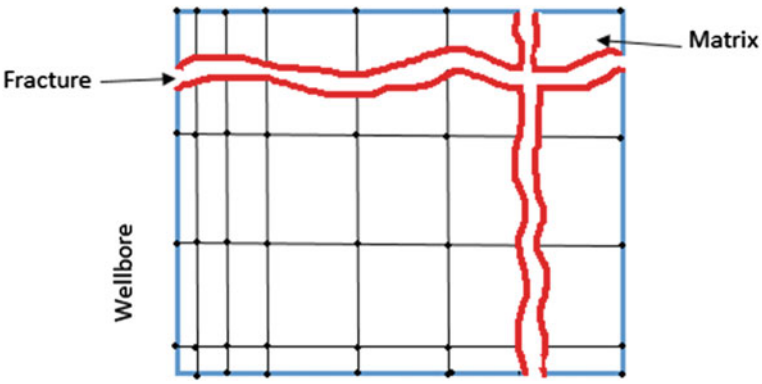

Fig. 2.3 Dual porosity idealisation by Kazemi (1969)

differential equation. In his study, he deduced equations that properly described the transitional period taking into account the unsteady state behaviour of the matrix. He also showed that the behaviour of a uniformly fractured reservoir can be fully described by four parameters each of which is a function of two or more of the five basic reservoir parameters (fracture and matrix porosity, fracture and matrix permeability and fracture spacing).

2.1.2 Discrete Fracture Network

DFN relies more on the spatial mapping of the fractures to construct an interconnected network of the fractures. It is seen as a more recent development.

According to Dershowitz et al. (2004), DFN may be defined as an analysis and modelling which explicitly incorporates the geometry and properties of the discrete features as a central component controlling flow and transport. The equation of flow is solved on each individual fracture network (McClure and Horne 2013).

One distinction between DFN and continuum model is that continuum model averages fracture properties into effective properties over volumetric grid blocks.

McClure and Horne (2013) discussed the benefit of using DFN in describing the complex nature of the fracture networks in low-permeability medium. With low-permeability rocks, individual fractures in close proximity with no intersection are mostly not well connected. Due to this, fluid flow between the locations will depend on the nature of the fracture network geometry. Sometimes more distant fractures provide a better connectivity than closer fractures (McCabe et al. 1983; McClure and Horne 2013).

Also, another useful benefit of using DFN is that stresses in the rock can be handled more accurately. According to McClure and Horne (2013), stresses caused by fracture opening or sliding are very heterogeneous spatially and its effect on neighbouring fractures is dependent on their relative orientation and location. There are two main types of DFN used: deterministic model and stochastic model.

The deterministic model defines explicitly the location, orientation and dimensions of the individual fracture which is then included in the model. The challenge with this modelling is the fact that for a complex system of fractures, it will be impossible to define accurately the location and properties explicitly of each of the fractures within the reservoir.

Stochastic models analyse certain properties of the fracture such as fracture height, length, aperture, orientation and spacing together with some statistical scaling rule that defines the fracture architecture. A statistical approach is adopted where the properties of the fracture system are generated randomly. To have an accurate representation of the flow system, many realisations of the fracture network flow system will have to be simulated.

According to Herbert (1996), it is not always possible in practice to simulate efficiently many realisations and often more qualitative bounds are estimated from a smaller sample of model results.

2.2 Diffusion Models in Shale

One of the key characteristics of shale gas reservoirs is the flow of gas in the pore network. The pores of shale gas reservoirs are within the ranges of 1–200 nm (Lee and Kim 2015).

Javadpour et al. (2007) conducted experiments on 152 core samples from nine shale reservoirs and reported that the average permeability of shale gas reservoirs is of the range 54 nD (5.43×10^{-20} m^2).

The flow of gas within this nano-pore is essential for gas production as well as accurate simulations of shale gas reservoirs. Due to the nano-pores of the reservoir, the apparent permeability is mostly dependent on the pore pressure, fluid type and the pore structure (Guo et al. 2015).

In conventional reservoirs flow is continuous, whereas in shale gas reservoirs gas can flow in the nano-pores in the slip flow regime, the transitional regime and the molecular regime in addition to the continuum regime (Geng et al. 2016).

Darcy's law which is used in conventional reservoirs to capture continuum flow regimes is inadequate to describe other flow regimes that occur in the nano-pores.

The nature of the nano-pores, therefore, plays a significant role in the dynamics of the fluid flow and its interactions with the surfaces of the shale. These are different from conventional reservoirs where the pore network is much bigger and flow can easily be described by Darcy's law. The application of Darcy's law in nano-pores of the shale reservoirs will only underestimate the flow rate, thus conventional Darcy's law is not applicable in shale gas reservoirs and caution must be exercised whenever it is used.

Under certain pressure and temperature conditions, the mean free path might exceed the size of the pores and this might cause the gas molecules to move singly through the pores. When this happens, the concept of continuum or bulk flow may not be applicable (Lee and Kim 2015).

The gas diffusing through a porous media may involve collisions between the gas molecules as well as collisions between the gas molecules and the walls of the porous media.

The flow of fluid within any porous medium can be distinguished using the Knudsen number. The Knudsen number is the ratio of the gas mean free path to the diameter of the pore size.

$$K_n = \frac{\lambda}{d_p} \tag{2.1}$$

where d_p is the diameter of the pores and λ is the gas mean free path. A K_n greater than 10 implies collision between gas molecules and the walls of the porous media. Knudsen diffusion is dominant in such case with negligible molecular diffusion and viscous diffusion. If K_n is much smaller than 0.1, collisions and interaction of the gas molecules become dominant and Knudsen diffusion becomes negligible compared with molecular and viscous diffusion.

Table 2.1 Flow regimes with corresponding Knudsen number

Knudsen number	Flow regime
(a) 0–10^{-3}	Continuum/Darcy flow (no-slip flow)
(b) 10^{-3}–10^{-1}	Slip flow
(c) 10^{-1}–10^{1}	Transition flow
(d) 10^{1}–∞	Free molecule flow

Rathakrishnan (2013) presented a table of different flow regimes corresponding to Knudsen numbers (see Table 2.1).

For Knudsen number between 0 and 10^{-3}, the continuum assumptions are valid and flow can be described by the Navier–Stokes (N–S) equations with no-slip boundary conditions. However, for Knudsen number between 10^{-3} and 10^{-1}, the flow can be described as slip flow and N–S equations become invalid. For Knudsen number between 10^{-1} and 10^{1}, flow is said to be in the transitional region between slip and free molecule flow and finally with Knudsen number greater than 10, the free molecular regime is encountered with collisions between the gas molecules and the walls of the media dominating (see Fig. 2.4).

Collisions of the gas molecules with the walls of the porous media are predominant especially for shale gas reservoirs due to the nano-pores which also makes permeability measurement a challenge. There are, however, negligible collisions between the gas molecules themselves compared with the collisions with the wall surfaces of the media. For typical shale gas reservoirs, the Knudsen number ranges from 2×10^{-4} to 6.0. As shown in Fig. 2.5, the slip flow occurs for most pore sizes at the initial reservoir pressure. With the pore pressure decreasing, the transition flow generally becomes dominant.

In such cases, the use of N–S equations is no longer valid. These equations are derived from the basic principles of conservation of mass, conservation of energy and conservation of momentum. It is based on the assumption that the fluid is a continuum, that is, it is not made up of discrete particles but rather a continuous substance.

According to Gad-el-hak (1999), the N–S model ignores the molecular nature of gases and liquids and regards the fluid as a continuous medium describable in terms of the spatial and temporal variations of density, velocity, pressure, temperature and other macroscopic flow quantities. The assumption of N–S can only be valid when the three fundamental assumptions of Newtonian framework (fluid with Newtonian viscosity), continuum approximation (mean free path much less than flow conduit dimensions) and thermodynamic equilibrium are satisfied (Gad-el-hak 1999; Moghaddam and Jamiolahmady 2016).

N–S equation has been modified by various other researchers to account for slip boundary condition. Other models have been developed to address the flow of fluid in a media at the molecular level when the N–S equations become invalid. These models are, however, excessively time-consuming and unrealistic to simulate gas flow. They include molecular dynamic (MD), direct simulation Monte Carlo (DSMC) or solution of linearised Boltzmann equation (LBE).

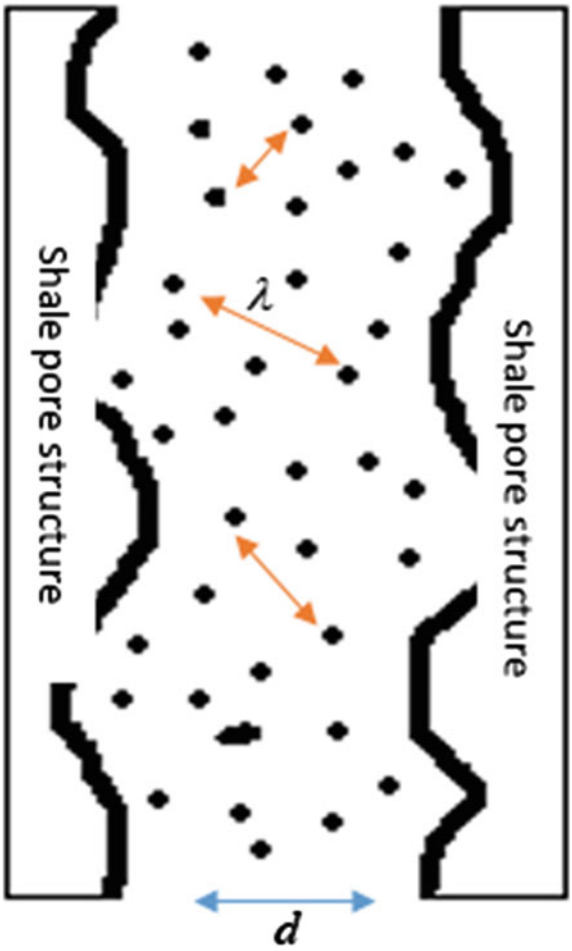

Fig. 2.4 Flow within a shale pore structure with gas molecules collisions

There have been a number of methods which accounts for slip boundary condition such as the Maxwell slip and second-order slip. Maxwell slip condition is a first-order approximation from the kinetic theory of gases and its being widely applied to predict the mass flow in micro- and nano-channels.

For a complete description of the flow in tight media, the model developed should be able to account for Knudsen diffusion as well as slip flow and the processes of adsorption and desorption. Thus, gas flow through shale nano-pores has been described by several models that account for Knudsen diffusion, slip flow and desorption.

Klinkenberg (1941) conducted experiments to explain the phenomenon of gas transport through porous media. He concluded that gas permeability is a function of mean pressure and gas composition and that the equivalent liquid permeability is independent of both mean pressure and gas composition. He showed that a linear

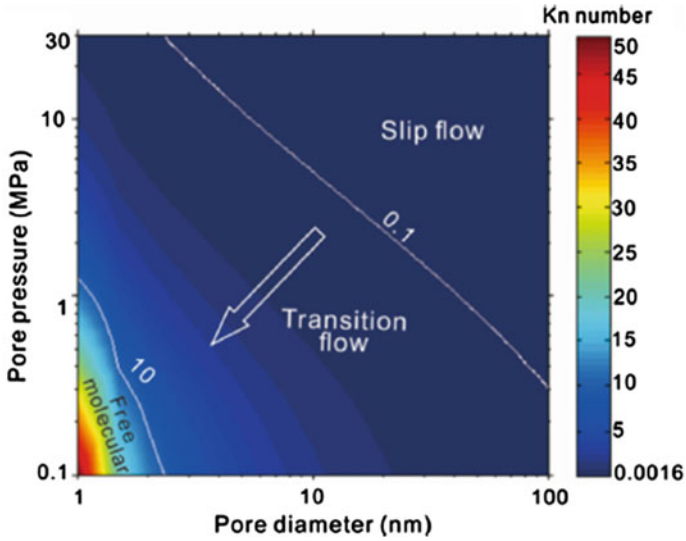

Fig. 2.5 Contour plot of the Knudsen number versus pore pressure size (Geng et al. 2016). Slip flow occurring at initial reservoir pressure

relationship exists between the Darcy permeability and the reciprocal of the mean pressure of the system.

$$k(p_{\text{avg}}) = k_{\text{D}}\left(1 + \frac{b}{p_{\text{avg}}}\right) \tag{2.2}$$

where $k(p_{\text{avg}})$ is the gas permeability at mean pressure p_{avg}, k_{D} the Darcy permeability or liquid permeability and b the Klinkenberg parameter. Conventional gas reservoirs have been modelled with the Klinkenberg effect, and recent use has been made for tight gas reservoirs with pores of 1–10 μm in size. Thus, slippage effect of the gas molecules can be accounted for when using Klinkenberg's model.

Javadpour (2009) developed a new model that accounted for a no-slip boundary and Knudsen diffusion using Maxwell theory. The new model presents an equation that is derived from the theoretical basis as in molecular dynamics but written in a format compatible with the Darcy equation. According to Javadpour (2009), this can be easily incorporated into commercial reservoir simulators to study gas production from mud rock systems. Javadpour (2009) model converges to the Knudsen diffusion model when the average pore size decreases and when the sizes increases, it converges to the continuum model.

$$k_{\text{app}} = \frac{2r\mu}{3 \times 10^3 p_{\text{avg}}}\left(\frac{8\text{RT}}{\pi M}\right)^{0.5} + \frac{r^2}{8}\left\{1 + \left(\frac{8\pi\text{RT}}{M}\right)^{0.5}\left(\frac{2}{\alpha} - 1\right)\frac{\mu}{rp_{\text{avg}}}\right\} \tag{2.3}$$

k_{app} is the apparent permeability for a porous medium in a straight cylindrical nanotube. The apparent permeability relationship with Klinkenberg can be written in the form

$K_{app} = k_D\left(1 + \frac{b}{p_{avg}}\right)$, where b is given as

$$b = \frac{16\mu}{3 \times 10^3 r}\left(\frac{8RT}{\pi M}\right)^{0.5} + \left(\frac{8\pi RT}{M}\right)^{0.5}\left(\frac{2}{\alpha} - 1\right)\frac{\mu}{r}, \tag{2.4}$$

This model is simple as it assumed an ideal gas and no desorption.

Azom and Javadpour (2012) corrected the above equation to account for real gas flowing in a porous medium. The final modified equation remained the same as above with b given as

$$b = \frac{16\mu c_g p_{avg}}{3 \times 10^3 r}\left(\frac{8ZRT}{\pi M}\right)^{0.5} + \left(\frac{8\pi RT}{M}\right)^{0.5}\left(\frac{2}{\alpha} - 1\right)\frac{\mu}{r} \tag{2.5}$$

to account for the gas compressibility factor. As the gas becomes ideal, Eq. (2.2) changes to Eq. (2.1) since the gas compressibility $c_g = \frac{1}{p_{avg}}$ and $Z = 1$.

Civan (2010) developed a model under slip flow assumptions represented by second-order slip approximations. This was based on Beskok and Karniadakis (1999) model of rarefied gas flow in a micro-channel, ducts and pipes. The model assumes that permeability is a function of the intrinsic permeability, the Knudsen number, the rarefication coefficient and the slip coefficient. Thus,

$$k = k_D(1 + \alpha_r k_n)\left(1 + \frac{4k_n}{1 - bk_n}\right) \tag{2.6}$$

with rarefication coefficient given as:

$$\alpha_r = \alpha_0\left(\frac{K_n^B}{A + K_n^B}\right) \tag{2.7}$$

The drawbacks of this model are the use of several empirical parameters which require performing several experiments.

Darabi et al. (2012) formulated a pressure-dependent permeability function known as apparent permeability function (APF). The APF model describes gas flow in ultra-tight natural porous media characterised by a network of interconnected tortuous micro-pores and nano-pores. Darabi et al. (2012) adapted the model developed by Javadpour (2009) to include surface roughness as well as Knudsen diffusion and slip flow (Maxwell theory). The APF in porous media is given as:

$$k_{\text{app}} = \frac{\mu M}{\text{RT}\rho_{\text{avg}}} \frac{\phi}{\tau} (\delta')^{D_f - 2} D_{\text{k}} + k_{\text{D}} \left(1 + \frac{b}{p}\right) \tag{2.8}$$

D_{k} is the Knudsen diffusion coefficient and δ' is the ratio of normalised molecular size (d_{m}) to local average pore diameter (d_{p}), $\delta' = d_{\text{m}}/d_{\text{p}}$. R_{avg} is the average pore radius, approximated by $R_{\text{avg}} = (8k_D)^{0.5}$.

Singh and Javadpour (2016) proposed a different approach to modelling apparent permeability in shale gas reservoirs. This approach deviated from the empirical approach used by earlier researchers. The term non-empirical apparent permeability (NAP) is used to describe this model which is an analytical equation that depends on the pore size, pore geometry, temperature, gas properties and average reservoir pressure. The NAP model was derived without the assumption of slip flow at the pore walls. The proposed model also showed that the pore surface roughness and mineralogy have negligible influence on gas flow rate under a complete range of reservoir operating conditions. Singh and Javadpour (2016) model accounts for both Knudsen diffusion and sorption in a porous medium but ignores slip flow.

Singh and Javadpour (2015) extended the analytical model for apparent permeability determination in shale gas reservoirs by developing a new permeability model that goes away with the shortcomings of Maxwell slip condition, uses readily available Langmuir sorption data to determine the slip coefficient for gas flow and also includes a higher-order slip effect on gas flow. This model is referred to as the Langmuir slip permeability (LSP). The LSP is based on the Langmuir slip condition of Myong (2003) which considers the gas surface molecular interactions.

Geng et al. (2016) developed a new model for gas flow based on the extended Navier–Stokes equations without adsorption and desorption. The model takes into account all the possible flow regimes including continuum regime, slip flow regime, the transitional regime and molecular regime. However, without incorporating the adsorption or desorption component, this model falls short in capturing the real phenomena of the flow process in the nano-pores.

A finite difference method called finite difference geometrical pore approximation (FDGPA) was introduced by Shabro et al. (2012) to simulate pore scale fluid flow in a porous media. In this model, geometrical parameters are defined in interstitial space domain to characterise pore scale images. This method is relatively six times faster on average than the Lattice Boltzmann method (LBM) which requires significant computational effort.

Comparison of different models describing fluid flow in porous media together with the pros and cons has been summarised by Singh and Javadpour (2015) in Fig. 2.6 and Table 2.2.

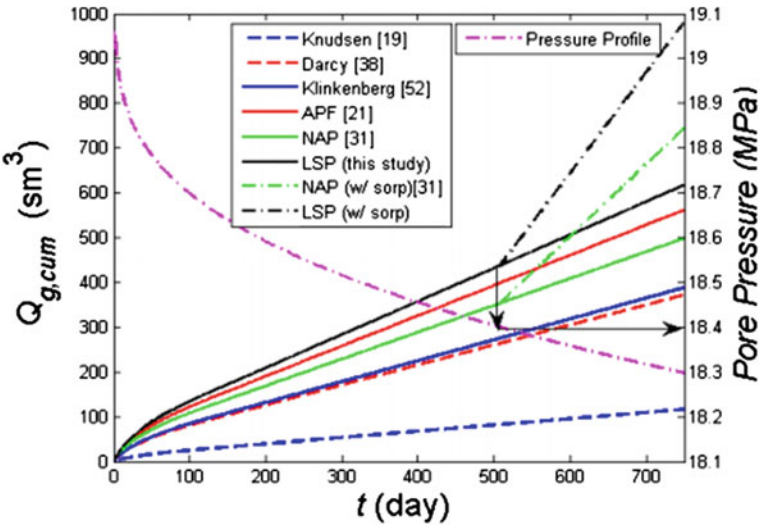

Fig. 2.6 Comparison of different models to predict cumulative gas production (Singh and Javadpour 2015)

2.3 Modelling of Fracture Propagation

In shale gas reservoirs, low permeability of shale implies very little or no recovery of gas through conventional drilling. Thus, to initiate flow to the wellbore, complex network of fractures are required to allow the gas to flow through them and into the well for production. Hydraulic fracturing is the key in creating these fractures that allow for an increase in the permeability to assist in fluid flow.

There is, therefore, the need to understand how these fractures will propagate through the formation. Various analytical and numerical techniques have been developed to model fracture propagation in shale gas reservoirs. These models are sometimes incorporated into reservoir simulators to assist in predicting shale gas performance.

Modelling of hydraulic fractures requires the application of three fundamental equations which are the continuity equation, momentum or fracture fluid flow and the linear elastic fracture mechanics (LEFM).

Both the continuity equations together with the fluid flow are coupled using a relation between the fracture width and fluid pressure, whereas the resulting deformation is modelled through LEFM.

2D modelling techniques were first to be used in modelling the fracture propagation; however, these models require the use of several assumptions that limit their use. The development of planar 3D and pseudo-3D models has helped to bridge this limitation while allowing for easier computational analysis.

All of these models require the understanding of the fracture geometry which includes the height of the fracture, its length and also the width. Commonly used

Table 2.2 Summary of models for diffusion in shale gas (Singh and Javadpour 2015)

Model	Description	Pros	Cons
Javadpour (2009)	Model developed using slip assumption, represented by Maxwell theory. Accounts for Knudsen diffusion. Modelled only for straight capillary tubes	Simple	Limited to straight tubes ideal gas. Ignores desorption
Civan (2010)	Model developed using slip flow assumption, represented by simplified second-order slip model. Contains several empirical parameters	Higher-order slip flow	Several empirical parameters
Darabi et al. (2012)	Model developed using slip flow assumption. Represented by Maxwell theory. Accounts for surface roughness and Knudsen diffusion in a porous medium	Includes tortuosity and pore surface roughness	Needs TMAC values. Ideal gas ignores desorption
Akkutlu and Fathi (2011)	Model includes dual porosity continua of matrix/fracture system where the matrix is composed of both organic and inorganic pores. Accounts for surface diffusion in a porous medium	Dual porosity system	Complex numerical model
Shabro et al. (2012)	A finite difference-based numerical model and geometrical parameters are used to reconstruct the porous structure of shale, which is then used for pore scale characterisation. Permeability equation is borrowed from Javadpour 1	Spatial characterisation and geometry of porous media included	Complex numerical model. Ideal gas ignores desorption. Needs TMAC values
Sakhaee-pour and Bryant (2011)	Model developed using slip flow assumptions, represented by Maxwell theory. Accounts for Knudsen diffusion	Spatial characterisation and geometry of porous media included	Needs TMAC values. Ideal gas
Mehmani et al. (2013)	Model developed by employing flow equation from Javadpour in pore network interconnected on Nano and micro length scales	Spatial characterisation and geometry of porous media included	Complex numerical model. Ideal gas. Ignores desorption. Needs TMAC values

(continued)

Table 2.2 (continued)

Model	Description	Pros	Cons
Singh and Javadpour (2016)	Model developed using Navier–Stokes equation and kinetic theory (no-slip flow assumption). Accounts for Knudsen diffusion, porous medium and sorption	Simple. No empirical coefficient	Ignores slip flow
Rezaveisi et al. (2014)	Numerical model developed to study components of produced gas with time from nanometre-sized pores. Relevant physics includes advection, slip flow and Knudsen diffusion	Distinguishes different gas types	Needs TMAC values
Kelly et al. (2015)	The porous structure of shale is reconstructed using FIB-SEM image stacks and numerical study using LBM is performed to study petro-physical properties of shale. Permeability estimation is done using pressure driven flow	Spatial characterisation and geometry of porous media included	Complex numerical model. Ignores slip, diffusion, and desorption
Chen et al. (2015)	The porous structure of shale is constructed using Markov Chain Monte Carlo (MCMC) on SEM images and its pore scale characterisation is performed. Apparent permeability includes flow from advection. Knudsen diffusion and slip. LBM is used to simulate fluid flow	Spatial characterisation and geometry of porous media included	Complex numerical model. Ignores desorption. Several empirical parameters
Naraghi and Javadpour (2015)	Model developed by stochastically characterising organic and inorganic pores. Accounts for slip flow. Knudsen diffusion, surface roughness and desorption	Distinguishes different pore systems in the organic and inorganic matter. Real gases	Needs additional information from SEM images. Needs TMAC values
Singh and Javadpour (2015)	Model developed using Langmuir slip condition and it does not carry several shortcomings associated with the use of Maxwell slip. Reliably predicts apparent permeability in shale	Simple and analytic. Gets slip coefficient from sorption data. Real gas	Ignores local heterogeneity

2D models include Perkins-Kern-Nordgren (PKN), Khristianovic-Geertsma-de Klerk (KGD) and circular fracture model.

Howard and Fast (1957) developed a mathematical model for fracture treatment which assumed the fracture width to be constant everywhere. A growing number of other 2D models have been developed since such as PKN and KGD. Usually with a 2D model, the fracture height is normally fixed and the fracture width and length will then be calculated.

Perkins and Kern (1961) developed the PKN model with modifications by (Nordgren 1972) to account for fluid loss. This model is usually used when the fracture length is greater than the fracture height or when there is a large length/height ratio. There are a number of assumptions that need to be satisfied for this model to be used successfully. These assumptions are best summarised by Nordgren (1972), Yew et al. (2015):

1. The fractures are assumed to be in a plane strain state in the vertical plane,
2. The vertical cross section is elliptical,
3. Fracture toughness has no effect on the fracture geometry since the energy needed for the fracture to propagate is less than that required for the fluid to flow along the fracture length,
4. Vertical fracture propagation in a straight line from the well,
5. Restricted vertical height,
6. Fracture is in plane strain in the vertical,
7. Isotropic, homogeneous, linear elastic rock mass.

PKN model is mostly used for long fractures with limited height and elliptical vertical cross section. The elliptical shape of the fracture propagation implies the width is not constant along the fracture height and length.

From Fig. 2.7, the maximum fracture width occurs where the fracture wing touches the wellbore and this width is a function of a distance from the wellbore.

$$x_{\mathrm{f}} = 0.68\left[\frac{GQ_o^3}{(1-v)\mu h_f^4}\right]^{1/5} t^{4/5} \tag{2.9}$$

$$w_0 = 2.5\left[\frac{(1-v)\mu Q_o^2}{Gh_f}\right]^{1/5} t^{1/5} \tag{2.10}$$

$$p_{\mathrm{w}} = \sigma_3 + 2.5\left[\frac{G^4\mu\, Q_o^2}{(1-v)^4 h_f^6}\right]^{1/5} t^{1/5} \tag{2.11}$$

where x_{f} is the fracture half length, w_0 is the maximum fracture opening, p_{w} is the wellbore pressure, G is the shear modulus, Q is the fluid injection rate, μ is the fluid viscosity and t is the time.

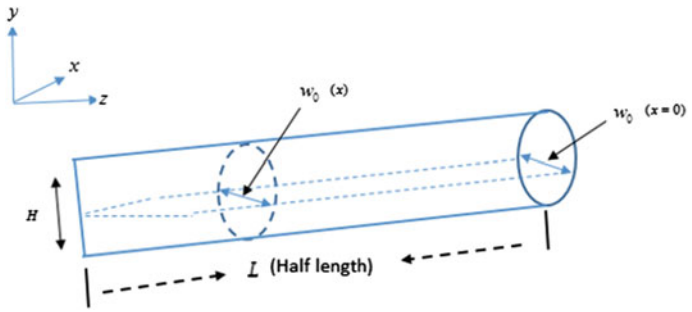

Fig. 2.7 Schematic model of PKN [modified from frackoptima.com ([1]http://www.frackoptima.com/userguide/theory/pkn.html)]

The KGD model is independent of height for width calculation and used often for very short fractures where plane strain assumptions are only applicable to horizontal sections (Adachi et al. 2007). Thus, KGD models are used when the fracture height is more than the fracture length. The geometry used in developing KGD model is illustrated in Fig. 2.8. The main assumptions under which KGD model is valid according to Geertsma and De Klerk (1969) are:

1. Vertical fracture propagating in a straight line from the well,
2. Restricted fracture height,
3. Homogeneous, isotropic, linear elastic rock mass,
4. Purely viscous fluid in laminar flow regime,
5. Rectangular vertical cross section of fracture,
6. Plane strain conditions in the horizontal plane.

Since the fracture is assumed to be at a plane strain condition in the horizontal plane, the KGD model is best suited for fractures whose length/height ratio is less or near unity (Yew et al. 2015).

$$x_{\mathrm{f}} = 0.48\left[\frac{8GQ_o^3}{(1-v)\mu h_f^4}\right]^{1/6} t^{2/3} \tag{2.12}$$

$$w_0 = 1.32\left[\frac{8(1-v)\mu Q_o^3}{G}\right]^{1/6} t^{1/3} \tag{2.13}$$

$$p_{\mathrm{w}} = \sigma_3 + 0.96\left[\frac{2G^3\mu Q_o}{(1-v)^3 x_f^2}\right]^{1/4} \tag{2.14}$$

Daneshy (1973) extended the KGD model for the case of power-law fluids or non-Newtonian fluids. He argued that the inclusion of non-Newtonian fluids allows

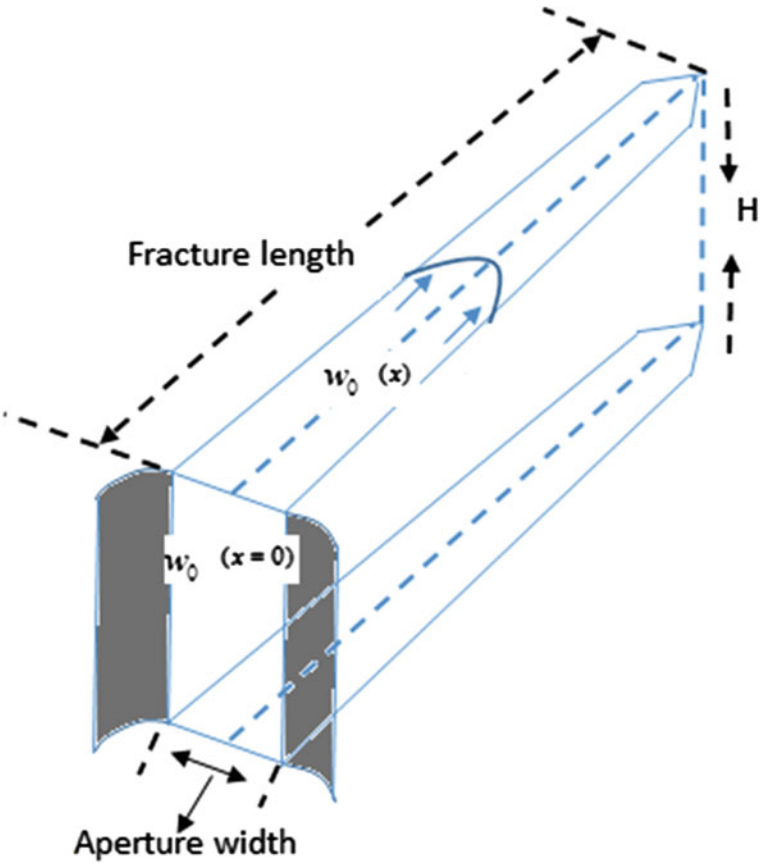

Fig. 2.8 Model geometry of KGD (modified from Weng 2015)

a more accurate consideration of most industrial fluids. By critically examining the assumptions involved in designing vertical hydraulic fractures, they found that some of these assumptions greatly affected the end results and that their presence does not necessarily affect the solution of the problem and their validity has not been tested. This was done on the basis of a new width equation and a numerical design procedure.

Settari and Cleary (1986) were the first to develop a pseudo-three-dimensional model (P3D) to describe the varying geometry of a 3D hydraulic fracture. According to Adachi et al. (2007), P3D is a crude yet effective attempt to capture the physical behaviour of planar 3D hydraulic fractures at minimal computational cost. Though this method might not be as accurate as numerical simulators, it requires less computing time and hence less expensive to develop. The P3D model does not consider the varying nature of the fracture geometry but instead modifies

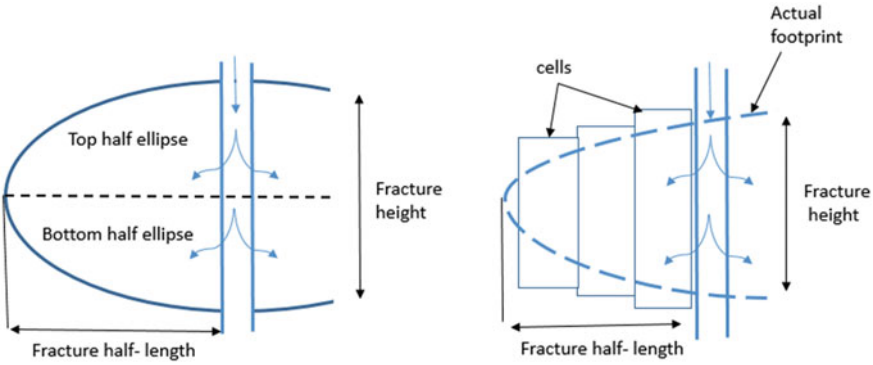

Fig. 2.9 Schematics showing fracture geometry based on 3D lumped elliptical model (**a**) and cell-based pseudo-3D geometry (**b**) (adapted from Weng 2015)

the 2D models by adding the varying height along the fracture length and its effect on the fracture width (Rahman and Rahman 2010). There are two types normally considered: lumped and cell-based (Mack and Warpinski 2000). The lumped model assumes that the vertical profile of the fracture consists of two half ellipses joined at the centre (Fig. 2.9a), whereas the cell-based models treat the fracture as a series of connected cells (Fig. 2.9b).

Though 2D models are simple, they are limited in that they require fracture height to be specified by the engineer and also by assuming that a radial fracture will develop. Another limitation is the fact that the fracture height is never the same especially from the well to fracture tip. The use of planar 3D models and pseudo-3D models has therefore been designed to address these limitations.

With respect to the planar three-dimensional models, the fracture geometry is defined by its width and the shape of its periphery which is, in turn, specified by the height at any distance from the well and length (Mack and Warpinski 2000). Planar 3D models describe the fracture propagation using either a 2D mesh of cells, either a triangular mesh or a fixed rectangular mesh. Planar 3D models have been developed also to address some of the limitations encountered when using the P3D models. An example of these limitations is that when there is an unconfined height growth, the P3D model tends to break down numerically.

2.4 Adsorption and Desorption Models in Shale

The composition of gas in shale gas reservoir is thought to be primarily made up of free gas stored within the pore network of the matrix and fractures and adsorbed gas on the surfaces of the shale matrix. The adsorbed gas is believed to be in the organic matter (kerogen).

Clarkson and Haghshenas (2013) outlined multiple mechanisms for gas storage in coals and in organic-rich shales. These are:

1. Adsorption upon internal surface area,
2. Conventional (compressed gas) storage in natural and hydraulic (induced) fractures,
3. Conventional storage in matrix porosity (organic and inorganic),
4. Solution in formation water,
5. Adsorption (solution) in organic matter.

The adsorption capacity of shale gas depends on a number of factors such as specific surface area, pressure, temperature, pore size and sorption affinity (Leahy-dios et al. 2011).

Total amount of gas in place is strongly affected by the TOC, clays and the adsorption ability of methane on the internal surface of the solid (Martin et al. 2010; Yu et al. 2014). Organic matter in shale is considered to have a strong adsorption potential due to its large surface area and its affinity to methane (Yu et al. 2014, 2015).

In shale gas reservoirs, the adsorption process is mainly considered to be a physical process such that both adsorption and desorption of gas molecules are reversible.

There are basically six different types of adsorption which the international union of pure and applied chemistry (IUPAC) has classified. Of the six categories, adsorption on shale gas reservoirs is normally classified under the Type I, also known as the Langmuir isotherm. The adsorption behaviour of the gas in shale gas reservoirs is normally described by the monolayer Langmuir isotherm. This means a single layer of molecules covering the solid surfaces.

The Langmuir isotherm assumes that the adsorbed gas behaves as an ideal gas under isothermal conditions. Hence, there is a dynamic equilibrium at constant temperature and pressure between the adsorbed and non-absorbed gas.

Freeman et al. (2012) and Chao et al. (1994) concurred that instantaneous equilibrium of the sorbing surfaces and the storage in the pore space is assumed to be established under the Langmuir isotherm.

According to Freeman et al. (2012), this means there is no transient lag between pressure drop and desorption response when considered under modelling perspective.

Chao et al. (1994) concluded that due to the very low permeability of the shale, flow through the media is extremely slow and hence the assumption of instantaneous equilibrium is justified.

Langmuir isotherm is given by the formulae:

$$V = \frac{V_L P}{P + P_L}, \tag{2.15}$$

where V the volume of adsorbed gas at pressure P, V_L is the Langmuir volume or maximum gas adsorption at infinite pressure and P_L is the Langmuir pressure

corresponding to one half of the Langmuir volume. This formula will give the volume of adsorbed gas in scf/ft^3. In order to convert the gas content from scf/ft^3 to scf/ton, the bulk density of shale is needed.

The contribution of adsorbed gas to overall gas recovery has been modelled by various researchers in an effort to ascertain the role adsorption and desorption play in the recovery process. According to Cipolla et al. (2010), the contribution from adsorbed gas made up a low percentage of the overall gas recovery due to the ultra-low permeability of the rock. He also observed that the impact of desorption decreases when the network fracture spacing is smaller using the Barnett shale play. Accroding to their study, it is expected that gas adsorption will play a small role in the well performance with the desorption mainly occuring at the later life of the well when pressures in the tight matrix have become very low. Frantz et al. (2005) also concluded that in the Barnett shale, desorption is a less important factor in evaluating the well performance.

Mengal and Wattenbarger (2011) developed a shale gas pseudo-steady state model (SGPSS) to describe the contribution of adsorption on the life of the field and the calculation of original gas in place (OGIP). They found that incorporating the adsorbed gas to the model results in a 30% increase in OGIP and a 17% decrease in recovery factor. Stimulated reservoir volume estimates were found to be 5% less when adsorbed gas is considered. Mengal and Wattenbarger (2011) also pointed out that adsorption has little contribution during early times but contributes significantly at late times and low reservoir pressures.

Stephen Brunauer, P. H. Emmet and Edward Teller developed the BET isotherm in 1938 in which they assumed that the adsorption layers on the surface of the organic carbon were infinite. Unlike the Langmuir isotherm which assumed a monolayer adsorption, BET isotherm extended Langmuir's application to include a multi-layer adsorption. See Fig. 2.10 for the difference between single-layer and multi-layer adsorption.

With several key assumptions such as homogeneous surface, no lateral interactions between molecules and saturation pressure conditions, the number of layers becomes infinite. BET isotherm is considered a better fit to describing the adsorption processes in shale gas reservoir.

BET isotherm is classified as Type 2 isotherm which occurs in a non-porous or a macro-porous material (Kuila and Prasad 2013). The general form of the BET isotherm can be given as

$$V(P) = \frac{V_{\mathrm{m}} C \frac{P}{P_O}}{1 - \frac{P}{P_O}} \left[\frac{1 - (n+1)\left(\frac{P}{P_O}\right)^n + n\left(\frac{P}{P_O}\right)^{n+1}}{1 + (C-1)\frac{P}{P_O} - C\left(\frac{P}{P_O}\right)^{n+1}} \right] \tag{2.16}$$

V_{m} is the maximum adsorption gas volume when the entire adsorbent surface is being covered with a complete monolayer, C is a constant related to the net heat of adsorption, P_O is the saturation pressure of the gas and n is the maximum number of

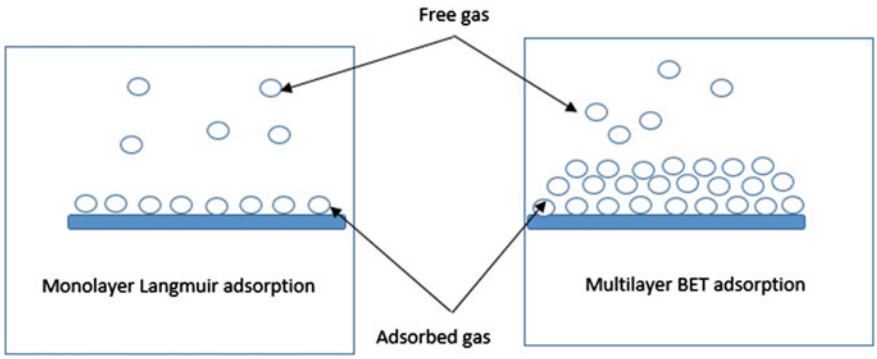

Fig. 2.10 Monolayer and multi-layer Langmuir isotherm

adsorption layers. When $n = 1$, the equation will be reduced to the Langmuir isotherm and when $n = \infty$, the equation reduces to

$$V_{\mathrm{L}} = \frac{V_{\mathrm{m}} CP}{(P_o - P)\left[1 + \frac{(C-1)P}{P_o}\right]} \tag{2.17}$$

A comparison of Langmuir and BET isotherm is shown in Fig. 2.11.

Yu et al. (2015) described for the first time that methane adsorption in shale gas reservoir behaved similar to multi-layer adsorption. Core samples from Marcellus shale were analysed and found to deviate from Langmuir isotherm but obey the Brunaeur-Emmett-Teller (BET) isotherm.

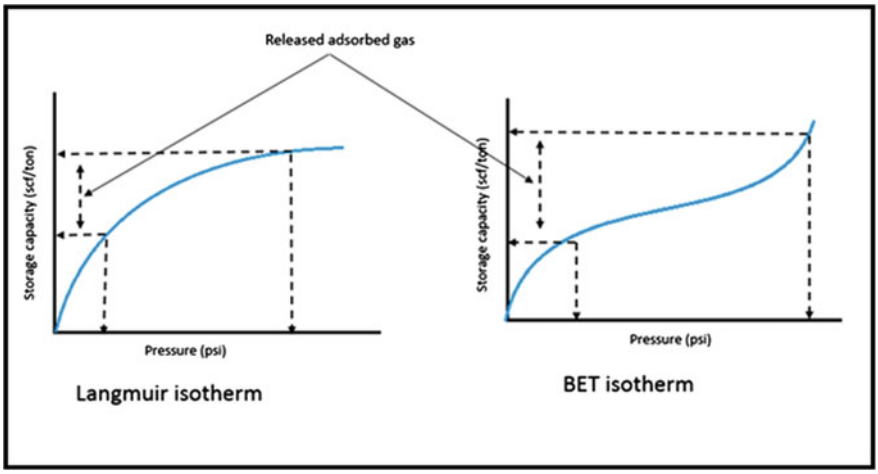

Fig. 2.11 Comparison of Langmuir and BET isotherms

Yu et al. (2015) also found that gas adsorption obeying the BET isotherm contributes to more production than gas adsorption obeying the Langmuir isotherm. They also argue that at very high pressures, the gas that is finally sorbed on the organic carbon surfaces forms multi-molecular layers and Langmuir isotherm may not be a good approximation of the amount of gas stored on the surfaces of the organic carbon.

Pure methane might not be the only component adsorbed on shale, with the presence of carbon dioxide, nitrogen and other heavier components. The presence of CO_2 with methane in the free gas makes the gas desorption behaviour and measurement most difficult. There is always competition for the same adsorption site by the components. Thus, the total volume of any of the gas will be less when they act independently.

Thus, the presence of more than one component within the pore network means that a better and more representative isotherm model will have to be taken into account.

Leahy-dios et al. (2011) suggested the use of multi-component adsorption isotherm model. According to Leahy-dios et al. (2011), a general form of expressing the multi-component adsorption is the extended Langmuir isotherm. They conducted experiments on the effect of multi-component adsorption and desorption on estimation and calculation of OGIP by using the extended Langmuir isotherm. By proposing a new multi-component adsorption model that allows the binary interaction parameters to capture non-ideal adsorption and also the fitting of adsorption isotherms for multi-component data sets, cumulative gas production could be increased by 10% over the life of the well.

Ambrose et al. (2011) also proposed a multi-component adsorption model that can be used to determine the composition and the amount of an adsorbed phase that is present. The extended Langmuir isotherm was chosen among other multi-component adsorption models such as ideal adsorbed solution (IAS) and the 2D equation of state (2D EOS) due to its wider use in the petroleum industry. Ambrose et al. (2011) proposed a new gas in place equation that combined the extended Langmuir model with volumetrics and the free gas composition; this method of calculating the gas in place showed a 20% decrease in gas in place compared with when the conventional approach was used in the calculation.

Ruthven (1984) proposed a general equation that represents the extended Langmuir isotherm as

$$V_{\mathrm{ads},i} = \frac{V_{\mathrm{L},i}\left(\frac{p_i}{p_{\mathrm{L},i}}\right)}{1 + \sum\left(\frac{p_i}{p_{\mathrm{L},j}}\right)} \tag{2.18}$$

where $V_{\mathrm{L},i}$ the Langmuir volume for component is i, $p_{\mathrm{L},i}$ is the Langmuir pressure component for i and $\sum\left(\frac{p_i}{p_{\mathrm{L},j}}\right)$ is the summation of all component pressure ratios i and j, p_i is the partial pressure of component i.

2.5 Stress-Dependent Permeability in Shale

In modelling of shale gas reservoirs, it is important to consider permeability changes due to overburden pressure. Very often in conventional reservoirs where the rocks are assumed permeable, permeability is modelled as insensitive to the effective pressure as the large pore throats of the rocks may not see a complete closure when effective pressure increases (Faulkner and Rutter 1998).

However, for unconventional reservoirs such as shale gas, the small grain size and pore spaces mean that they are easily affected by the influence of pressure. Thus, pressure changes throughout the reservoir have the effect of changing the permeability of the formation. The pore spaces can eventually be closed under effective pressure (i.e. Total pressure–Pore fluid pressure).

Previous modelling of shale gas reservoirs neglected the effect of stress-dependent fracture permeability on well productivity and gas recovery (Cipolla et al. 2009a). Cipolla et al. (2009b) showed the impact of closure stress and Young's modulus on unpropped fracture conductivity. Fracture conductivity decreased considerably as the closure stress increased and with decreasing Young's modulus. They conducted a number of simulation using Barnett shale properties and demonstrated the more severe effect of stress-dependent fracture conductivity on reducing gas recovery. According to them, for shales of lower Young's modulus, the corresponding increase in the closure stress and its effect on the fracture conductivity will be greater.

Pedrosa (1986) obtained pressure transient response in stress-sensitive formations by analytically solving the radial flow equation with pressure-dependent rock properties. In his model, he considered the reduction in permeability as a result of increase in effective stress. A new parameter known as the permeability modulus was included in his model to account for the permeability dependence on pressure. This permeability modulus is the fractional change in permeability with a unit change in pressure.

Lowering pore pressure has the effect of increasing the effective stress in the formation, and with low-permeability reservoirs, this has a major impact on the permeability of the formation. Thus, an essential feature of low-permeability reservoirs and fractured rocks is their sensitivity to effective stress in terms of both porosity and permeability (Pedrosa 1986).

Vairogs et al. (1971) conducted experimental studies to demonstrate that low-permeability reservoirs exhibit a much greater permeability reduction than reservoirs with much higher permeability. The authors proposed a mathematical model that incorporated the effect of stress on the permeability of tight reservoirs and used this model to predict production performance as a result of the effect of stress on the permeability of tight rocks.

Raghavan and Chin (2002) presented correlations in order to assess the production loss in stress-dependent permeability reservoirs. They believed that these correlations could be easily incorporated into reservoir simulators to do production forecasts and account for productivity changes. A rigorous mathematical model was

developed that combines geo-mechanical and fluid flow to correlate reductions that occur in production with time. They used three fundamental principles of linear momentum, mass conservation and Darcy's law in their model to compute pressure responses. The results from their studies showed that a high drawdown pressure, high overburden stress and an initially low reservoir pressure will increase stress-induced loss in productivity.

Cho et al. (2012) conducted a number of experimental studies to verify and calibrate existing pressure-dependent permeability correlations. These correlations were supported by a number of field examples and synthetic data with results indicating the loss of initial permeability of unpropped natural fractures following pressure depletion in the reservoir. Nevertheless, the authors cautioned against the use of fracture closure with pressure drop data without considering the complex interactions between the natural fractures and the shale matrix. A table of the correlations used in the studies of Cho et al. (2012) are presented (see Table 2.3).

Best and Katsube (1995) stated that there is no agreement on whether the relationship between permeability and pressure could be represented by a single mathematical expression. They, however, postulated that this relationship between pressure and permeability for shale can be expressed exponentially by the form

Table 2.3 Table of selected correlations (Cho et al. 2012)

	References	Correlation
1.	Rutqvist et al. (2002)	$k_f = k_{fi}\mathrm{e}^{c_1\left(\frac{\phi}{\phi_i}-1\right)}$, $\phi = \phi_{r1} + (\phi_i - \phi_{r1})\mathrm{e}^{a1\Delta p}$
2.	Rutqvist et al. (2002)	$k = k_{\mathrm{i}}F_k$, $F_k = \frac{\left[b_{\max 2}\left(\mathrm{e}^{d_2 d_y} - \mathrm{e}^{d_2\sigma' yi}\right)\right]^3 + \left[b_{\max 2}\left(\mathrm{e}^{d_2 d_z} - \mathrm{e}^{d_2\sigma' zi}\right)\right]^3}{b_{i2}^3 + b_{i2}^3}$
3.	Raghavan and Chin (2002) (rock type I)	$k_f = k_{fi}\mathrm{e}^{-d_{f3}\Delta p}$
4.	Raghavan and Chin (2002) (rock type II)	$k_f = k_{fi}\left(1 - m_{f4}\Delta p\right)$
5.	Raghavan and Chin (2002) (rock type III)	$k_f = k_{fi}\left(\frac{\phi_f}{\phi_{fi}}\right)^n$ with $\phi_f^{n+1} = 1 - \frac{1-\phi_f^n}{\mathrm{e}^{\Delta\varepsilon_v}}$, $\Delta\varepsilon_v = \frac{\alpha_5\Delta p(1+v_5)(2v_5-1)}{E_5(1-v_5)}$
6.	Raghavan and Chin (2002) and Celis et al. (1994)	$k_f = k_{fi}\left(\frac{\phi_f}{\phi_{fi}}\right)^n$, $\phi_f = \phi_{fi}\mathrm{e}^{-d_{f6}\Delta p}$
7.	Raghavan and Chin (2002) and Rutqvist et al. (2002)	$k_f = k_{fi}\left(\frac{\phi_f}{\phi_{fi}}\right)^n$, $\phi_f = \phi_{fi}F_\phi$, $F_\phi = \frac{b_1+b_2+b_3}{b_{1i}+b_{2i}+b_{3i}}$, $b = b_{f7} + b_{\max 7}\left[\mathrm{e}^{d_{f7}\sigma' n} - \mathrm{e}^{d_{f7}\sigma' ni}\right]$
8.	Raghavan and Chin (2002) and Minkoff et al. (2003)	$k_f = k_{fi}\left(\frac{\phi_f}{\phi_{fi}}\right)^n$, $\phi_f = \phi_{fi}\left(1 - m_{f8}\Delta p\right)$
9.	Raghavan and Chin (2002) and Minkoff et al. (2003)	$k_f = k_{fi}\left(\frac{\phi_f}{\phi_{fi}}\right)^n$, $\phi = 1 - \frac{(1-\phi_i)}{\mathrm{e}^{\varepsilon_v}}$, $\varepsilon_v = \frac{\alpha_g\Delta p\left(1+v_g\right)\left(2v_g-1\right)}{E_g\left(1-v_g\right)}$

$$k = k_o e^{-\alpha P_e} \tag{2.19}$$

where k_o is the permeability at atmospheric condition, P_e is the effective pressure and α is the slope of the curve of permeability versus effective pressure.

Gutierrez et al. (2000) conducted experimental studies to describe how fracture permeability varies with mechanical loading and to determine whether mechanical deformation can completely close a hydraulic fracture. The results from the experiments showed reduction in fracture permeability when increasing normal stress. But they observed that the fracture is never completely closed under this stress and the permeability remained higher compared to the shale matrix permeability.

Franquet et al. (2004) noted that substantial errors are likely to be obtained if proper appreciation of the mechanics of rock compressibility under various states of stress is not examined. Pressure-dependent permeability data are very rare to come by and hence most analysis of permeability in well test analysis is done with the assumption of a constant permeability. They attempted to evaluate the error caused by ignoring the pressure-dependent permeability in tight gas reservoirs by simulating the pressure-dependent permeability using an exponential form for the permeability versus pressure drop. This simulation model, therefore, required only one parameter γ which is the permeability modulus, psia^{-1}.

$$k = k_i e^{-\gamma(p_i - p)} \tag{2.20}$$

k, k_i are the current and initial permeability, respectively, while p, p_i are the current and initial pressures.

Navarro (2012) conducted field studies of wells in Robore III reservoir, Bolivia, to investigate the decline in production by analysing compressibility, production and pressure data. It was found that production decline was primary as a result of the closure of fractures due to an increase in the effective stress. The closure of the natural fractures leads to the reservoir becoming more of a matrix permeability reservoir.

Tao et al. (2009) conducted numerical modelling combining a fully coupled poro-elastic displacement discontinuity method and nonlinear fracture deformation model to analyse the change in fracture permeability in fractured reservoirs. Their studies focussed on fractures since they are susceptible to change under stress compared to that of the matrix. Their work showed that fracture permeability reduces due to the increases in effective normal stress. Thus under isotropic stress conditions, fracture permeability was found to be decreasing. According to Tao et al. (2009), fracture permeability may increase during production especially in high anisotropic stress.

Wu and Pruess (2000) presented integral solutions for transient flow through a porous media by considering pressure-dependent permeability. They observed the effects of pressure on permeability by using integral solutions for one-dimensional

single-phase, slightly compressible linear and radial flow through a horizontal fracture. The results of their studies also showed that ignoring pressure dependence on permeability may lead to significant errors in flow behaviour under high-pressure operations.

Berumen and Tiab (1996) presented new numerical approach for interpreting the effect of permeability changes in artificially fractured rocks. By considering non-linear effect of pressure dependence, new type curves were generated for pressure sensitive fracture formations. The use of conventional techniques in evaluating fractured wells was found to be insufficient and led to inaccurate estimates.

According to Wheaton (2017), there has been no analytically derived relationship that relates shale permeability to pressure and geo-mechanical properties. Wheaton (2017), therefore, tried to examine the theoretical dependence of shale permeability on pressure and geo-mechanical properties of shale using Young's modulus and poison ratio. By developing a simple equation to relate shale permeability to pressure, Young's modulus and poison ratio, he was able to predict shale permeability on the basis of geo-mechanical properties.

$$\frac{k(p_i)}{k(p_o)} = \left[1 + \frac{3p_i(1-2v)}{E\phi_o}\right]^3 \tag{2.21}$$

where p_i = initial producing pressure, $k(p_o)$ = shale permeability under surface conditions and $k(p_i)$ = estimated shale permeability under initial production conditions. Also E, v represents Young's modulus and poison ratio, respectively.

The model equation though cannot be verified due to the absence of any experimental data which relates the dependence of shale permeability to pressure as a function of Young's modulus and poison ratio in shale.

References

Adachi J, Siebrits E, Peirce A, Desroches J (2007) Computer simulation of hydraulic fractures. Int J Rock Mech Min Sci 44:739–757. https://doi.org/10.1016/j.ijrmms.2006.11.006

Akkutlu IY, Fathi E (2011) Gas transport in shales with local kerogen heterogeneities. In: SPE annual technical conference and exhibition. SPE 146422, p 13. https://doi.org/10.2118/146422-MS

Ambrose RJ, Hartman RC, Labs W, Akkutlu IY (2011) Multi-component sorbed-phase considerations for shale gas-in-place calculations. In: SPE production and operations symposium. SPE 141416, pp 1–10. https://doi.org/10.2118/141416-MS

Azom PN, Javadpour F (2012) Dual continuum Modeling of shale and tight gas reservoirs. Society of petroleum engineers. doi:10.2118/159584-MS

Bai M, Elsworth D, Roegiers JC (1993) Modeling of naturally fractured reservoirs using deformation dependent flow mechanism. In: International journal of rock mechanics and mining sciences & geomechanics abstracts. 30(7):1185–1191. Pergamon

Barenblatt GI, Zheltov IP, Kochina IN (1960) Basic concepts in the theory of seepage of homogeneous liquids in fissured rocks [strata]. J Appl Math Mech 24:1286–1303

Berumen S, Tiab D (1996) Effect of pore pressure on conductivity and permeability of fractured rocks. In: Proceedings of SPE western regional meeting, pp 445–460. https://doi.org/10.2523/35694-MS

Beskok A, Karniadakis GE (1999) A model for flows in channels, pipes, and ducts at micro and nano scales. Microscale Thermophys Eng 3:43–77. https://doi.org/10.1080/108939599199864

Best ME, Katsube TJ (1995) Shale permeability and its significance in hydrocarbon exploration. Lead. Edge 14:165–170. https://doi.org/10.1190/1.1437104

Celis V, Silva R, Ramones M, Guerra J, Da Prat G (1994) A New Model for Pressure Transient Analysis in Stress Sensitive Naturally Fractured Reservoirs. Soc Pet Eng doi:10.2118/23668-PA

Chen L, Zhang L, Kang Q, Yao J, Tao W (2015) Nanoscale simulation of shale transport properties using the lattice Boltzmann method: permeability and diffusivity Li Chen. Sci Rep 25(7):134–139

Chao C, Lee J, Spivey JP, Semmelbeck ME (1994) Modeling multilayer gas reservoirs including sorption effects. Society of Petroleum Engineers. doi:10.2118/29173-MS

Cho Y, Apaydin O, Ozkan E (2012) Pressure-dependent natural-fracture permeability in shale and its effect on shale-gas well production. Soc Pet Eng. SPE 159801, 1–18. https://doi.org/10.2118/159801-PA

Cipolla C, Lolon E, Erdle J, Rubin B (2010) Reservoir modeling in shale-gas reservoirs. SPE Reserv Eval Eng 13:23–25. https://doi.org/10.2118/125530-PA

Cipolla CL, Lolon E, Mayerhofer MJ, Warpinski NR (2009a) Fracture Design Considerations in Horizontal Wells Drilled in Unconventional Gas Reservoirs. Soc Pet Eng. doi:10.2118/119366-MS

Cipolla CL, Lolon EP, Erdle JC, Tathed V (2009b) Modeling well performance in shale-gas reservoirs. SPE 125532, pp 19–21. https://doi.org/10.2118/125532-MS

Civan F (2010) Effective correlation of apparent gas permeability in tight porous media. Transp Porous Media 82:375–384. https://doi.org/10.1007/s11242-009-9432-z

Clarkson CR, Haghshenas B (2013) Modeling of supercritical fluid adsorption on organic-rich shales and coal. In: SPE unconventional resources conference, pp 1–24. https://doi.org/10.2118/164532-MS

Daneshy AA (1973) On the design of vertical hydraulic fractures. J Pet Technol 25:83–97. https://doi.org/10.2118/3654-PA

Darabi H, Ettehad A, Javadpour F, Sepehrnoori K (2012) Gas flow in ultra-tight shale strata. J Fluid Mech 710:641–658. https://doi.org/10.1017/jfm.2012.424

de Swaan OA (1976) Analytic solutions for determining naturally fractured reservoir properties by well testing. https://doi.org/10.2118/5346-PA

Dershowitz WS, La Pointe PR, Doe TW et al (2004) Advances in discrete fracture network modeling. In: Proceedings of the US EPA/NGWA fractured rock conference, Portland, pp 882–894

Faulkner DR, Rutter EH (1998) The gas permeability of clay-bearing fault gouge at 20 °C. Geol Soc London Spec Publ 147:147–156. https://doi.org/10.1144/gsl.sp.1998.147.01.10

Franquet M, Ibrahim M, Wattenbarger R, Maggard J (2004) Effect of pressure-dependent permeability in tight gas reservoirs, transient radial flow. Proc Can Int Pet Conf, 1–10. https://doi.org/10.2118/2004-089

Frantz J, Sawyer W, MacDonald R, Williamson J, Johnston D, Waters G (2005) Evaluating barnett shale production performance using an integrated approach. Proc SPE Annu Tech Conf Exhib, 1–18. https://doi.org/10.2523/96917-MS

Freeman C, Moridis GJ, Michael GE, Blasingame TA (2012) Measurement, modeling, and diagnostics of flowing gas composition changes in shale gas wells. SPE 153391. doi:10.2118/153391-MS

Gad-el-hak M (1999) The fluid mechanics of microdevices—the freeman scholar lecture. Transactions-American Society of Mechanical Engineers Journal of FLUIDS Engineering, 121:5–33

Geertsma J, De Klerk F (1969) A rapid method of predicting width and extent of hydraulically induced fractures. J Pet Technol 21:1571–1581. https://doi.org/10.2118/2458-PA

Geng L, Li G, Zitha P, Tian S, Sheng M, Fan X (2016) A diffusion–viscous flow model for simulating shale gas transport in nano-pores. Fuel 181:887–894. https://doi.org/10.1016/j.fuel.2016.05.036

Guo C, Xu J, Wu K, Wei M, Liu S (2015) Study on gas flow through nano pores of shale gas reservoirs. Fuel 143:107–117. https://doi.org/10.1016/j.fuel.2014.11.032

Gutierrez M, Øino LE, Nygård R (2000) Stress-dependent permeability of a de-mineralised fracture in shale. Mar Pet Geol 17:895–907. https://doi.org/10.1016/S0264-8172(00)00027-1

Herbert AW (1996) Modelling approaches for discrete fracture network flow analysis. Dev Geotech Eng 79:213–229

Howard G, Fast CR (1957) Optimum fluid characteristics for fracture extension? In: Proceedings of American Petroleum Institute, pp 261–270. API-57-261

Javadpour F (2009) Nanopores and apparent permeability of gas flow in mudrocks (Shales and Siltstone). Soc Pet Eng J 48:1–6. https://doi.org/10.2118/09-08-16-DA

Javadpour F, Fisher D, Unsworth M (2007) Nanoscale gas flow in shale gas sediments. J Can Pet Technol 46:55–61. https://doi.org/10.2118/07-10-06

Kazemi H (1969) Pressure transient analysis of naturally fractured reservoirs with uniform fracture distribution. https://doi.org/10.2118/2156-A

Kelly S, El-Sobky H, Torres-Verdín C, Balhoff MT (2015) Assessing the utility of FIB-SEM images for shale digital rock physics. Adv Water Resour, 1–15. https://doi.org/10.1016/j.advwatres.2015.06.010

Klinkenberg LJ (1941) The permeability of porous media to liquids and gases. Drilling and production practice, pp 200–213. American Petroleum Institute

Kuila U, Prasad M (2013) Specific surface area and pore-size distribution in clays and shales. Geophys Prospect 61:341–362. https://doi.org/10.1111/1365-2478.12028

Leahy-dios A, Das M, Agarwal A, Kaminsky RD, Upstream E (2011) Modeling of transport phenomena and multicomponent sorption for shale gas and coalbed methane in an unstructured grid simulator adsorbed gas, scf/tonne. SPE Annu, 1–9. https://doi.org/10.2118/147352-MS

Lee KS, Kim TH (2015) Integrative understanding of shale gas reservoirs, 1st edn. Springer, Berlin. https://doi.org/10.1007/978-3-319-29296-0

Mack MG, Warpinski NR (2000) Mechanics of hydraulic fracturing. Reservoir stimulation. MJ Economides and KG Nolte

Martin JP, Hill DG, Lombardi TE, Nyahay R (2010) A Primer on New York's gas shales, pp 1–32

McCabe WJ, Barry BJ, Manning MR (1983) Radioactive tracers in geothermal underground water flow studies. Geothermics 12:83–110

McClure M, Horne RN (2013) Discrete fracture network modeling of hydraulic stimulation: coupling flow and geomechanics. Springer, Berlin

Mehmani A, Prodanović M, Javadpour F (2013) Multiscale, multiphysics network modeling of shale matrix gas flows. Transp Porous Media 99:377–390. https://doi.org/10.1007/s11242-013-0191-5

Mengal SA, Wattenbarger RA (2011) Accounting for adsorbed gas in shale gas reservoirs. SPE Conf, 25–28. https://doi.org/10.2118/141085-MS

Minkoff SE, Stone CM, Bryant S, Peszynska M, Wheeler MF (2003) Coupled fluid flow and geomechanical deformation modeling. J Petrol Sci Eng. 38(1):37–56

Moghaddam R, Jamiolahmady M (2016) Slip flow in porous media. Fuel 173:298–310. https://doi.org/10.1016/j.fuel.2016.01.057

Myong RS (2003) Gaseous slip models based on the Langmuir adsorption isotherm. Phys Fluids 16:104–117. https://doi.org/10.1063/1.1630799

Najurieta HL (1980) A theory for pressure transient analysis in naturally fractured reservoirs. https://doi.org/10.2118/6017-PA

Naraghi ME, Javadpour F (2015) A stochastic permeability model for the shale-gas systems. Int J Coal Geol 140:111–124. https://doi.org/10.1016/j.coal.2015.02.004

Navarro VOG (2012) Closure of natural fractures caused by increased effective stress, a case study: Reservoir Robore III, Bulo Bulo Field, Bolivia. Soc Pet Eng. SPE 153609, 1–11. https://doi.org/10.2118/153609-MS

Nordgren RRP (1972) Propagation of a vertical hydraulic fracture. Soc Pet Eng J 12:306–314. https://doi.org/10.2118/3009-PA

Odeh AS (1965) Unsteady-state behavior of naturally fractured reservoirs. https://doi.org/10.2118/966-PA

Pedrosa OA (1986) Pressure transient response in stress-sensitive formations. SPE 15115. https://doi.org/10.2118/23312-MS

Perkins TK, Kern LR (1961) Widths of hydraulic fractures. J Pet Technol 13:937–949. https://doi.org/10.2118/89-PA

Raghavan R, Chin LY (2002) Productivity changes in reservoirs with stress-dependent permeability. Soc Pet Eng. SPE 88870, 308–315. https://doi.org/10.2118/77535-MS

Rahman MM, Rahman MK (2010) A review of hydraulic fracture models and development of an improved pseudo-3D model for stimulating tight oil/gas sand. Energy Sources Part A Recover Util Environ Eff 32:1416–1436. https://doi.org/10.1080/15567030903060523

Rathakrishnan E (2013) Gas dynamics. PHI Learning Pvt. Ltd, New Delhi

Rezaveisi M, Javadpour F, Sepehrnoori K (2014) Modeling chromatographic separation of produced gas in shale wells. Int J Coal Geol 121:110–122. https://doi.org/10.1016/j.coal.2013.11.005

Ruthven DM (1984) Principles of adsorption and adsorption processes. John Wiley & Sons

Rutqvist J, Wu YS, Tsang CF, Bodvarsson G (2002) A modeling approach for analysis of coupled multiphase fluid flow, heat transfer, and deformation in fractured porous rock. Int J Rock Mech Min Sci 39(4):429–442

Sakhaee-pour A, Bryant SL (2011) Gas Permeability of Shale. Soc Pet Eng. doi:10.2118/146944-MS

Serra K, Reynolds AC, Raghavan R (1983) New pressure transient analysis methods for naturally fractured reservoirs. https://doi.org/10.2118/10780-PA

Settari A, Cleary MP (1986) Development and testing of a pseudo-three-dimensional model of hydraulic fracture geometry. SPE Prod Eng 1:449–466. https://doi.org/10.2118/10505-PA

Shabro V, Torres-Verdín C, Javadpour F, Sepehrnoori K (2012) Finite-difference approximation for fluid-flow simulation and calculation of permeability in porous media. Transp Porous Media 94:775–793. https://doi.org/10.1007/s11242-012-0024-y

Singh H, Javadpour F (2015) Langmuir slip-Langmuir sorption permeability model of shale. Fuel 164:28–37. https://doi.org/10.1016/j.fuel.2015.09.073

Singh H, Javadpour F (2016) Langmuir slip-Langmuir sorption permeability model of shale. Fuel, 164:28–37

Tao Q, Ehlig-Economides CA, Ghassemi A (2009) Investigation of stress-dependent fracture permeability in naturally fractured reservoirs using a fully coupled poroelastic displacement discontinuity model. Proc SPE Annu Tech Conf Exhib 5:2996–3003. https://doi.org/10.2118/124745-MS

Vairogs J, Hearn CL, Dareing DW, Rhoades VW (1971) Effect of rock stress on gas production from low-permeability reservoirs. Soc Pet Eng 5:1161–1167. https://doi.org/10.2118/3001-PA

Walton I, Mclennan J (2013) The role of natural fractures in shale gas production. https://doi.org/10.5772/56404

Warren JEE, Root PJJ (1963) The behavior of naturally fractured reservoirs. Soc Pet Eng J 3:245–255. https://doi.org/10.2118/426-PA

Weng X (2015) Modeling of complex hydraulic fractures in naturally fractured formation. J Unconv Oil Gas Resour 9:114–135. https://doi.org/10.1016/j.juogr.2014.07.001

Wheaton R (2017) Dependence of shale permeability on pressure. Society of petroleum engineers. doi:10.2118/183629-PA

Wu Y-S, Pruess K (2000) Integral solutions for transient fluid flow through a porous medium with pressure-dependent permeability. Int J Rock Mech Min Sci 37:51–61. https://doi.org/10.1016/S1365-1609(99)00091-X

Yew CH, Weng X, Yew CH, Weng X (2015) Fracturing of a wellbore and 2D fracture models (Chapter 1). In: Mechanics of hydraulic fracturing, pp 1–22. https://doi.org/10.1016/B978-0-12-420003-6.00001-X

Yu W, Sepehrnoori K, Patzek TW (2014) Evaluation of gas adsorption in marcellus shale. Society of petroleum engineers. pp 27–29. doi:10.2118/170801-MS

Yu W, Sepehrnoori K, Patzek TW (2015) Modeling gas adsorption in marcellus shale with Langmuir and BET isotherms. SPE J. https://doi.org/10.2118/170801-PA

Chapter 3
Numerical Study of Shale Gas Flow Behaviour in Reservoir and Hydraulic Fractures

Abstract Some of the inappropriate assumptions that are often made in the use of commercial simulators for shale gas simulations are discussed in this chapter. For shale gas reservoirs characterised by very small pore size network, these approximations could lead to serious errors. Modelling of the geological complexities of shale gas requires the use of appropriate grid structures within the simulator to handle these complexities. Also, implementation of appropriate numerical methods that can adequately solve the set of mathematical equations associated with the simulation of shale gas reservoirs is the key to obtain sensible simulation results. This chapter provides a review of these inherent challenges in shale gas modelling. The concept of instantaneous capillary equilibrium within the pore networks as well as the non-Darcy flow that occurs within the matrix of the pore network is critically reviewed while the existing theories for proppant transport within the fractures are examined.

3.1 Instantaneous Capillary Equilibrium

In nano-pore networks, the displacement of different phases may take considerable amount of time to reach equilibrium. This is especially true for shale gas reservoirs which feature such smaller pores. In such systems, it would be inappropriate to represent the transport mechanism between the interfaces as instantaneous in response to an external pressure gradient. In most commercial reservoir simulators, reservoir modelling of two fluids is made under such an assumption of instantaneous capillary equilibrium. Devegowda et al. (2014) explain that for shales, phase displacement will take considerable amount of time before it reaches equilibrium under an imposed pressure gradient and thus for multi-phase flow in shales, assuming instantaneous equilibrium will be inaccurate. Also due to the large capillary pressures expected for nano-pore scales, capillary forces may sometimes be comparable to pore pressures and may restrict the movement of the different phases, especially if they act in opposition to the imposed pressure gradient (Devegowda et al. 2014).

J. Gholinezhad et al., *Challenges in Modelling and Simulation of Shale Gas Reservoirs*, SpringerBriefs in Petroleum Geoscience & Engineering,
https://doi.org/10.1007/978-3-319-70769-3_3

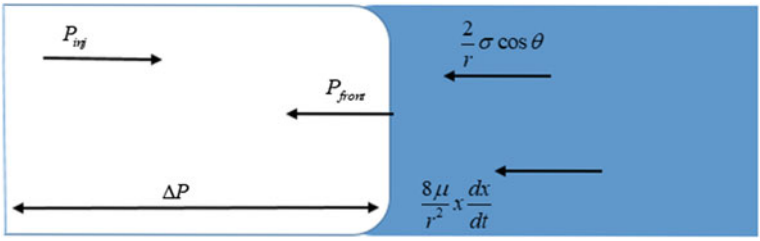

Fig. 3.1 Gas displacing water (adapted from Devegowda et al. 2014)

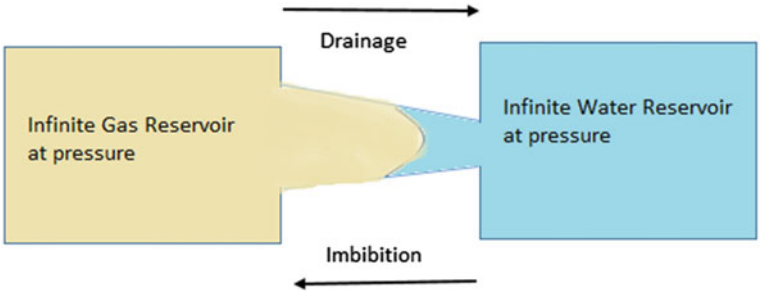

Fig. 3.2 Instantaneous equilibrium problem (adapted from Andrade et al. 2010)

Figure 3.1 shows gas displacing water with the speed of the interface being governed by the difference between the imposed pressure forces, capillary and viscous forces (Devegowda et al. 2014).

Andrade et al. (2010) conducted numerical simulations by incorporating the effects of non-instantaneous capillary equilibrium for oil–water and gas–water systems to study the impact of the new physics on the movement of saturation front within a 1D core flood. They considered a cone-shaped water-wet capillary tube with an infinite water and gas reservoir as seen from Fig. 3.2.

Decreasing the pressure in the gas reservoir will decrease the pressure of the gas in the capillary tube and due to the limited compressibility of water coupled with small flow rate out of the water reservoir; it may not advance quickly to replace the gas. Thus for significantly large capillary pressure values, the water phase pressure can only become negative and hence the use of instantaneous equilibrium for shale becomes inaccurate. The results of their studies showed that the saturation profiles changed significantly when non-instantaneous equilibrium was included in the simulation study for shale.

3.2 Non-Darcy Flow Simulation

Darcy's law is not suitable to be used in unconventional reservoirs to simulate flow through the nano-pores of shale matrix. The use of Darcy's law is only valid over a limited range of flow rates. For such shale gas reservoirs, modification of Darcy's formula to account for turbulent flow of the gas, especially within the fractures where inertial forces are high, is important.

In cases of high gas flow rate or highly fractured reservoir such as shale gas reservoirs, the use of Darcy's law to describe the fluid behaviour will lead to misleading results. Nguyen (1986) showed that using standard Darcy flow analysis will result in over predicting the productivity by as much as 100% in some cases.

In such cases, Forchheimer equation is used to address the non-Darcy flow. This equation, however, is only used to describe single-phase non-Darcy flow and may also be limited to a range of flow rates or pore types (Barree and Conway 2004).

Forchheimer observed that at very high flow rates, the relationship between pressure gradient and fluid velocities is no longer linear as described by Darcy's law. The pressure gradient under such conditions was usually higher than that predicted by Darcy's law. He introduced a second proportionality constant in addition to the permeability k that would account for the nonlinearity. This was called the non-Darcy flow coefficient β. The equation is given as

$$-\frac{\mathrm{d}p}{\mathrm{d}x} = \frac{\mu v}{k} + \beta \rho v^2 \tag{3.1}$$

The additional quadratic term introduced by Forchheimer to address the non-linearity was found to be limited in describing all of Forchheimer data, thus Forchheimer added another cubic term to account for the deviations. Forchheimer equation inability yet to describe all data sets was observed by other authors such as Barree and Conway (2004). Lai et al. (2012) noted that without addressing these discrepancies, a significant impact will be noticed for the flow rate or pressure distribution in a porous medium.

$$-\frac{\partial p}{\partial x} = \frac{\mu v}{k} + \beta \rho v^2 + \gamma \rho v^3 \tag{3.2}$$

ρ is the density of the fluid.

Martins et al. (1990) showed using Fig. 3.3 based on experimental data that the β factor is not constant in a porous media. Thus for very high flow rates, Forchheimer equation will make inaccurate predictions.

There have been a lot of interest in developing correlations for the non-Darcy coefficient β. Li and Engler (2001) gave an excellent review of the correlations of the non-Darcy coefficient in one phase and multi-phase cases. For theoretical correlations, both parallel type and serial type models were reviewed. In the parallel type models, the assumption is made that the porous medium is made up of bundle

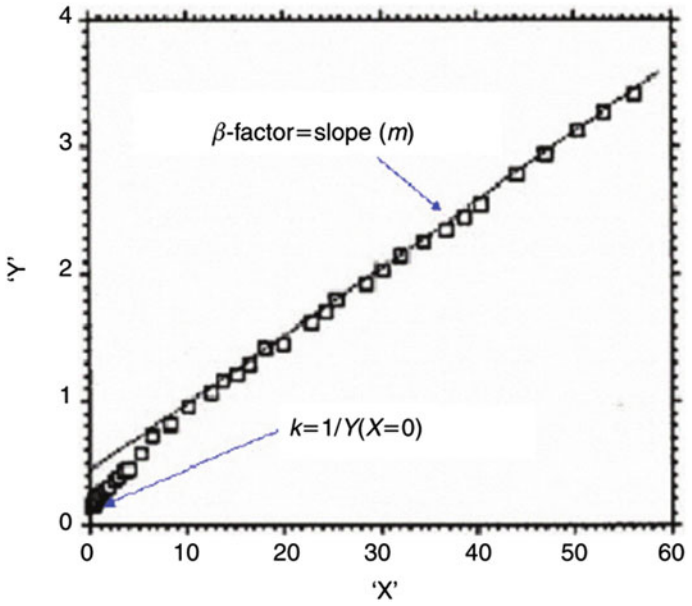

Fig. 3.3 Forchheimer plot showing that β is not a constant for increased flow rates (Lai et al. 2013; Martins et al. 1990)

of straight, parallel capillaries of uniform diameter (Fig. 3.4a). Whereas for the serial type models, the pore space is assumed to be serially lined up (Fig. 3.4b). The derivation of the non-Darcy coefficient for the parallel type model (Irmay 1958) and for serial type model (Scheidegger 1974) is given below

$$\beta = \frac{c}{K^{0.5}\phi^{1.5}} \text{ Parallel type model} \tag{3.3}$$

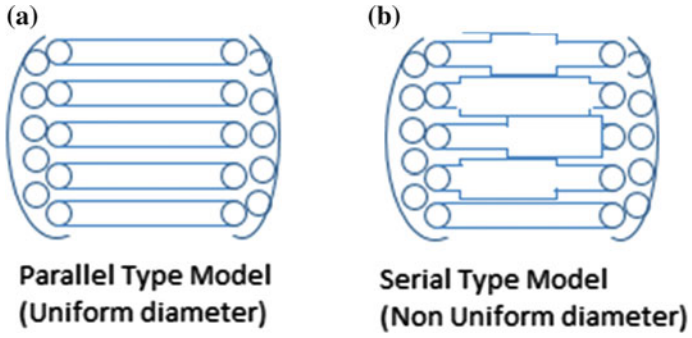

Fig. 3.4 Schematics of both parallel (**a**) and serial type model (**b**) (Li and Engler 2001)

$$\beta = \frac{c''\tau}{K\phi} \text{ Serial type model} \tag{3.4}$$

where c is a constant, c″ is a constant related to pore size distribution, ϕ is porosity, τ is tortuosity and K the permeability. Also, Li and Engler (2001) reviewed the empirical correlations that have been developed for the non-Darcy coefficient for both single-phase and multi-phase.

Under single phase, Cooke (1973) addressed the effects of non-Darcy flow in propped fractures by using permeability to predict the non-Darcy coefficient.

$$\beta = bK^{-a},$$

where a, b are constants determined by experiments based on proppant type.

Geertsma (1974) developed a correlation for one phase system by proposing a non-Darcy coefficient derived based on data measured from unconsolidated and consolidated media. He proposed that parallel type model developed by Irmay (1958) was not applicable to consolidated materials but rather to unconsolidated media. Thus from his empirical correlation, he developed a non-Darcy coefficient as

$$\beta = \frac{0.005}{K^{0.5}\phi^{5.5}} \tag{3.5}$$

Liu et al. (1995) incorporated the effect of tortuosity of the porous media on the non-Darcy coefficient by developing a correlation that gave β as

$$\beta = 8.91 \times 10^{8} K^{-1}\phi^{-1}\tau \tag{3.6}$$

They found that the Geertsma's formulae for the non-Darcy coefficient were inaccurate after plotting Geertsma's equation with other data obtained by other researchers.

Geertsma (1974) also proposed a β correlation for two-phase system where permeability was replaced by effective gas permeability at some water saturation, and porosity was replaced by void fraction occupied by the gas in the equation below

$$\beta = \frac{0.005}{K^{0.5}\phi^{5.5}} \cdot \frac{1}{(1 - S_{\text{wr}})^{5.5} K_{\text{rel}}^{0.5}} \tag{3.7}$$

where S_{wr} is residual water saturation and K_{rel} is relative gas permeability.

There have been many models proposed to account for multi-phase flow. Bennethum et al. (1997) derived a generalised Forchheimer equation to describe both single-phase and multi-phase flow.

A numerical model developed by Ewing et al. (1999) described the non-Darcy flow through isotropic porous media. For high flow rate wells, well equations were described using Forchheimer equation developed using finite difference, Galerkin

finite element and mixed finite element techniques. Ewing et al. (1999) observed that bottomhole well pressure is affected greatly by the Forchheimer coefficient beta (β). Therefore, for numerical simulation used in prediction of well performance for non-Darcy flow to be accurate, the incorporation of Forchheimer coefficient based on field measurement should be applied.

A new model that did not rely on the assumptions of a constant permeability or a constant β was proposed by (Barree and Conway 2004, 2009). Whereas Darcy's law still applied, the constant in Forchheimer work is introduced as a general nonlinear function (Barree and Conway 2009; Lai et al. 2013). The model can be described by the Darcy permeability and constant T thus according to the authors, by choosing the correct value of k_d and T, the whole porous media can be described using the same generalised equation for apparent permeability in Darcy's law.

$$\frac{\partial p}{\partial L} = \mu v / k_d \left[k_{mr} + \frac{(1 + k_{mr})}{\left(1 + \frac{\rho v}{\mu T}\right)} \right] \tag{3.8}$$

k_d constant Darcy permeability, Darcy
k_{mr} minimum permeability relative to Darcy permeability, fraction.

Barree and Conway (2009) further deduced a new Forchheimer type equation to address the non-Darcy flow. Wu et al. (2011) later extended and discussed Barree and Conway (2009) model for multi-phase flow in porous media. Wu et al. (2011) presented a mathematical and numerical model for incorporating the Barree Conway Model (BCM) in a general reservoir simulator to simulate multi-phase non-Darcy flow in porous media.

Choi et al. (1997) demonstrated that the use of Darcy's law in both fracture and matrix of the fractured system is not adequate. They proposed the use of Forchheimer model in the fracture while maintaining conventional Darcy's law in the matrix instead of using the conventional dual porosity/dual permeability formulation. The limitations of Choi et al. (1997) model are the use of single-phase flow.

Belhaj et al. (2003) proposed a comprehensive numerical simulation and experimental model that describes the non-Darcy behaviour in a porous media. This was achieved based on a careful selection of the non-Darcy coefficient (β). They concluded that the numerical model is valid for both single-phase flow and is functioning in all ranges of flow regimes in porous medium. According to them, this can also be applied to multi-phase flow cases.

Al-otaibi et al. (2011) developed a 3D numerical model according to Forchheimer and BCM specifically for pressure transient analysis of a single-phase fluid flow in porous and fractured reservoirs. An equivalent non-Darcy flow coefficient was derived based on the apparent permeability of non-Darcy flow for both the Forchheimer and BCM equations. The model was able to simulate all near-wellbore effects coupled with non-Darcy flow behaviour.

Rubin (2010) conducted simulation studies on Darcy and non-Darcy flow using finely gridded single well reference solutions within an explicitly modelled SRV complex fracture network. The reference solutions were compared with standard dual permeability, MINC and LS-LR-DK models. Rubin (2010) found that a non-Darcy flow permeability correction factor k_{corr} will allow non-Darcy flow to be accurately modelled in fracture conduits as wide as 2 ft. Thus by combining the LS-LR-DK models with this correction factor, the reference solutions were accurately matched. However, the limitations to this simulation modelling were the use of only single-phase fluid and the absence of desorption effect.

3.3 Proppant Transport

Due to the complex nature of the network of fractures created by hydraulic fracturing, the correct placement of proppants within the fracture network is critical if the well is to produce more gas. Proppant is pumped in a slurry to hold the fractures open, thereby increasing their ability to conduct fluid. Without the proppant, the fracture will close back on itself once the injection is stopped and the fluid pressure decreases. The location of proppant within the fracture network is difficult to predict especially when there is an interconnecting complex network of fractures and hence the modelling of proppant transport has become a challenge. In characterising the flow capacity or conductivity of induced fracture network, the following three key parameters should be determined according to Cipolla et al. (2009): location of proppants within the fracture network and conductivity of the propped and unpropped fracture network.

Cipolla et al. (2009) discussed how propped and unpropped fracture conductivity can affect shale gas performance. They investigated two different scenarios (see Fig. 3.5). One case is where the proppant is distributed evenly throughout the complex network of fractures. This case was found to be the least beneficial as only limited proppants is able to effectively prop the large fracture networks, thereby making it behave as if they were unpropped.

The second case occurs when the proppant flows towards a more dominant primary fracture, thereby increasing the average proppant concentration. The effect of this is a much more increased conductivity in the primary fracture and a better connection between the fracture network and the wellbore.

Numerical simulation of proppant transport can be undertaken using several approaches with the two most common frameworks being Eulerian–Eulerian and Eulerian–Lagrangian (Shiozawa and McClure 2016; Tsai et al. 2013; Zhang and Chen 2007).

Zhang and Chen (2007) described Eulerian method as treating the particle phase as a continuum and developed its conservation equations on a control volume basis similar to the fluid phase. In contrary, the Lagrangian method considers particles as a discrete phase and tracks the pathway of each individual particle. According to Zhang and Chen (2007), both methods can predict the steady-state particle

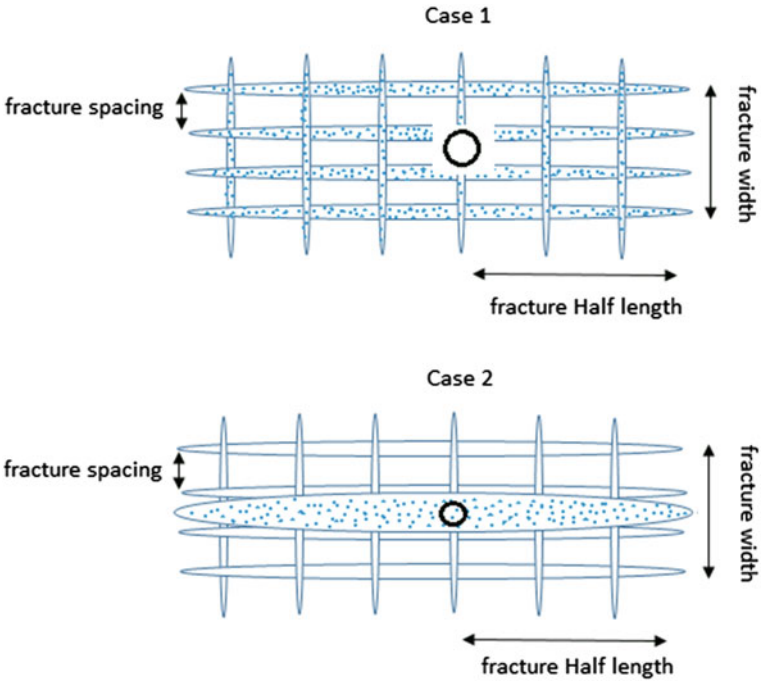

Fig. 3.5 Proppant transport scenarios (adapted from Cipolla et al. 2009)

concentration distribution while the Lagrangian method is computationally more demanding.

The problems of gravitational settling and tip screen out effect were addressed by Dontsov and Peirce (2015) by modelling proppant transport in hydraulic fractures that were able to capture both effects. This was achieved based on numerical simulations that allowed proppant plug formation and growth as well as gravitational settling to be properly captured. Their results demonstrated that it was possible to capture plug formation and growth and also to be able to capture gravitational settling when using both fracture geometries of KGD and P3D. The main limitation of their model as reported by the authors was the fact that it could not capture asymmetry caused by gravitational settling. The solution to this as suggested by the authors was to add a proppant transport module into a fully planar 3D fracture propagation model.

Based on the approach by Dontsov and Peirce (2015), Shiozawa and McClure, (2016) conducted numerical simulation of proppant transport in 3D hydraulic fracturing simulator using an Eulerian–Eulerian framework. Their simulation of hydraulic fracture propagation through a complex network showed how the proppants tend to accumulate at the intersections between the natural fracture and the hydraulic fractures and for low permeability formations such as shale, proppant

settling is a major problem for proppant placement since the proppant settles quickly due to gravity even before the fracture closure can occur.

3.4 Structured and Unstructured Grid

The unique geological complexities of shale gas reservoirs make it a challenge to model it using conventional approaches. Cartesian grids have been used extensively in modelling conventional reservoirs. However, it is inadequate to be used in modelling the complex geologies of unconventional reservoirs such as fractured shale gas formations. These complexities include non-planar and non-orthogonal fracture network that exists within the reservoir. Therefore, the representation of the fracture geometry within a numerical simulation model is a challenge and requires unstructured gridding. The fracture system in shale gas has been identified by Moridis et al. (2010) to include primary or hydraulic fractures caused by the injection of fluids into the formation, secondary fractures which occur as a result of changes in rocks when the primary fractures are created, natural fractures which are pre-existing fractures in the formation and finally radial fractures which are created as a result of the stress release in the immediate neighbourhood of the horizontal well. These fractures for the sake of simplicity in numerical simulations are assumed to be planar and orthogonal and are represented as such using Cartesian or structured gridding. For conventional reservoir simulators that use Cartesian gridding, modelling of the matrix and the fracture simultaneously as well as the flow transport within the ultra-tight permeability of the shale is a complicated task. Due to the complex geological nature of shale gas reservoirs, generating grid to represent these complexities in numerical simulation requires huge amount of effort and time. Therefore, structured grids only have mostly been employed for fast and accurate solutions in the past.

Aziz and Settari (1979) were one of the few people that utilised structured gridding in reservoir simulation, and their work was later extended to accommodate local grid refinement by Heinemann et al. (1991), Nacul (1991). The structured Cartesian grid and its local refinement are shown schematically in Fig. 3.6.

Structured grids are seen as the best in terms of computational time and efficiency when modelling shale gas reservoir, and it has been widely applied to model complex geometries using Cartesian grid approach. They allow for easy and uniform discretization of flow equations; however, due to their limited flexibility, they cannot represent accurately complex geological features such as various fracture geometries in shale gas reservoirs.

The performance of Cartesian or structured grid techniques has been improved by the introduction of local grid refinements and nine-point difference schemes (Heinemann et al. 1991).

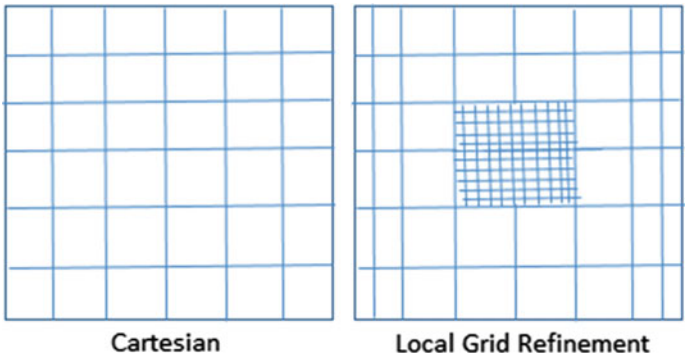

Fig. 3.6 Cartesian and local grid refinement (LGR)

3.4.1 Unstructured (PEBI) Grid

Heinemann et al. (1991) was the first to introduce the concept of Voronoi or perpendicular bisector (PEBI) grid in the petroleum industry. These grids are defined by the perpendicular bisectors of the lines joining neighbouring centres (Heinemann et al. 1991) (see Fig. 3.7).

One of the key properties of PEBI or Voronoi grids that makes its application useful in many areas of studies in petroleum engineering, mathematics and physics is the fact that the grid points could be specified anywhere inside the domain regardless of the position of any other points (Palagi and Aziz 1994).

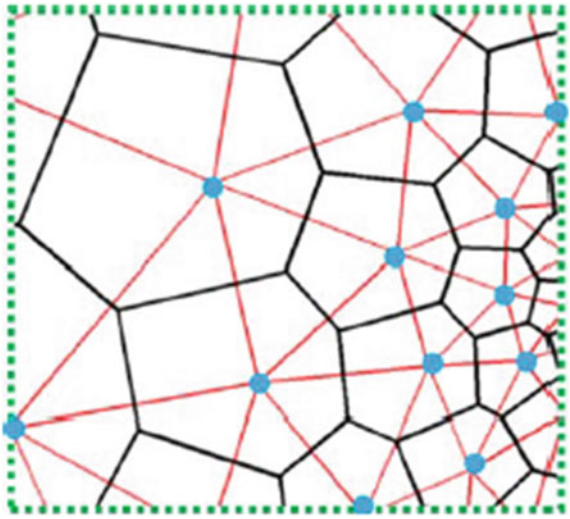

Fig. 3.7 Unstructured PEBI grid and Delaunay triangulation (red triangles) (Sun et al. 2016)

Zhang et al. (2015) developed a compositional model based on unstructured PEBI grid to characterise non-Darcy flow and multi-component adsorption in shale gas reservoirs. The model allows for the characterisation of non-Darcy flow including slip flow, transitional flow and free molecular flow. They discussed the following advantages of using unstructured grid compared with Cartesian grid:

1. Flexibility in the sense that it can represent complex boundary such as pinch out and faults in a formation much more easily.
2. Easiness of local refinement. Due to its flexibility and arbitrariness of arranging PEBI grid points, it is much easier to refine grids in the local section such as a domain around wells.
3. Less grid orientation effect. Grid orientation is less significant compared with structured grids due to the unstructured hexagonal grids.
4. And finally, the easiness of discretising and solving equations. This can easily be done using finite volume method to discretise and solve equations.

Sun et al. (2016) applied unstructured grids to generate simulation meshes for complex fracture networks by proposing new unstructured gridding and discretization workflow that could handle non-orthogonal and non-uniform apertures. They reported the accuracy of simulation results can be improved with refinement in the background mesh. An unstructured gridding approach such as PEBI was shown to be the best in terms of CPU performance and accuracy of simulation results.

3.5 FDM, FEM and FVM

The reservoir is represented by a set of mathematical equations which often cannot be solved by analytical methods. In these instances, numerical methods are used to solve the equations. Since the 1950s, numerical methods have been used to solve complex fluid flow processes involved in most petroleum reservoirs. They provide approximate solutions to nonlinear partial differential equations that cannot be solved analytically. The commonly used numerical methods in the petroleum industry are the finite difference method (FDM), finite element method (FEM) and finite volume method (FVM).

3.5.1 Finite Difference Method

This is the most commonly used numerical method in reservoir simulation. The technique involves discretising continuous ordinary and partial differential equations. A system of nonlinear partial differential equations which represents fluid

flow in porous media is solved using finite difference method. The implementation of the finite difference method is achieved by superimposing a finite difference grid over the reservoir to be modelled. At each boundary point, flow is calculated using pressure information obtained at a particular point of each block. This means that the distribution of grid points in space and the location of block boundaries with respect to grid points influence the accuracy of finite difference approximations (Nacul 1991). Once the spatial derivatives of the continuous equations are approximated, the unknown variables (usually pressure) are solved for by truncating the Taylor series expansion (Ertekin et al. 2001). Finite difference method is often seen as faster than finite element method and also very easy to implement. It is mostly represented by rectangular shapes and can also use curvilinear coordinates. In terms of simplicity and ease with extension from 1D to 2D and 3D, finite difference method is far superior but with the added problems of numerical dispersion and grid dependence (Firoozabadi 1999).

3.5.2 Finite Element Method

The use of finite element modelling has been seen to be more accurate compared to finite difference approach in numerical simulations. Finite element modelling yields a linear approximation of solution as opposed to piecewise constant approximation solution (Jayakumar et al. 2011). One of the advantages of the use of finite element modelling in reservoir simulation is the fact that it is very flexible in accommodating other shapes, allowing the mesh to be unstructured and flexible even though it is typically tetrahedral in shape. It is able to capture minute details of flow that occurs through the matrix to the fracture. According to Logan et al. (1985), FEM provides excellent efficiency and flexibility when handling complex reservoir geometry.

Jayakumar et al. (2011) demonstrated the use of finite element methods in modelling three Haynesville shale gas wells. With the benefit of modelling down even to the minute scale of flow from the reservoir through to the fracture faces, a finite element numerical simulator was used to successfully model shale gas. Jayakumar et al. (2011) argues that though a conventional simulator can be used to explicitly model shale gas flow, the large ratio between the average and minimum cell size would make computations impractical.

3.5.3 Finite Volume Methods

Compared to finite element methods, finite volume methods are said to be fairly recent technique used in numerical methods for solving problems in reservoir

simulations involving complex geometries. The use of finite volume method in unstructured meshes has presented significant development mainly in discretisation methodologies (Neyval et al. 2001). FVM is faster and easier to implement compared with finite element method while at the same time providing accurate solutions and versatility compared with the finite difference approach.

3.6 Reservoir Simulators for Shale Simulation

Several reservoir simulators have been designed that are capable of simulating shale gas reservoir performance. These reservoir simulators can be used for a wide range of processes such as history matching of gas production and reproducing complex hydraulic fracture network. Despite the success achieved by most of these simulators in modelling shale gas reservoirs, they fail to address all of the challenges identified in this chapter with some of the simulators tackling only a few distinctive features of shale gas reservoirs. It is, therefore, important to note that when using these available commercial and non-commercial simulators, care must be taken to identify the underlying assumptions made in developing them. Among some of the commercial simulators that is widely used for shale gas simulation are CMG/GEM™ by Computer Modelling Group (CMG), Eclipse 300™ by Schlumberger, COMET3™ by Advanced Resources International Inc. and GCOMP™ by PHH petroleum consultants. The non-commercial simulators include UTCHEM™ by the University of Texas and PSU-COALCOMP™ by Penn State university (Andrade et al. 2011). The key feature that is mostly offered by these simulators includes the ability to model gas adsorption either as a single-component or multi-component fluid. Almost all of the mentioned commercial simulators have the ability to model gas adsorption using Langmuir isotherm for single-component and using the extended Langmuir isotherm for multi-component systems. The PSU-COALCOMP simulator can additionally model multi-component gas adsorption using the ideal adsorbed solution (IAS). In terms of the reservoir model description, the available simulators can model single porosity (SP), dual porosity–single permeability (DP-SK) and dual porosity–dual permeability (DP-DK).

A general overview of the main features of the simulation packages available for shale gas simulation has been provided by Andrade et al. (2011) (see Tables 3.1 and 3.2).

Table 3.1 Overview of main features used in shale gas reservoir simulators part one (Andrade et al. 2011)

Software	Commercial	Non-commercial	Dimension	Solution method		Formulation	Num. phases		Num. wells	
				Num	Analytical		Single	Multi	Single	Multi
ECLIPSE	X		3D	X		Fully implicit, IMPES, AIM		X		X
CMG	X		3D	X		Explicit, Fully implicit, AIM		X		X
UTCHEM		X	3D	X		IMPES		X		X
PMTx	X		N/A		X	N/A	X		X	
COMET3	X		3D	X		Fully implicit		X		X
PSU-COALCOMP		X	3D	X		Fully implicit		X		X
GCOMP		X	3D	X		NR		X		X

AIM Adaptive implicit mode, *ARI* Advanced Resources International, *DP* Dual porosity, *DK* Dual permeability, *MIC* Multiple interacting continua, *NR* No record, *Num* Numerical, *N/A* Not applicable, *R* Peng Robinson, *R–K* Redlich–Kwong, *SK* Single permeability, *SP* Single porosity, *S–R–K* Soave–Redlich–Kwong, *TP* triple porosity, *Z–J–R–K* Zudkevitch–Joffe–Redlich–Kwong

Table 3.2 Overview of main features used in shale gas reservoir simulators part two

Software	Solid adsorption modelling	Compositional model	Reservoir model	Adsorption/desorption			EOS	Enhanced recovery	LGR
				Instant sorption	Unsteadystate	Pseudo-steady state			
ECLIPSE	Ext. Langmuir	Eclipse 300	SP, DP-SK, DP-DK	X	X	X	P-R, R-K, S-R-K, Z-J-R-K	X	X
CMG	Ext. Langmuir	GEM	TP-DP, DP-DK, MIC, subdomain, DP		X	X	P-RS-R-K	X	X
UTCHEM	Langmuir isotherm	X	TP-DK DP-DK		NR	NR	–	NR	X
PMTx	X	NR	DP		X	X	Dranchuk and Abou-Kassem	N/A	N/A
COMET3	Ext. Langmuir	X	TP-DK			X	–	X	X
PSU-COALCOMP	IAS/Lang. Isotherm	X	DP-DK, TP-DK	NR	NR	NR	P-R	X	NR
GCOMP	NR	X	DP-DK	NR	NR	NR	NR	X	NR

References

Al-otaibi A, Studies T, Wu Y (2011) An alternative approach to modeling non-Darcy flow for pressure transient analysis in porous and fractured reservoirs. Soc Pet Eng, SPE, p 149123

Andrade J, Civan F, Devegowda D, Sigal R (2010) Accurate simulation of shale-gas reservoirs. SPE Annu, 19–22. https://doi.org/10.2118/135564-MS

Andrade J, Civan F, Devegowda D, Sigal R (2011) Design and examination of requirements for a rigorous shale-gas reservoir simulator compared to current shale-gas simulators. SPE Pap. https://doi.org/10.2118/144401-MS

Aziz K, Settari A (1979) Petroleum reservoir simulation. Chapman & Hall

Barree RD, Conway MW (2004) Beyond beta factors: a complete model for Darcy, Forchheimer, and Trans- Forchheimer flow in porous media. SPE 89325 8. https://doi.org/10.2523/89325-MS

Barree RD, Conway MW (2009) Multiphase Non-Darcy flow in proppant packs. SPE Prod Oper. 257–268. https://doi.org/10.2118/109561-MS

Belhaj HA, Agha KR, Nouri AM, Butt SD, Islam MR (2003) Numerical and experimental modeling of non-Darcy flow in porous media. Am Caribb Pet Eng Conf, SPE Lat. https://doi.org/10.2118/81037-MS

Bennethum LS, Murad MA, Cushman JH (1997) Modified Darcy's law, Terzaghi's effective stress principle and Fick's law for swelling clay soils. Comput Geotech 20:245–266. https://doi.org/10.1016/S0266-352X(97)00005-0

Choi ES, Cheema T, Islam MR (1997) A new dual-porosity/dual-permeability model with non-Darcian flow through fractures. J Pet Sci Eng 17:331–344. https://doi.org/10.1016/S0920-4105(96)00050-2

Cipolla CL, Lolon EP, Erdle JC, Tathed V (2009) Modeling well performance in shale-gas reservoirs. SPE 125532:19–21. https://doi.org/10.2118/125532-MS

Cooke CE (1973) Conductivity of fracture proppants in multiple layers. J Pet Technol 25:1101–1107. https://doi.org/10.2118/4117-PA

Devegowda D, Civan F, Sigal R (2014) Simulation of shale gas reservoirs incorporating appropriate geometry and the correct physics of capillarity and fluid transport. Project 09122.11.FINAL.RPSEA. http://www.rpsea.org/media/files/project/d376660e/09122-11-PFS-Simulation_Shale_Gas_Reservoirs_Incorporating_Correct_Physics_Capillarity_Fluid_Transport-05-21-15.pdf

Dontsov EV, Peirce AP (2015) Proppant transport in hydraulic fracturing: crack tip screen-out in KGD and P3D models. Int J Solids Struct 63:206–218. https://doi.org/10.1016/j.ijsolstr.2015.02.051

Ertekin T, Abou-Kassen JH, King GR (2001) Basic applied reservoir simulations. Society of Petroleum Engineers

Ewing RE, Lazarov R, Lyons SL, Papavassiliou DV, Pasciak J, Qin G (1999) Numerical well model for non-Darcy flow through isotropic porous media. Comput Geosci 3:185–204

Firoozabadi A (1999) Thermodynamics of hydrocarbon reservoirs. McGraw-Hill Education, USA

Geertsma J (1974) Estimating the Coefficient of Inertial Resistance in Fluid Flow Through Porous Media. Soc Pet Eng J 14:1–6. https://doi.org/10.2118/4706-PA

Heinemann ZE, Brand CW, Munka M, Chen YM (1991) Modeling reservoir geometry with irregular grids. SPE Reserv Eng 6:225–232. https://doi.org/10.2118/18412-PA

Irmay S (1958) On the theoretical derivation of Darcy and Forchheimer formulas. Trans Am Geophys Union 39:702. https://doi.org/10.1029/TR039i004p00702

Jayakumar R, Sahai V, Boulis A (2011) A better understanding of finite element simulation for shale gas reservoirs through a series of different case histories. SPE Middle East Unconv Gas Conf Exhib, Proc. https://doi.org/10.2118/142464-MS

Lai B, Miskimins JL, Wu Y (2012) Non-Darcy porous media flow according to the Barree and Conway Model: laboratory and numerical modeling studies. Society of Petroleum Engineers.doi:10.2118/122611-PA

Lai B, Miskimins JL, Wu Y-S (2013) Non-Darcy porous-media flow according to the Barree and Conway model: laboratory and numerical-modeling studies. Soc Pet Eng J 17:70–79. https://doi.org/10.2118/122611-PA

Li D, Engler TW (2001) Literature review on correlations of the non-Darcy coefficient. SPE Permian Basin Oil Gas Recover Conf, 1–8. https://doi.org/10.2118/70015-MS

Liu X, Civan F, Evans RD (1995) Correlation of the non-Darcy flow coefficient. J Can Pet Technol 34:50–54. https://doi.org/10.2118/95-10-05

Logan RW, Lee RL, Tek MR (1985) Microcomputer gas reservoir simulation using finite element methods. https://doi.org/10.2118/14449-MS

Martins JP, Milton-Tayler D, Leung HK (1990) The effects of non-Darcy flow in propped hydraulic fractures. Society of Petroleum Engineers. doi:10.2118/20709-MS

Moridis GJ, Blasingame TA, Freeman CM (2010) Analysis of mechanisms of flow in fractured tight-gas and shale-gas reservoirs. SPE Lat Am Caribb Pet Eng Conf Proc 2:1310–1331. https://doi.org/10.2118/139250-MS

Nacul EC (1991) Use of domain decomposition and local grid refinement in reservoir simulation. Stanford University, Stanford

Neyval CR, Souza AF, De Lopes RHC (2001) Petroleum reservoir simulation using finite volume method with non -structured grids and parallel distributed computing. 22nd CILANCE, Campinas, Brasil, November 2001. http://www.inf.ufes.br/∼alberto/papers/cil491.pdf

Nguyen T (1986) Experimental study of non-Darcy flow through perforations. Society of Petroleum Engineers. doi:10.2118/15473-MS

Palagi CL, Aziz K (1994) Use of Voronoi grid in reservoir simulation. SPE Adv Technol Ser 2:69–77. https://doi.org/10.2118/22889-PA

Rubin B (2010) Accurate simulation of non Darcy flow in stimulated fractured shale reservoirs. SPE Conf, 1–6. https://doi.org/10.2118/132093-MS

Scheidegger AE (1974) The physics of flow through porous media, 3rd edn. University of Toronto Press, Toronto and Buffalo

Shiozawa S, McClure M (2016) Simulation of proppant transport with gravitational settling and fracture closure in a three-dimensional hydraulic fracturing simulator. J Pet Sci Eng 138:298–314. https://doi.org/10.1016/j.petrol.2016.01.002

Sun J, Schechter D, Texas A, Huang C (2016) Grid-sensitivity analysis and comparison between unstructured perpendicular bisector and structured tartan/local-grid-refinement grids for hydraulically fractured horizontal wells in eagle ford formation with complicated natural fractures. Society of Petroleum Engineers. doi:10.2118/177480-PA

Tsai K, Fonseca E, Lake E, Degaleesan S (2013) Advanced computational modeling of proppant settling in water fractures for shale gas production. SPE J 18:50–56. https://doi.org/10.2118/151607-PA

Wu YS, Lai B, Miskimins JL, Fakcharoenphol P, Di Y (2011) Analysis of multiphase non-Darcy flow in porous media. Transp Porous Media 88:205–223. https://doi.org/10.1007/s11242-011-9735-8

Zhang L, Li D, Wang L, Lu D (2015) Simulation of gas transport in tight/shale gas reservoirs by a multicomponent model based on PEBI grid. J Chem

Zhang Z, Chen Q (2007) Comparison of the Eulerian and Lagrangian methods for predicting particle transport in enclosed spaces. Atmos Environ 41:5236–5248. https://doi.org/10.1016/j.atmosenv.2006.05.086

Chapter 4
Production Performance Analysis of Shale Gas Reservoirs

Abstract Prediction of production performance in shale gas reservoirs can be achieved through a number of techniques designed to produce information about the estimated ultimate recovery and also about the reservoir parameters such as permeability, skin and fracture properties. These methods sometimes involve obtaining well production data and making future predictions from them. This chapter looks at some of the analytical and semi-analytical models for production performance calculations associated with shale gas reservoirs. The techniques discussed in this chapter include decline curve analysis, pressure transient analysis and rate transient analysis.

4.1 Decline Curve Analysis and Prediction of Future Potential

Production decline curve analysis mainly consists of trying to predict the estimated ultimate recovery (EUR). This is achieved through analysing well production data and predicting well performance during the life of the well. Due to the different flow regimes that are experienced during the life of a shale gas well, accurate analysis is essential to estimate the production performance and eventually the expected ultimate recovery. Decline curve analysis provides simple and practical method for making such analysis. Production decline analysis used in conventional oil and gas fields (Arps 1945; Duong 2011; Fetkovich 1980) can also be applied in the analysis of shale gas wells. Besides these, other decline curve analyses such as power law exponential decline, stretched exponential (SEDM) and logistic growth model (LGM) have all been used to analyse and predict EUR.

J. Gholinezhad et al., *Challenges in Modelling and Simulation of Shale Gas Reservoirs*, SpringerBriefs in Petroleum Geoscience & Engineering,
https://doi.org/10.1007/978-3-319-70769-3_4

4.1.1 Arp's Decline Curve Analysis

Arp's (1945) proposed a method of analysing production performance based on empirical approach. Several assumptions were made in the derivation of the general Arp's equation that is used in the prediction of the EUR. These assumptions include the well to be producing at or near capacity and at a constant bottomhole pressure. For shale gas reservoirs, where transient flow is dominant, Arp's method is proven not to be suitable. This is because Arp's method is only useful when the reservoir is experiencing a boundary-dominated flow or is in a semi-steady state (pseudo-steady state) condition. Three forms of Arp's equation can be identified based on the value of the declining exponent b [see Eqs. (4.1)–(4.3)]. When the decline exponent b is equal to 1, Arp's equation is normally referred to as harmonic decline. Hyperbolic decline occurs when the value of b is between zero and one. Exponential decline occurs when the value of b is equal to zero. In this case, there is a linear relationship when the flow rate is plotted against time on a semi-log plot or the cumulative production is plotted against flow rate on a Cartesian plot. Three forms of Arp's equation are illustrated in Fig. 4.1.

Harmonic equation

$$q = \frac{q_i}{(1 + D_i t)} \tag{4.1}$$

Hyperbolic equation

$$q = \frac{q_i}{(1 + bD_i t)^{1/b}} \tag{4.2}$$

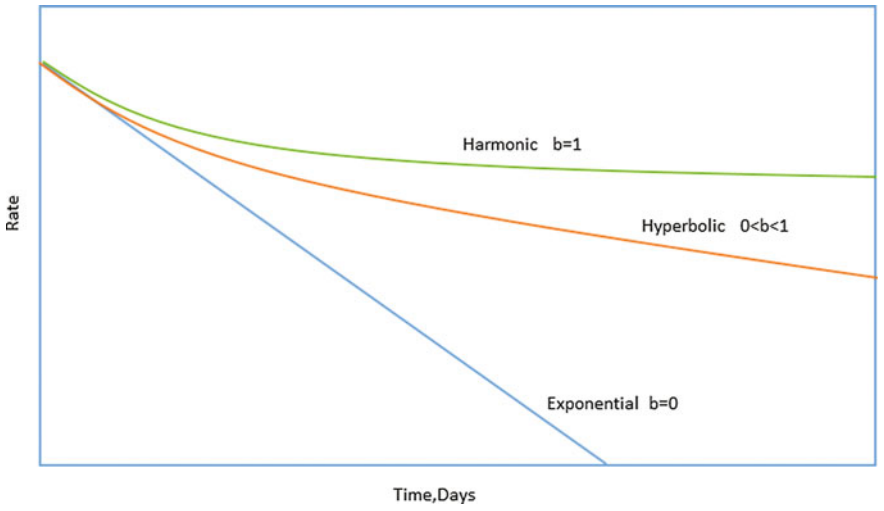

Fig. 4.1 Three types of Arp's decline

Exponential equation

$$q_i = q_i e^{-Dt} \tag{4.3}$$

where D_i is the initial decline rate, t is the time, b is the degree of curvature of the curve and q_i is the initial rate.

4.1.2 Power Law Exponential Decline (PLE)

The power law exponential decline is much suited to production forecast of shale or tight gas reservoirs. This is because it does not assume boundary-dominated flow as compared to the Arp's model. The power law exponential decline was introduced by Ilk et al. (2008). The model assumes that the loss ratio follows a power law function at early time and becomes constant at late time. The power law exponential loss ratio is given as

$$D = D_\infty + D_1 t^{-(1-n)}. \tag{4.4}$$

With final PLE rate–time relation as

$$q = q_i \exp\left(-D_\infty t - \frac{D_1}{n} t^n\right) \tag{4.5}$$

where D is Arp's "loss ratio", D_∞ is decline constant at "infinite time", D_1 is decline constant "intercept" at 1 time unit and n is time exponent.

From the equation provided by Ilk et al. (2008), there are four parameters that will have to be fitted to the production data by fine-tuning. Other factors also present some difficulties when using the power law as outlined by Seshadri and Mattar (2010). There is confusion about D_i being instantaneous decline at $t = 1$ divided by n rather than an initial instantaneous decline. Also, q_i and D_i are so large that they tend to lose their meaning. Long-term forecasts are sensitive to the choice of n; however, with power law exponential decline, many values can reasonably fit a data set.

4.1.3 Stretched Exponential Decline Model (SEDM)

Similar to the power law exponential model is the stretched exponential decline proposed by Valko (2009). Due to the limited number of parameters used in the equation, the SEDM is a much more suitable model to be used in unconventional reservoirs. In terms of its application in shale gas/tight gas, it is a much preferred

model compared with Arp's model since it can be used both in a transient flow regime and boundary-dominated flow regime. When compared with the power law exponential model, the D_∞ is considered to be zero and one key advantage over the PLE model is the provision of the cumulative–time relation (Kanfar and Wattenbarger 2012). With this relation, data fitting of cumulative production can be achieved which enables regression to be easily done as compared to when the regression is done on the scattered production rate trends.

The rate–time relation is given as

$$q = q_0 \exp\left(\left(-\frac{t}{\tau}\right)^n\right). \tag{4.6}$$

And the cumulative–time relation is also given as

$$Q = \frac{q_0 \tau}{n}\left\{\Gamma\left(\frac{1}{n}\right) - \Gamma\left(\frac{1}{n}, \left(\frac{\tau}{n}\right)^n\right)\right\} \tag{4.7}$$

where q_0 is the flow rate at time $t = 0$, Q is the cumulative production, τ is the characteristics time parameter for SEPD model, in days.

The first and second terms inside the brackets refer to the complete and incomplete gamma function, respectively.

4.1.4 Duong's Model

Duong (2011) method has been developed specifically for reservoirs that have low permeability like shale gas/tight gas. For such wells, fracture flow is dominant and matrix contribution to flow is negligible. This means for wells with transient flow periods, estimation of EUR can be done using Duong's method. Duong (2011) developed the model based on the fact that the production rate and time have a power law relation or form a straight line when plotted on a log-log scale (Kanfar and Wattenbarger 2012). Studies by Duong (2011) showed a straight line in all unconventional reservoir cases studied when a log–log plot of rate over cumulative production was constructed against time. The liquid content, operational conditions, fracture stimulation and the reservoir rock characteristics can all be determined from the slope and intercept of this straight line.

Cumulative rate and production rate are defined by the following Duong's equations:

$$q = q_1 t(a, m) + q_\infty \tag{4.8}$$

$$Q = \frac{q_1 t(a, m)}{a t^{-m}} \tag{4.9}$$

where

$$t(a,m) = t^{-m} \exp\left(\frac{a}{1-m}\left(t^{1-m} - 1\right)\right) \tag{4.10}$$

q_∞ is the flow rate at time $t = \infty$, q_1 is the flow rate at $t = 1$, m is the slope, a is the intercept constant.

q_∞ can be either negative or positive and this was added by Duong to provide a better fit to some field data that showed an intercept instead of a straight line to the origin when rate, q was plotted against the Duong's time function $t(a,m)$ (Kanfar and Wattenbarger 2012).

4.2 Pressure Transient Analysis in Complex Fracture Networks

Key characteristics of shale such as low permeability within the range of 1–100 nano-Darcy imply considerable time for flow to reach the boundaries of the reservoir, thus flow normally occurs in a transient flow regime. In order to fully comprehend the production performance of such reservoirs and especially for shale reservoirs where the reservoir is hydraulically fractured with long horizontal wells, the pressure transient behaviour needs to be understood. Also, for such tight and multiple transverse fractures coupled with a horizontal well, pressure transient analysis is useful for evaluating the various fracturing techniques or treatments. The use of pressure transient analysis provides reasonable estimates of the reservoir properties and fracture parameters needed for the estimation of the production performance of the well.

An important concept when undertaking transient analysis involves being able to clearly identify the different flow regimes and their characteristic trends from the production data (Vera and Ehlig-Economides 2014). The fluid flow regime that occurs in a reservoir is dependent on several factors including, but not limited to, the time and can occur differently at different times. Also, the size and shape of the reservoir account for the flow pattern of the fluid. In addition, depending on the wellbore type whether vertical or horizontal, several flow regimes may be encountered. The pressure transient characteristics involve mostly the derivation of pseudo-pressure derivative plot; this is seen as an efficient way of analysing flow regimes than the use of pseudo-pressure curves (Kim et al. 2014). The different times for derivative plots are usually broken down into early time, middle time and late time.

The understanding of pressure transient behaviour of hydraulically fractured horizontal wells is important for characterising the reservoir and the hydraulic fractures. This is supported by the fact that the production of hydraulically fractured

horizontal wells takes place under long transient flow regimes periods; hence, the production performance of these wells is often dominated by the characteristics of the transient flow regimes (Medeiros et al. 2006, 2007).

4.2.1 Flow Regimes of MTFHW in Shale Gas Reservoirs

Multiple transverse fracture horizontal well (MTFHW) drilling has become an inextricable element in the production of gas from the ultra-tight shale matrix. The success of shale gas drilling is primarily due to the advancement seen in the combination of horizontal drilling coupled with hydraulic fracturing.

In horizontal fracture drilling, fracturing can be implemented in two forms: longitudinal or transverse. These two cases are shown in Fig. 4.2. Most shale gas reservoirs use the transverse method for horizontal fracture drilling (Wei and Economides 2005). The choice of MTFHW is based on the optimization of the contact area between the reservoir and the wellbore. Different flow regimes are associated with either of these types of fracturing, which can normally be identified by the analysis of recorded pressure data.

Availability of recorded pressure data on a regular basis ensures long-term production data to be analysed in a more confident manner compared with when there are no pressure data available.

Many authors have studied the different flow regimes that are associated especially with a fractured horizontal gas wells. The presence of the multi-stage fractures, their interaction with reservoir natural fractures and the different flow regimes associated with it make the pressure transient analysis in shale gas reservoirs even more complicated (Kim et al. 2014).

Al-Kobaisi et al. (2006) provided a study on the early time flow regimes and the responses of the pressure transient analysis at that time stage. They identified several flow regimes for a multiple transverse fractured horizontal wells as fracture

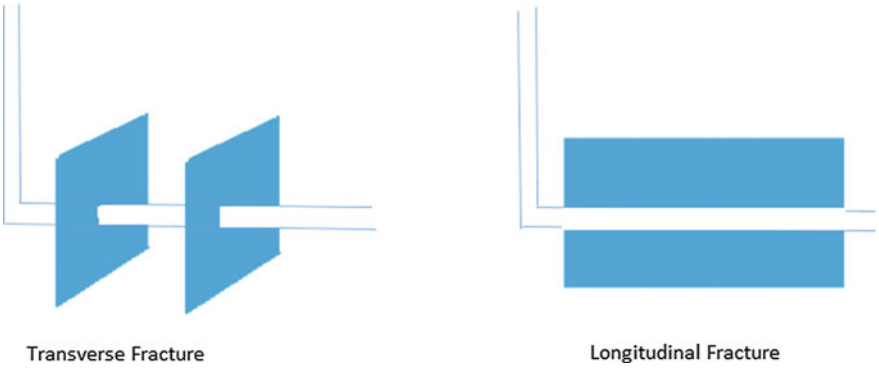

Fig. 4.2 Horizontal well with transverse and longitudinal fracture

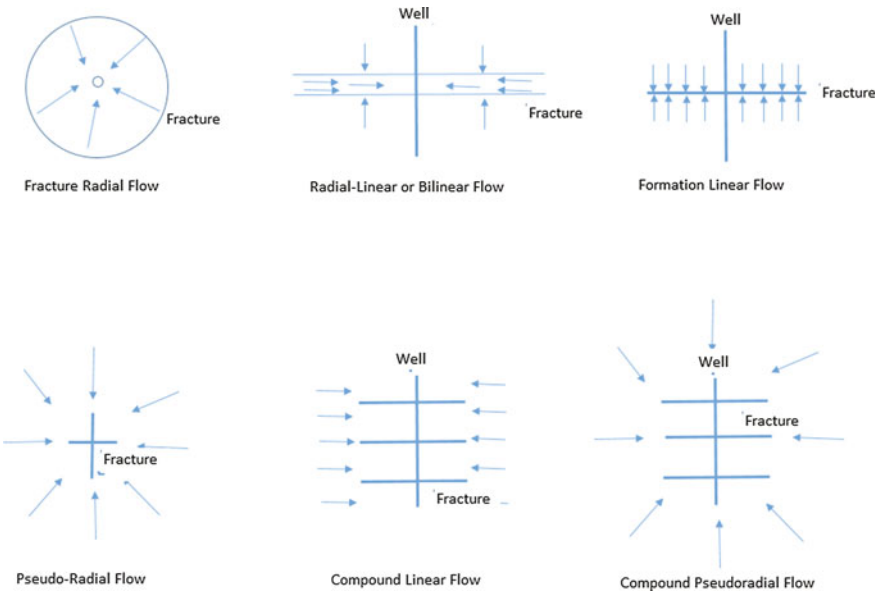

Fig. 4.3 Flow regimes as identified by Al-kobaisi for a MTFHW

radial, radial-linear flow and bilinear flow (Fig. 4.3). Their studies also showed that fracture geometry and the location of the well affect to a large extent the flow into a horizontal well fracture that results in different early time flow regimes from that of vertical well fracture.

Wang et al. (2013), identified five basic flow regimes of MTFHW in their studies of pressure transient analysis including early time linear flow, pseudo-pseudo-steady state flow, compound linear flow, pseudo-radial flow and boundary-dominated flow. They demonstrated throughout their work using numerical analysis that the early time linear flow that occurs before fracture interference and fracture interference dominated pseudo-steady state flow regimes are key due to the fact that oil in place calculations depend on those flow regimes.

For vertical fractured wells, the semi-analytical model presented by Cinco et al. (1978) provided a standard model for other authors to investigate the pressure transient responses of hydraulically fractured vertical wells and later horizontal wells (Al-Kobaisi et al. 2006). The semi-analytical model uses a numerical method to obtain pressure distribution along the fractures by coupling the analytical solutions for the reservoir and the fracture flow. Further studies by Cinco and Samaniego (1981) identified four flow regime periods which included fracture linear flow, bilinear flow, formation linear flow and pseudo-radial flow. The finite conductivity fractures were shown to display at early times a fracture linear and bilinear flow regimes in addition to the reservoir linear and pseudo-radial flow regimes for infinite conductivity fractures. Raghavan et al. (1997), Rodriguez et al. (1984a, b), Schulte (1986) also studied the pressure transient responses of finite and

infinite conductivity vertical fractures by identifying different flow regimes that are associated with it.

Kruysdijk and Dullaert (1989) conducted numerical simulation studies to identify the different complex flow regimes that are normally exhibited by a tight/shale gas system. Their approach provided key understanding in terms of the different flow regimes surrounding horizontal wells with multiple transverse fractures. Numerical simulation studies conducted by the authors demonstrated that the dominant flow in the early time is linear flow which is perpendicular to the fracture faces until the neighbouring fractures begins to interfere at which point a compound linear flow regime occurs, as shown in Fig. 4.4.

For a hydraulically fractured horizontal wells, Larsen and Hegre (1991, 1994) studied the pressure transient behaviour by providing a description of the various transient flow regimes. The flow regimes were described by analytical solutions developed by the authors. Flow periods exhibited by both single and multi-fractured horizontal well under various ideal conditions were discussed by the authors. The key flow regimes identified for a transverse or radial fracture included fracture radial, radial-linear, formation linear and pseudo-radial fractures, whereas for longitudinal fractures, the early flow regimes were fracture linear and bilinear flow.

Several factors affect the pressure transient response of a well. These factors include, among others, the number of fractures, the location and also orientation of the fractures. Raghavan et al. (1997) studied the effects of all of these factors on the pressure transient responses mostly in conventional reservoirs. A mathematical model was developed by the authors to describe the characteristic responses of a multiple fractured horizontal well. The model assumes distinct fractures are created and that each fracture has distinct properties. The authors identified three main flow regimes which primarily consisted of an early time flow period. For this flow period, the system is assumed to behave as if it had n number of fractures. The second flow regime reflects an interference between the neighbouring fractures and

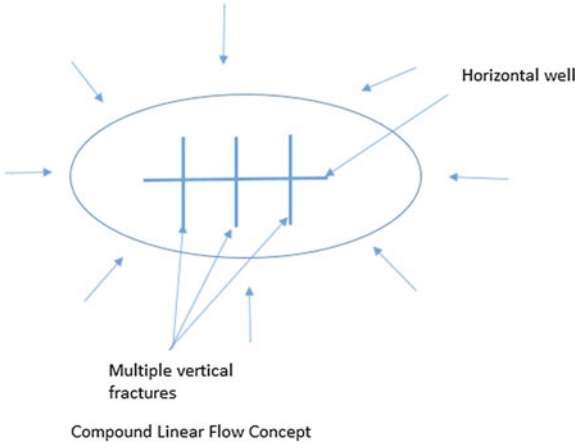

Fig. 4.4 Compound linear flow concept by Kruijsdik and Dullaert

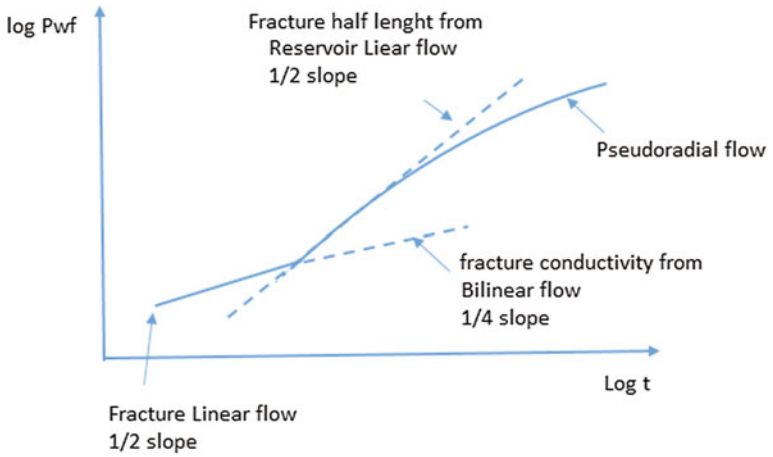

Fig. 4.5 Fracture property estimation from characteristics of PTA flow regimes

finally a late flow period during which the composite fracture system behaves as a single fracture length equal to the spacing between the outermost fractures.

A hybrid numerical/analytical model was developed by Al-Kobaisi et al. (2006) to represent the responses of pressure transient for a finite conductivity fracture intercepted by a horizontal well. The model developed combines a numerical fracture model together with an analytical reservoir model to develop a rigorous horizontal well fracture model of finite conductivity. The characteristics of the pressure transient flow regimes are used to interpret or estimate the different fracture properties as shown in Fig. 4.5.

The effects of different fracture properties on the pressure transient characteristics of a single, finite conductivity horizontal well fracture were also studied. Different fracture properties can cause different flow regimes to be created in horizontal well fractures that are different to those of vertical well fractures. With the focus on a single horizontal well fracture model, Al-Kobaisi et al. (2006) showed that fracture geometry and the fracture properties greatly affect the flow behaviour of the well.

A semi-analytical model was developed by Medeiros et al. (2006) which can model the overall range of the flow regime that surrounds the multiply fractured horizontal well system. Dual permeability region near the fracture faces was also considered to represent a complex fractured region around the hydraulic fracture. Medeiros et al. (2006) approach provides an alternative to numerical simulation of horizontal well pressure transient responses in a heterogeneous formation. Pressure and pressure-derivative curves were used by Medeiros et al. (2008) to analyse the effects of matrix permeability, fracture spacing and well spacing. Their discussion focussed on the performance and productivity of fractured horizontal wells in heterogeneous, tight gas formations. The different flow regimes that characterise a homogeneous tight gas system are illustrated in Fig. 4.6.

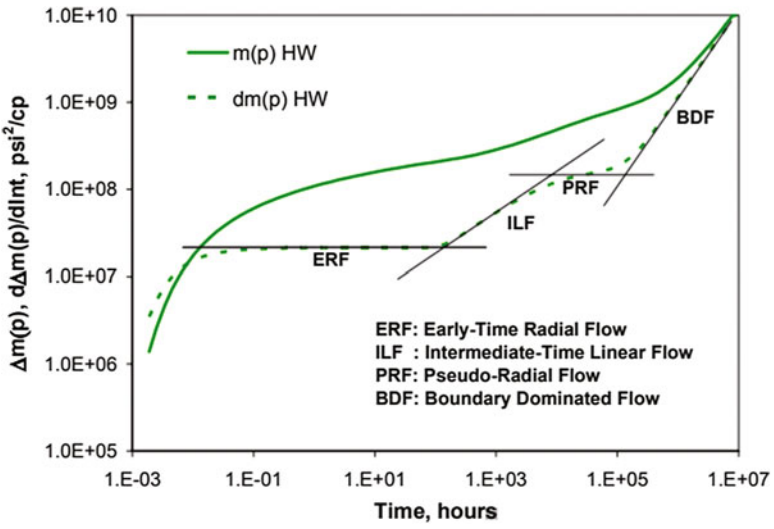

Fig. 4.6 Flow regimes of a homogeneous tight formation (Medioris et al. 2006)

Similarly, Freeman et al. (2009) studied the different flow regimes associated with multiple fractured horizontal well in shale gas reservoir by using a numerical simulator. They studied the characteristics of the pressure transient at later times, that is, towards the end of the fracture storage. For the various analytical, semi-analytical and empirical models used to characterise the pressure transient behaviour of shale gas systems with horizontal well and multiple fractures, there is little agreement concerning the large-scale flow behaviour, and in particular, the dominant flow regime and whether reservoir properties can be easily estimated from the well performance data (Freeman et al. 2009). The authors sought to show how the various reservoir and completion parameters affect the performance of a multiply fractured horizontal wells in a shale/tight gas reservoir system. Illustrations of the various flow regimes typical of a tight/shale gas system include an initial linear flow within the hydraulic fractures, compound formation linear flow and finally elliptical flow as shown in Fig. 4.7.

According to Cheng (2011), the pressure transient response for a horizontal shale gas well with multiple transverse fractures is controlled by a combination of reservoir properties and well configuration. The author investigated the behaviour of the pressure transient response under several factors and flow regimes in a Marcellus shale using properties within the range practical to Marcellus shale. Five distinctive flow regimes were identified which included fracture radial flow, bilinear flow, inner linear flow, quasi-steady state flow and late-time outer linear flow. Figure 4.8 shows the different flow regimes.

Production from a multiple fractured horizontal well in a shale gas reservoir was modelled by Brohi et al. (2011) by developing a linear composite model that included a dual porosity inner zone. Three key linear flow regimes were identified

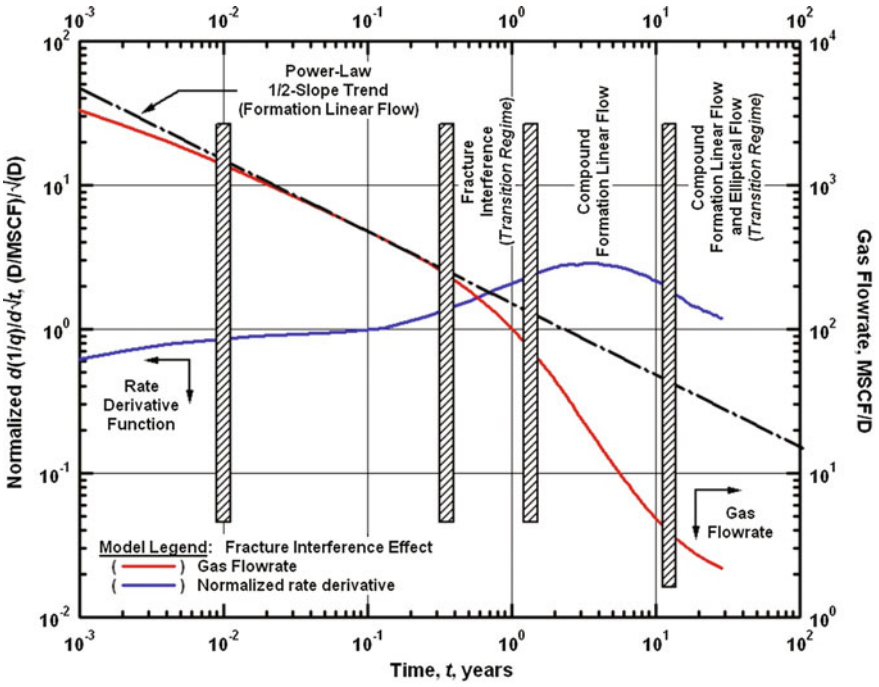

Fig. 4.7 Illustration of different flow regimes of a horizontal gas well with multiple (transverse) fractures (Freeman et al. 2009)

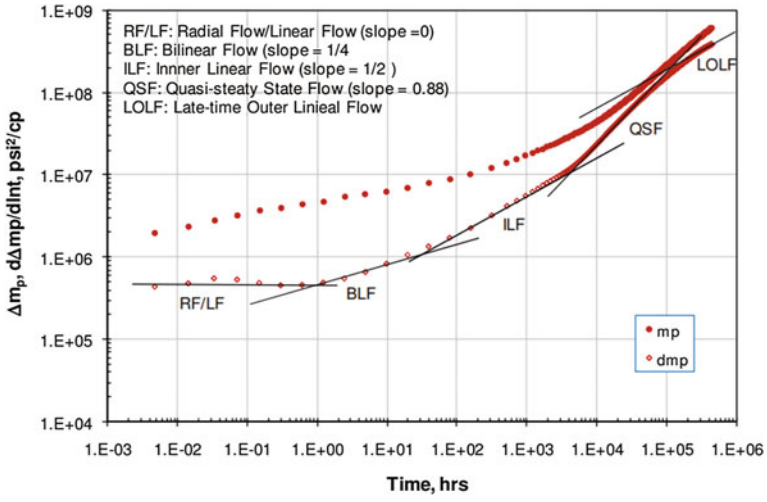

Fig. 4.8 Representation of different flow regimes of MTFHW by Cheng (2011)

by the authors within this model which included a linear flow at the initial stage where flow occurs from the fractures into the wellbore, this was then followed by linear flow in the matrix to the fractures and a linear flow in the outer single porosity to the inner reservoir. The five distinct flow regimes observed by the authors through their numerical simulation included fracture linear, fracture pseudo-steady state, matrix linear and fracture pseudo-steady state, matrix pseudo-steady state and fracture pseudo-steady state and formation linear.

Guo et al. (2014) identified possible nine flow regimes that can be associated with transient flow behaviour of a multiple hydraulically fractured horizontal well. These are based on the characteristics of the type curve. Their paper provided an improved multi-mechanism model for a finite conductivity hydraulic fracture with an account of diffusive flow and desorption within the matrix by investigating the pressure transient characteristics responses. The flow regimes identified included:

1. Wellbore storage period which is purely dominated by the effects of wellbore storage. During this period, the derivative curve together with the pseudo-pressure is represented by a unit slope.
2. Transitional flow period is represented by a hump in the curve for the derivative and pseudo-pressure. The hump is normally attributed to the combination of skin as well as wellbore storage effects.
3. Bilinear flow period is shown by a one-fourth slope straight line in both pseudo-pressure and derivative curves. Additionally, there is a simultaneous linear flow within the hydraulic fractures and reservoir.
4. First reservoir linear flow period is represented by a half slope in both the derivative and the pseudo-pressure curves. During this period, it is anticipated to be no interactions between other neighbouring hydraulic fractures.
5. First pseudo-radial flow period existence is dependent on the fracture length and the fracture spacing. This is marked by a plateau in the derivative curve.
6. Second reservoir linear flow period is also marked by half slope in both the derivative and pressure curves. Interference between the neighbouring hydraulic fractures will be felt at this stage.
7. Second pseudo-radial flow of natural fractures is represented by a flat behaviour of the derivative curves.
8. Inter-porosity diffusivity flow period representing flow between the matrix and the natural fracture is shown as a dip in the pressure-derivative plot.
9. Compound pseudo-radial flow period is marked by a flat behaviour of the derivative plot.

The different flow regimes identified by Guo et al. (2014) are shown in Fig. 4.9.

Both production data analysis (PDA) and pressure transient analysis (PTA) are used in the industry to analyse the behaviour of the well. PTA and PDA are performed independently thereby different interpretations from different people and software programs are produced. This often leads to conflicting results (Ehlig-Economides et al. 2009). Ehlig-Economides et al. (2009), therefore proposed a combination of PTA data and long-term PDA for analysis instead of stand-alone PTA or PDA. Their method supports flow regimes diagnosis for model

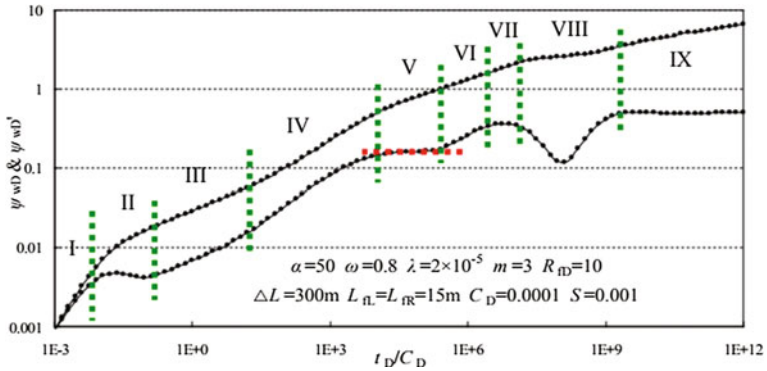

Fig. 4.9 Type curves for a horizontal well intercepted by multiple finitely conductive fractures (Guo et al. 2014)

identifications and helps to characterise the well and the reservoir beyond it. The authors improved the use of rate-normalised pressure (RNP) data to obtain a much more conclusive PDA. The combined PTA and PDA analysis is displayed on a plot of pressure change and its derivative from build-up (BU), and also the RNP and its derivative from injection/production data. The combined BU-RNP method provides a consistent and complete analysis compared to the stand-alone PTA or PDA by combining the short-duration PTA and long-term PDA data. Figure 4.10 illustrates a combined build-up and rate normalised pressure plot for a well with a long build-up.

The various flow regimes presented by different authors using PTA are summarized in Table 4.1.

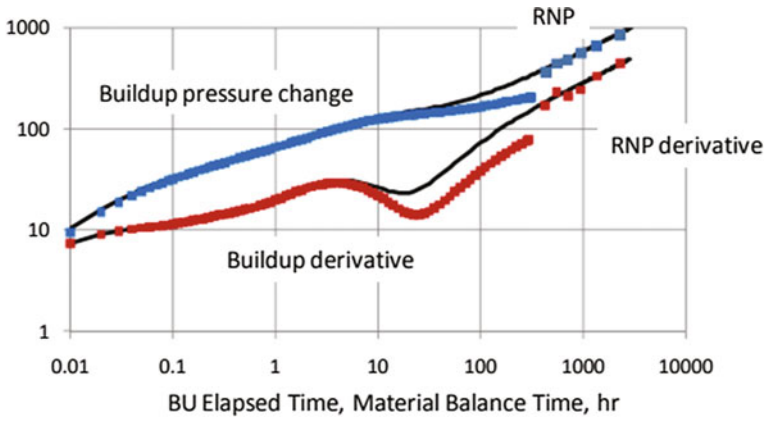

Fig. 4.10 Combined build-up and rate normalised plot (Ehlig-Economides et al. 2009)

Table 4.1 Summary of different flow regimes for fractured gas well

Authors	Well type	Flow regimes
Cinco et al. (1978)	Vertical fractured well	Fracture linear flow, bilinear flow, formation linear flow and pseudo-radial flow
Freeman et al. (2009)	MTFHW	Formation linear, compound formation linear, elliptical flow
Al-Kobaisi et al. (2006)	MTFHW	Fracture radial flow, radial-linear or bilinear flow, formation linear flow, pseudo-radial flow, compound linear flow, compound pseudo-radial flow
Cheng (2011)	Hydraulically fractured horizontal shale gas well	Radial flow/linear flow, bilinear flow, inner linear flow, quasi-steady state flow, late-time outer linear flow
Wang et al. (2013)	MTFHW	Early time linear or bilinear flow, pseudo-pseudo-steady state flow, compound linear flow, pseudo-radial flow and boundary-dominated flow
Guo et al. (2014)	MTFHW	Wellbore storage period, transition flow period, bilinear flow period, first reservoir linear flow period, first pseudo-radial flow period, second reservoir linear flow period, second pseudo-radial flow period, inter-porosity diffusive flow period and complex pseudo-radial flow period
Brohi et al. (2011)	Multiply fractured horizontal well	Fracture linear, fracture pseudo-steady state, matrix linear and fracture pseudo-steady state, matrix pseudo-steady state and fracture pseudo-steady state and formation linear
Clarkson (2011)	MFHW	Bilinear, early linear, early elliptical/ pseudo-radial, fracture interference and compound(late) linear

4.2.2 Straight Line Analysis of Pressure Transient Responses

The straight line analysis technique is often used to estimate the properties of the fracture and also the determination of oil in place in the stimulated reservoir volume by expressing a plot of straight line equation with slope and intercept. A set of equations are used in the straight line analysis to determine fracture half length, stimulated pore volume, formation permeability and reservoir pore volume among others. One of the key advantages of the use of straight line analysis is its simplicity in implementation and identification of the flow regime. Given the flow regimes exhibited by a MTFHW, the pressure transient mathematical equation dominating each flow regime is presented from (Wang et al. 2013).

Early Time Linear Flow

The early time linear flow period is governed by a pressure response equation given as

$$\Delta p_{wf} = 4.0641 \frac{qB}{nhx_f} \sqrt{\frac{\mu t}{k\varphi c_t} + \frac{141.2qB\mu}{kh}\left[s + s_{\mathrm{p}}\right]} \tag{4.11}$$

where s is the fracture surface skin and s_{p} is the pseudo-skin factor. The early time linear flow period is characterised by a half slope straight line on the derivative plot. The slope from Eq. (4.11) can be defined as

$$m = 4.0641 \frac{qB}{nhx_f} \sqrt{\frac{\mu}{k\varphi c_t}} \tag{4.12}$$

From Eq. (4.12), the fracture half length x_f can be determined. The time at the end of the early time linear flow is determined as

$$t_e = \frac{x_s^2 \varphi \mu c_t}{4(0.029)^2 k} \tag{4.13}$$

where x_{s} is given as the fracture spacing in ft.

Pseudo Pseudo-Steady State Flow

The pressure drop during this flow regime is given by

$$\Delta p_{wf} = \frac{qBt}{24V_{\mathrm{p}}c_t} + \Delta p_{\mathrm{int}} \tag{4.14}$$

where Δp_{int} is the longitudinal intercept, V_{p} refers to the SRV pore volume. The slope is defined as

$$m_{qf} = \frac{qB}{24V_p c_t} \tag{4.15}$$

From Eq. (4.15), the SRV pore volume can be estimated.

Pseudo-Radial Flow

The pressure drop during this flow regime is given by

$$\Delta p_{wf} = \frac{162.6qB\mu}{kh}\left[\log\left(\frac{2.64 \times 10^{-4} kt}{\varphi \mu c_t r_w^2}\right) + \frac{s + s_{\mathrm{p}}}{1.1516} + 0.3513\right] \tag{4.16}$$

The formation permeability can be calculated from the slope of Eq. (4.16) as

$$\Delta p_{wf} = \frac{162.6qB\mu}{kh} \tag{4.17}$$

Pseudo-Steady State Flow

Pressure drop during the pseudo-steady state flow period is expressed as

$$\Delta p_{wf} = \frac{qBt}{24V_{\mathrm{r}}c_t} + \Delta p^*_{\mathrm{int}} \tag{4.18}$$

where $\Delta p^*_{\mathrm{int}}$ is defined as the longitudinal intercept. The reservoir pore volume V_{r} is calculated from the slope of Eq. (4.18) as

$$m_{ql} = \frac{qB}{24V_{\mathrm{r}}c_t} \tag{4.19}$$

4.3 Rate Transient Analysis in Shale Gas Reservoirs

Similar to pressure transient analysis, rate transient analysis involves analysing production data and for unconventional gas reservoirs such as tight gas or shale gas wells, this may involve characterising the different flow regimes which may be observed during production of the well. The development of permanent downhole pressure gauges has led to possible advancement in the use of RTA. Characterisation of the different flow regimes becomes useful in the determination of hydraulic fracture properties as well as reservoir properties. For instance, ultimate recovery and original gas in place can be determined from boundary-dominated flow data that is obtained from the well. Furthermore, hydraulic fracture properties such as half length, fracture permeability and conductivity as well as the matrix permeability can be determined from the transient flow data. Both flowing pressure data and production rates are used to account for the varying operating conditions of the wells (Clarkson 2011). According to Clarkson (2011), the flow geometries associated with hydraulic fracture geometries and reservoir properties are critical when interpreting rate transient of unconventional gas reservoirs.

When the pressure in the reservoir propagates away from the well during production, the flow regime associated with this is normally referred to as transient flow. Once the pressure propagation reaches the boundary of the reservoir such as a

fault or pinch out, the flow regime is normally referred to as a boundary-dominated flow regime. In terms of hydraulically fractured wells and especially for multiple fractured wells, the flow regimes sequence might be much more complex and one might require several different flow regimes to be able to characterise the reservoir for the estimation of both the fracture and reservoir properties as was also noted in Sect. 4.2.

Normalisation of the pressure data using the rate data is usually done under rate transient analysis for oil wells; however, for gas wells such as shale gas and tight gas, the bottomhole pressure is converted to a pseudo-pressure and the pseudo-pressure data are normalised using gas production data. When the bottomhole pressure data is missing, the well head pressure data can be converted to the bottomhole pressure data using a multi-phase flow well model correlations for rate transient analysis and for multi-fractured shale reservoirs, the t_{BDF} (time to reach boundary-dominated flow) and m_{LF} (slope of the straight line for linear flow regime) can be used (as seen in Fig 4.11) to characterise the SRV parameters (Bahrami et al. 2016).

The following RTA plots for characterising the SRV are made from the normalised pressure data (Bahrami et al. 2016; Malallah et al. 2007).

1. For gas wells, the normalised pseudo-pressure data should be plotted against time on a log- log scale. The linear flow regime based on 1/2 slope on the diagnostic plot can be identified. The time at which boundary-dominated flow (t_{BDF}) period starts occurs at higher values 1/2 slope.
2. Also, the normalised pseudo-pressure data plotted against time function can provide the slope of the linear flow regime straight line (m_{LF})

Various techniques for analysing production data can be grouped under three main methods. These include straight line method, type curves and analytical/numerical simulation (Clarkson 2011; Clarkson and Beierle 2011). Gatens et al. (1989) proposed the use of type curves, analytical model and empirical equations to analyse production data.

Type curve method requires the matching of production data to empirical solutions to flow equations in dimensionless variable format (Clarkson 2011). According to Clarkson (2011), reservoir, well length or stimulation information can be obtained following a match of the dimensionless type curves by defining the dimensionless variables. For analytical/ numerical simulation model, the model is fitted to the production data by history matching and once an acceptable fitting has been achieved, production forecast can then be made either for a single or multi-well production. Straight line methods use specialty plots that transform data obtained from specific flow regimes such that a linear trend is obtained. The straight line can then be used to obtain hydraulic fracture and reservoir information. Empirical methods that are normally used in production analysis involve production forecasting to obtain estimated ultimate recovery (EUR). They include Arp's decline equations and power law exponential decline which were already discussed in Sect. 4.1.

4.4 Type Curves

The concept of type curve was introduced into the petroleum industry for constant rate solutions to diffusivity equation by Agarwal et al. (1970). Several other authors (Carter 1985; Ehlig-Economides and Ramey 1981; Fetkovich 1980; Ozkan et al. 1987; Uraiet and Raghavan 1980) have already used the concept of type curve for constant wellbore pressure. The use of superposition theory assists in using the constant rate solution interchangeably for both pressure transient analysis and that of rate transient analysis. The principle of superposition states that the total pressure drop that occurs at any time is the sum of the pressure changes caused by variable rate changes of the system. Thus, the response of the system to a number of rate changes is equal to the sum of the responses to each of the rate changes as if they were present by themselves. With this superposition principle, constant rate solutions can be used for analysing production data.

Fetkovich (1980) advanced the use of decline curve analysis by developing a strong mathematical and theoretical ground for its application unlike the Arp's equation that merely had an empirical or semi-empirical basis. Fetkovich combined the constant pressure solution to the diffusivity equation with the Arp's equation to derive a simple single-type curve. The important concept of re-initialization was also introduced by Fetkovich to DCA. It states that at any point that flow regime changes, the production data re-initialize in both time and rate. Thus, the reference pressure and rate change and the time reset back to zero.

Assuming a circular reservoir and a pseudo-steady inflow, Fetkovich (1980) proposed that

$$q_{\mathrm{i}} = \frac{kh\left(p_{\mathrm{i}} - p_{wf}\right)}{141.2\,\mu B\left[\ln\left(\frac{r_e}{r_w}\right) - 0.5\right]} \tag{4.20}$$

$$t_{\mathrm{d}} = \frac{\frac{0.00634kt}{\phi\mu c_t r_w^2}}{0.5\left[\ln\left(\frac{r_e}{r_w}\right) - 0.5\right]\left[\left(\frac{r_e}{r_w}\right)^2 - 1\right]}. \tag{4.21}$$

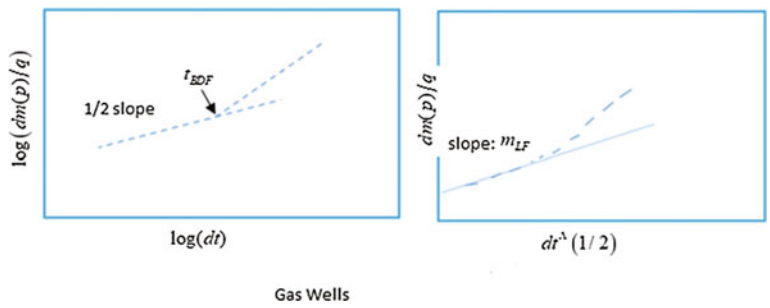

Fig. 4.11 RTA plots for characterising SRV (modified from Bahrami et al. 2016)

With

$$q_{\mathrm{Dd}} = q(t)/q_{\mathrm{i}} \tag{4.22}$$

$$q_{\mathrm{Dd}} = \frac{q(t)/kh\left(p_{\mathrm{i}} - p_{wf}\right)}{141.2\mu B\left[\ln\left(\frac{r_e}{r_w}\right) - 0.5\right]} = q_d\left[\ln\left(\frac{r_e}{r_w}\right) - 0.5\right] \tag{4.23}$$

where the dimensionless flow rate is given by q_{d},

$$q_{\mathrm{d}} = \frac{141.2q\mu B}{kh\left(p_{\mathrm{i}} - p_{wf}\right)} \tag{4.24}$$

In the above equations, q_{Dd} refers to decline curve dimensionless rate, t_{d} dimensionless time.

Figure 4.12 shows the classic Fetkovich plot with t_{Dd} versus q_{Dd} (Fetkovich et al. 1987).

With the gas system, Carter (1981) recognised that assuming very small and constant compressibility led to inaccurate results especially for gas reservoirs that produced at very high drawdown pressure. Carter (1981) therefore developed a variable λ to represent variations in the decline curves from real gas properties (Fraim and Wattenbarger 1987).

$$\lambda = \frac{\left(\mu c_g\right)_i\left(m(p_{\mathrm{i}}) - m(p_{wf})\right)}{2\left((p/z)_i - (p/z)_{wf}\right)} \tag{4.25}$$

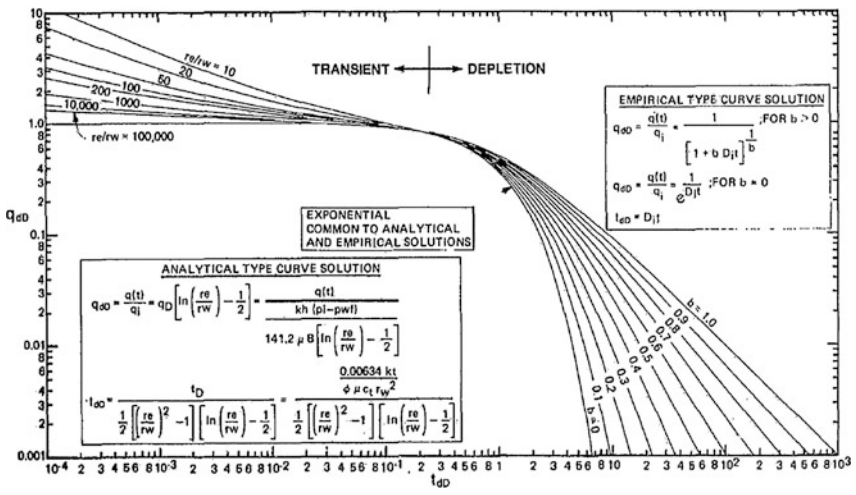

Fig. 4.12 Fetkovich type curve (Fetkovich et al. 1987)

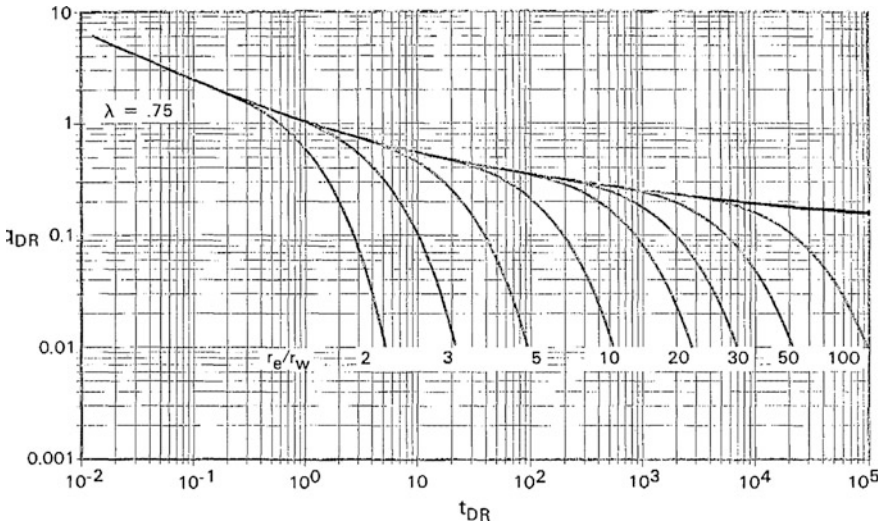

Fig. 4.13 Radial type curve based on ideal gas flow (Carter 1981)

When $\lambda = 1$, this represents a liquid case, and as $\lambda < 1$, this represents the degree of the severity of the drawdown. An example of Carter's (1981) type curve is seen in Fig. 4.13.

Fraim and Wattenbarger (1987) also contributed significantly to the analysis of decline curves. Most of their concepts were taken from Carter (1981), Fetkovich (1980) and also from the concept of pressure transient analysis. They introduced normalised time that applied to viscosity and compressibility at the average reservoir pressure rather than the wellbore pressure. Fraim and Wattenbarger (1987) was able to show that for a closed real gas reservoir, when a normalised time is used, an exponential decline would be expected. The following equation was, therefore, derived for a bounded radial gas reservoir:

$$\ln\left(\frac{q}{q_{\mathrm{i}}}\right) = \frac{-2J_g(p/z)_i}{G(\mu_g c_g)_i} t_n \tag{4.26}$$

Normalised time is defined as

$$t_n = \int_0^t \left(\frac{(\mu c_t)_i}{\bar{\mu}\bar{c}_g}\right) \mathrm{d}t \tag{4.27}$$

$$J_{\mathrm{g}} = \frac{1.9875\,E^{-5} k_g h}{0.5 \ln\left(\frac{2.2458\,A}{C_{\mathrm{A}} r_w^2}\right)} \frac{T_{\mathrm{sc}}}{p_{\mathrm{sc}} T} \tag{4.28}$$

where J_{g} is the gas productivity index, C_{A} is Dietz shape factor and A is the area.

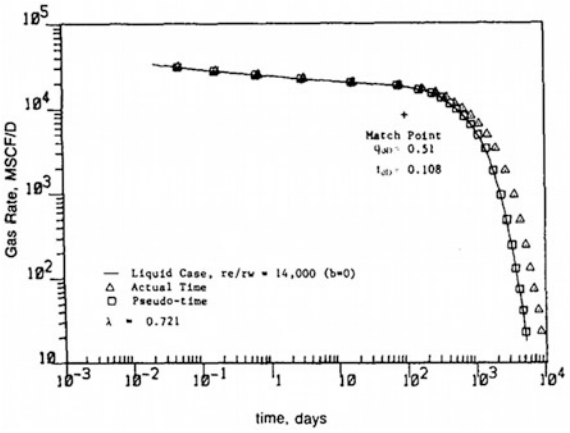

Fig. 4.14 Actual time and pseudo-time compared with liquid exponential decline case (Fraim and Wattenbarger 1987)

Figure 4.14 shows the difference between an actual time and pseudo-time with liquid exponential decline case.

The accuracy of DCA is normally affected by variable rates and pressure production histories. To reduce these effects, Palacio and Blasingame (1993) presented the use of material balance functions. The use of Palacio and Blasingame (1993) type curve overrides the limitations imposed by either using constant bottomhole pressure or constant rate but actual field conditions are used instead to analyse the production data. Based on previous work by both (Carter 1981; Fetkovich 1980), Palacio and Blasingame (1993) modified type curve analyses several possibilities of both single-phase gas and liquid. They proposed the use of material balance pseudo-time which is based on the real gas pseudo-pressure (Lewis and Hughes 2008), with the decline equation for gas given as:

$$\frac{q_g}{p_{pi} - p_{\text{pwf}}} b_{a,pss} = \frac{1}{1 + \left(\frac{m_a}{b_{a,\text{pss}}}\right)\overline{t_a}} \tag{4.29}$$

where

$$m_a = \frac{1}{G_{\text{c}_\text{ti}}} \tag{4.30}$$

$$b_{a,\text{pss}} = 141.2 \frac{\mu_{gi} B_{gi}}{k_g h} \left[1/2 \ln \left(\frac{4}{e^{\gamma}} \frac{A}{C_A r_w^2} \right) \right]. \tag{4.31}$$

Combining the above equations gives:

$$p_{pi} - p_{\text{pwf}} = \Delta m(p) = q_g 141.2 \frac{\mu_g B_{gi}}{k_g h} \left[1/2 \ln \left(\frac{4}{e^{\gamma}} \frac{A}{C_A r_w^2} \right) \right] + \frac{q_g}{G_{\text{cti}}} t_a \tag{4.32}$$

The material balance time can be written as

$$\bar{t}_a = \frac{\mu_{gi} c_{ti}}{q_g} \left(-\frac{G z_i}{p_i} \right) \int_{p_i}^{\bar{p}} \frac{p}{z \mu_g} \mathrm{d}p \tag{4.33}$$

With the integral term expressing the real gas pseudo-pressure difference, the final equation for gas material balance pseudo-time is, therefore, given as

$$\bar{t}_a = \frac{\mu_{gi} c_{ti}}{q_g} \left(\frac{G z_i}{2 p_i} \right) \Delta m(p) \tag{4.34}$$

Agarwal et al. (1998) pointed out that Palacio and Blasingame type curve can be useful for estimating gas in place, permeability and skin but it may not be suitable for analysing gas wells with long vertical hydraulic fractures of infinite/finite conductivity. They developed a numerical simulator that was used to verify Palacio and Blasingame findings and that the constant rate and constant pressure solutions for both liquid and gas systems can be converted to an equivalent constant rate liquid solution using the material balance time transformation.

Agarwal et al. (1998) presented new decline type curve under three categories: rate-time, rate cumulative production and cumulative production-time. The dimensionless time function based on Area (A) is given as:

$$t_{DA} = t_{aD} \left(\frac{r_w^2}{A} \right) \tag{4.35}$$

whereas both the dimensionless wellbore pressure and dimensionless cumulative production based on Area (A) are given as

$$\frac{1}{p_{wD}} = \frac{1422 T q(t)}{k h \Delta m(p)} \tag{4.36}$$

$$Q_{aD} = \frac{4.5 T z_i G_i}{\phi h r_{wa}^2 p_i} \frac{\Delta m(\bar{p})}{\Delta m(p)} \tag{4.37}$$

These important additions made by Agarwal et al. (1998) in their new decline type curve use derivatives to aid in the identification of the transition period between the transient and pseudo-steady state flow regimes and in the matching process.

References

Agarwal RG, Al-Hussainy R, Ramey HJ (1970) An investigation of wellbore storage and skin effect in unsteady liquid flow: I. Analytical treatment. Soc Pet Eng J 10:279–290. https://doi.org/10.2118/2466-PA

Agarwal RG, Gardner DC, Kleinsteiber SW, Fussell DD (1998) Analysing well production data using combined type curve and decline curve analysis concepts. Society of Petroleum Engineers. doi:10.2118/49222-MS

Al-Kobaisi M, Ozkan E, Kazemi H (2006) A hybrid numerical/analytical model of a finite-conductivity vertical fracture intercepted by a horizontal well. SPE Reserv Eval Eng. 9:345. https://doi.org/10.2118/92040-PA

Arps JJ (1945) Analysis of decline curves. Trans AIME. https://doi.org/10.2118/945228-G

Bahrami N, Pena D, Lusted I (2016) Well test, rate transient analysis and reservoir simulation for characterizing multi-fractured unconventional oil and gas reservoirs. J Pet Explor Prod Technol 6:675–689. https://doi.org/10.1007/s13202-015-0219-1

Brohi I, Pooladi-Darvish M, Aguilera R (2011) Modeling fractured horizontal wells as dual porosity composite reservoirs—application to tight gas, shale gas and tight oil cases. SPE West North Am Reg Meet. https://doi.org/10.2118/144057-MS

Carter RD (1981) Characteristic behavior of finite radial and linear gas flow systems—constant terminal pressure case. SPE/DOE Low Permeability Gas Reserv Symp. https://doi.org/10.2118/9887-MS

Carter R (1985) Type curves for finite radial and linear gas-flow systems: constant-terminal-pressure case. Soc Pet Eng J 25:719–728. https://doi.org/10.2118/12917-PA

Cheng Y (2011) Pressure transient characteristics of hydraulically fractured horizontal shale gas wells. SPE East Reg Meet, 1–10. https://doi.org/10.2118/149311-MS

Cinco LH, Samaniego F (1981) Transient pressure analysis for fractured wells. J Pet Technol 33:1749–1766. https://doi.org/10.2118/7490-PA

Cinco LH, Samaniego V, Dominguez A (1978) Transient pressure behavior for a well with a finite-conductivity vertical fracture. SPE J 18:253–264. https://doi.org/10.2118/6014-PA

Clarkson C (2011) Integration of rate-transient and microseismic analysis for unconventional gas reservoirs: where reservoir engineering meets geophysics. CSEG Rec 36:44–61

Clarkson CR, Beierle JJ (2011) Integration of microseismic and other post-fracture surveillance with production analysis: a tight gas study. J Nat Gas Sci Eng 3:382–401. https://doi.org/10.1016/j.jngse.2011.03.003

Duong A (2011) Rate-decline analysis for fracture-dominated shale reservoirs. SPE Reserv Eval Eng 14:19–21. https://doi.org/10.2118/137748-PA

Ehlig-Economides CA, Ramey HJ (1981) Transient rate decline analysis for wells produced at constant pressure. Soc Pet Eng J 21:98–104. https://doi.org/10.2118/8387-pa

Ehlig-Economides CA, Barron HM, Okunola D (2009) Unified PTA and PDA approach enhances well and reservoir characterization. Society of Petroleum Engineers. doi:10.2118/123042-MS

Fetkovich MJ (1980) Decline curve analysis using type curves. J Pet Technol 32:1065–1077. https://doi.org/10.2118/4629-PA

Fetkovich MJ, Vienot ME, Bradley MD, Kiesow UG (1987) Decline curve analysis using type curves: case histories. SPE Form Eval 2:637–656. https://doi.org/10.2118/13169-PA

Fraim ML, Wattenbarger RA (1987) Gas reservoir decline-curve analysis using type curves with real gas pseudopressure and normalized time. SPE Form Eval 2:671–682. https://doi.org/10.2118/14238-PA

Freeman CM, Moridis G, Ilk D, Blasingame TA (2009) A numerical study of performance for tight gas and shale gas reservoir systems. SPE Annu Tech Conf Exhib. https://doi.org/10.2118/124961-MS

Gatens MJ, Lee WJ, Lane HS, Watson AT, Stanley DK (1989) Analysis of eastern devonian gas shales production data. J Pet Technol 41:519–525

Guo J, Zhang L, Wang H (2014) Pressure transient characteristics of multi-stage fractured horizontal wells in shale gas reservoirs with consideration of multiple mechanisms

Ilk D, Perego aD, Rushing Ja, Blasingame Ta (2008) Exponential vs. hyperbolic decline in tight gas sands—understanding the origin and implications for reserve estimates using Arps' decline curves. Spe-116731 116731. https://doi.org/10.2118/116731-MS

Kanfar M, Wattenbarger R (2012) Comparison of empirical decline curve methods for shale wells. SPE Can Unconv Resour Conf, 1–12. https://doi.org/10.2118/162648-MS

Kim TH, Park P, Lee KS (2014) Development and application of type curves for pressure transient analysis of multiple fractured horizontal wells in shale gas reservoirs. Offshore Technology Conference. doi:10.4043/24881-MS

Kruysdijk V, Dullaert GM (1989) A boundary element solution to the transient pressure response of multiply fractured horizontal wells. In: ECMOR I-1st European conference on the mathematics of oil recovery

Larsen L, Hegre TM (1991) Pressure-transient behavior of horizontal wells with finite-conductivity vertical fractures. Methods. https://doi.org/10.2118/22076-ms

Larsen L, Hegre T (1994) Pressure transient analysis of multifractured horizontal wells. Society of Petroleum Engineers. doi:10.2118/28389-MS

Lewis AM, Hughes RG (2008) Production data analysis of shale gas reservoir. Society of Petroleum Engineers. doi:10.2118/116688-MS

Malallah A, Nashawi I, Algharaib M (2007) Constant-pressure analysis of oil wells intercepted by infinite-conductivity\nHydraulic fracture using rate and rate-derivative functions. Proc SPE Middle East Oil Gas Show Conf. https://doi.org/10.2523/105046-MS

Medeiros F, Ozkan E, Kazemi H (2006) A semianalytical, pressure-transient model for horizontal and multilateral wells in composite, layered, and compartmentalized reservoirs. Society of Petroleum Engineers. doi:10.2118/102834-MS

Medeiros F, Kurtoglu B, Ozkan E, Kazemi H (2007) Pressure-transient performances of hydraulically fractured horizontal wells in locally and globally naturally fractured formations. Int Pet Technol Conf. https://doi.org/10.2523/IPTC-11781-MS

Medeiros F, Ozkan E, Kazemi H (2008) Productivity and drainage area of fractured horizontal wells in tight gas reservoirs. SPE Reserv Eval Eng 11:16–18. https://doi.org/10.2118/108110-PA

Ozkan E, Ohaeri U, Raghavan R (1987) Unsteady flow to a well produced at a constant pressure in a fractured reservoir. SPE Form Eval, 187–200. SPE–9902–PA. https://doi.org/10.2118/9902-PA

Palacio JC, Blasingame TA (1993) Decline curve analysis using type curves: analysis of gas well production data. In: 1993 SPE Jt Rocky Mountain Regional/Low Permeability Reservoirs Symposium. https://doi.org/10.2118/25909-MS

Raghavan R, Chen C-C, Argawal B (1997) An analysis of horizontal wells intercepted by multiple fractures. SPE J 2:235–245. https://doi.org/10.2118/27652-PA

Rodriguez F, Horne RN, Cinco LH (1984a) Partially penetrating fractures: pressure transient analysis of an infinite conductivity fracture. Society of Petroleum Engineers. doi:10.2118/12743-MS

Rodriguez F, Horne RN, Cinco LH (1984b) Partially penetrating vertical fractures: pressure transient behavior of a finite-conductivity fracture. Society of Petroleum Engineers. doi:10.2118/13057-MS

Schulte WM (1986) Production from a fractured well with well inflow limited to part of the fractured height. Society of Petroleum Engineers. doi:10.2118/12882-PA

Seshadri J, Mattar L (2010) Comparison of power law and modified hyperbolic decline methods. Can Unconv Resour Int Pet Conf, 19–21. https://doi.org/10.2118/137320-MS

Uraiet aa, Raghavan R (1980) Unsteady flow to a well producing at a constant pressure. J Pet Technol 32:1803–1812. https://doi.org/10.2118/8768-PA

Valko P (2009) Assigning value to stimulation in the Barnett Shale: a simultaneous analysis of 7000 plus production histories and well completion records. Proceedings of SPE hydraulic fracturing technology conference, pp 1–19. https://doi.org/10.2118/119369-MS

Vera F, Ehlig-Economides C (2014) Describing shale well performance using transient well analysis. The Way Ahead 10(02):24–28

Wang F, Zhang S, Liu B (2013) Pressure transient analysis of multi-stage hydraulically fractured horizontal wells. J Pet Sci Res 2:162. https://doi.org/10.14355/jpsr.2013.0204.03

Wei Y, Economides MJ (2005) Transverse hydraulic fractures from a horizontal well. SPE Annu Tech Conf Exhib, 1–12. https://doi.org/10.2118/94671-MS